



HAL
open science

High Integrity Personal Tracking Using Fault Tolerant Multi-Sensor Data Fusion

Mohamad Daher

► **To cite this version:**

Mohamad Daher. High Integrity Personal Tracking Using Fault Tolerant Multi-Sensor Data Fusion. Automatic. Université de Lille 1, Sciences et Technologies; CRISTAL UMR 9189, 2017. English. NNT: . tel-01740905

HAL Id: tel-01740905

<https://hal.science/tel-01740905>

Submitted on 2 Apr 2018

HAL is a multi-disciplinary open access archive for the deposit and dissemination of scientific research documents, whether they are published or not. The documents may come from teaching and research institutions in France or abroad, or from public or private research centers.

L'archive ouverte pluridisciplinaire **HAL**, est destinée au dépôt et à la diffusion de documents scientifiques de niveau recherche, publiés ou non, émanant des établissements d'enseignement et de recherche français ou étrangers, des laboratoires publics ou privés.

Université de Lille

École doctorale **Sciences Pour l'Ingénieur**
Unité de recherche **CRISAL**

Thèse présentée par

Mohamad Daher

Soutenue le **13 décembre 2017**

En vue de l'obtention du grade de docteur de l'Université de Lille

Discipline **Automatique, Génie informatique, Traitement du Signal**

Fusion multi-capteurs tolérante aux fautes pour un niveau d'intégrité élevé du suivi de la personne

Composition du jury

<i>Rapporteurs</i>	Véronique Berge-Cherfaoui	Professeur à l'Université de Technologie de Compiègne
	Ghaleb Hoblos	Professeur à l'ESGIELEC
<i>Examineurs</i>	Claude Delpha	MCF HDR Université Paris Sud
	Ahmad Diab	MCF à l'Université Libanaise
	Mohamad Khalil	Professeur à l'Université Libanaise
	Christine Perret-Guillaume	PU PH CHRU Nancy
<i>Directeurs de thèse</i>	Maan El Badaoui El Najjar	Professeur à l'Université de Lille
	Francois Charpillet	Directeur de recherche INRIA, Nancy

Mots clés: système de localisation des personnes, reconnaissance des activités de la vie quotidienne, détection des chutes des personnes âgées, extraction des paramètres, sélection des paramètres, détection des signaux, fusion de données, filtre informationnel, détection et exclusion des défauts, divergence de Kullback-Leibler.

Keywords: personal localization system, activities daily living recognition, elderly fall detection, features extraction, features selection, signal detection, data fusion, information filter, fault detection and exclusion, Kullback-Leibler divergence.

Preface

This thesis is submitted to the Lille University - Science and Technology in partial fulfilment of the requirements for the degree of Doctor of Philosophy.

The work has been conducted at CRIStAL (Centre de Recherche en Informatique, Signal et Automatique de Lille) and has been achieved in partnership with the Institut National de Recherche en Informatique et en Automatique (INRIA) in Nancy - Grand Est and the Azm Center for Research in Biotechnology and its Applications.



Abstract

About one third of home-dwelling older people suffer a fall each year. The most painful falls occur when the person is alone and unable to get up, resulting in huge number of elders which are associated with institutionalization and high morbidity-mortality rate.

The PAL (Personally Assisted Living) system appears to be one of the solutions of this problem. This ambient intelligence system allows elderly people to live in an intelligent and pro-active environment. It is charged with the supervision and control of the entrusted space, monitoring events and detecting falls, recognizing human activities through a network sensors, and finally providing support through robotic actuators. Such services have the potential of increasing autonomy of elders while minimizing the risks of living alone. Therefore, they have been an active research topic due to the fact that health care industry has a big demand for their products and technology.

This thesis describes the ongoing work of in-home elder tracking, activities daily living recognition, and automatic fall detection system using a set of non-intrusive sensors that grants privacy and comfort to the elders. In addition, a fault-tolerant fusion method is proposed using a purely informational formalism: information filter on the one hand, and information theory tools on the other hand. Residues based on the Kullback-Leibler divergence are used. Using an appropriate thresholding, these residues lead to the detection and the exclusion of sensors faults.

The proposed algorithms were validated with many different scenarios containing the different activities: walking, sitting, standing, lying down, and falling. The performances of the developed methods showed a sensitivity of more than 94% for the fall detection of persons and more than 92% for the discrimination between the different ADLs (Activities of the daily life).

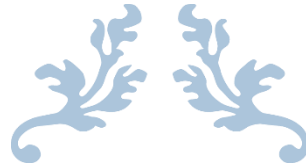
Résumé

Environ un tiers des personnes âgées vivant à domicile souffrent d'une chute chaque année. Les chutes les plus graves se produisent lorsque la personne est seule et incapable de se lever, ce qui entraîne un grand nombre de personnes âgées admis au service de gériatrique et un taux de mortalité malheureusement élevé.

Le système PAL (Personally Assisted Living) apparaît comme une des solutions de ce problème. Ce système d'intelligence ambiante permet aux personnes âgées de vivre dans un environnement intelligent et pro-actif. Il permet la supervision et le contrôle de l'espace confié, la surveillance des événements et la détection des chutes, tout en reconnaissant les activités humaines grâce à des réseaux de capteurs et en fournissant un support grâce à des actionneurs robotiques. Ces services ont le potentiel d'accroître l'autonomie des personnes âgées tout en minimisant les risques de vivre seuls. Par conséquent, ils ont été un sujet de recherche actif en raison du fait que l'industrie des soins de santé a émis une forte demande pour leurs produits et leur technologie.

Le travail de cette thèse s'inscrit dans le cadre de suivi des personnes âgées avec un maintien à domicile, la reconnaissance quotidienne des activités et le système automatique de détection des chutes à l'aide d'un ensemble de capteurs non intrusifs qui accorde l'intimité et le confort aux personnes âgées. En outre, une méthode de fusion tolérante aux fautes est proposée en utilisant un formalisme purement informationnel: filtre informationnel d'une part, et outils de la théorie de

l'information d'autre part. Des résidus basés sur la divergence de Kullback-Leibler sont utilisés. Via un seuillage adéquat, ces résidus conduisent à la détection et à l'exclusion des défauts capteurs. Les algorithmes proposés ont été validés avec plusieurs scénarii différents contenant les différentes activités: marcher, s'asseoir, debout, se coucher et tomber. Les performances des méthodes développées ont montré une sensibilité supérieure à 94% pour la détection de chutes de personnes et plus de 92% pour la discrimination entre les différentes ADL (Activités de la vie quotidienne).



Acknowledgements

First and above all, I praise God, the almighty for providing me this opportunity and granting me the capability to proceed successfully.

This thesis appears in its current form due to the assistance and guidance of several people. I would therefore like to offer my sincere thanks to all of them.

First, I wish to warmly thank my Research Director Professor Maan El-Badaoui El-Najjar and Mr. François Charpillet for having offered me the possibility to pursue this doctorate under their guidance.

I would also like to thank the Professor Mohamad Khalil; director of the Azm Center for Research in Biotechnology and its Applications; for hosting me in the laboratory.

I would like to express my deepest sense of gratitude to Mr. Ahmad Diab, who offered his continuous advice and encouragement throughout the course of this thesis.

I am very grateful to the official referees of this thesis: Pr. for having presided the jury; Mrs. Véronique Cherfaoui and Mr. Ghaleb Hoblos for reviewing my thesis; Mrs. Christine Perret-Guillaume and Mr. Claude Delpha for their valuable comments.

Mr. Abdallah Dib and Mr. Thomas Moinel, thanks for your excellent technical assistance in the INRIA laboratory, particularly for data acquisition technique, and your kindly answers to my general questions.

I am grateful to my CRIStAL laboratory colleague Ms. Joelle Al Hage for her continuous support.

I would also like to thank our assistant Mrs. Véronique Constant, who helped organizing all the missions to conferences and project meetings.

I cannot finish without thanking my family, I warmly thank and appreciate my beloved parents for their love and positive support on my life.

Finally I want to express my gratitude and deepest appreciation to my lovely sweet wife “Reem”, thank you for your love, your support, and your encouragement given to me in life and especially during the progression of this thesis.

My Daughters and my Son: Lynn, Lea, Ahmad and Celia, thank you my good for your presents.

Villeneuve d'Ascq, on November , 2017

Mohamad Daher



Table of contents

Abstract	v
Acknowledgements	vii
Table of contents	ix
Acronyms	xiv
Chapter I - Introduction	1
I.1 Ambient Intelligence (AmI).....	1
I.2 AmI System Flow	1
I.3 Aging population	2
I.4 Elderly falls in aging population.....	4
I.5 Causes of elderly falls	5
I.6 Consequences of elderly falls	5
I.7 Advances in AmI as a driver for seniors independent living.....	7
I.8 Existing AmI projects	7
I.9 Background of the thesis.....	9
I.10 Objectives and structure of the thesis	9
I.12 Key contributions of this thesis.....	11
I.13 Publication list	11
Chapter II - Fall detection systems and sensing floors: existing prototypes and related works	14
Overview	14
Section 1: Fall detection systems	15
II.1.1 Introduction	15
II.1.2 Fall detection system framework.....	16
II.1.2.1 Wearable sensors	16
II.1.2.2 Camera-Based sensing.....	18
II.1.2.3 Ambient sensing	18
II.1.3 System evaluation.....	19
II.1.4 Existing prototypes	20
II.1.5 Commercially available fall detection systems	26
II.1.6 Conclusion	27
Section 2: Sensing floors	29
II.2.1 Introduction	29
II.2.2 Existing prototypes	30

II.2.2.1 Monolithic pressure-sensing floors.....	30
II.2.2.2 Modular pressure-sensing floors.....	33
II.2.3 Commercially available sensing floors.....	39
II.2.4 Conclusion.....	40
Section 3: The Inria Nancy – Grand Est sensing floor prototype	42
II.3.1 Introduction	42
II.3.2 Origins of the Project.....	42
II.3.3 Research projects of the Inria Nancy – Grand Est research center.....	44
II.3.4 Intra and inter tiles communications	47
II.3.5 Inria sensing floor capabilities.....	47
II.3.6 Conclusion.....	48
General conclusion.....	49
Chapter III - Processing and simulating data from the Inria Nancy – Grand Est sensing floor	51
Overview	51
Section 1: Processing and simulating data from the load sensing floor.....	52
III.1.1 Introduction	52
III.1.2 The load pressure sensors of the Inria Nancy – Grand Est platform.....	52
III.1.2.1 Load frequency distribution and sensors calibration.....	53
III.1.3 Load data collection	54
III.1.4 Elder tracking and ADLs recognition using the load data	55
III.1.4.1 ADLs definition.....	56
III.1.4.2 Characteristics of all postures.....	56
III.1.4.3 Load data processing	57
III.1.4.4 Experiments and results.....	59
III.1.5 Conclusion.....	63
Section 2: Processing and simulating data from the accelerometers	65
III.2.1 Introduction	65
III.2.2 The accelerometers of the Inria Nancy – Grand Est platform.....	65
III.2.3 Accelerometer data collection	66
III.2.4 Fall detection using the accelerometer data	67
III.2.4.1 Accelerometer data preprocessing.....	68
III.2.4.2 Features extraction.....	69
III.2.4.3 Feature selection	73
III.2.4.4 Signal change detection.....	87
III.2.4.4.1 Results of signal changing detection	87
III.2.5 Evaluation.....	89
III.2.6 Conclusion.....	92

Section 3: Merging between the load pressure sensors results and the accelerometers decisions	94
III.3.1 Introduction	94
III.3.2 Merging between the load sensors results and the accelerometer decisions.....	95
III.3.3 Results	96
III.3.4 Conclusion.....	96
General Conclusion.....	98
Chapter IV - Multisensory data fusion with detection and exclusion of faults based on Kullback-Leibler divergence.....	100
Overview	100
Section 1: State of the art and work positioning	102
IV.1.1 Multisensory data fusion: definition and objectives	102
IV.1.2 Data fusion methods.....	102
IV.1.2.1 Bayes’ rule.....	103
IV.1.2.2 Kalman filter	103
IV.1.2.3 The information filter for data fusion.....	104
IV.1.2.4 Sequential Monte Carlo Methods.....	105
IV.1.2.5 Alternatives to probability.....	105
IV.1.3 Data fusion consequences	106
IV.1.4 Fault-tolerant multi-sensors data fusion.....	106
IV.1.4.1 Related works.....	106
IV.1.4.2 Information tools for fault-tolerant data fusion.....	108
IV.1.5 Multi-sensors data fusion for positioning systems.....	108
IV.1.5.1 PLS related works	109
Section 2: Proposed approach.....	112
IV.2.1 Problem statement.....	112
IV.2.2 Inertial measurement unit (IMU)	112
IV.2.2.1 IMU components, measurements and uses	113
IV.2.2.2 IMU performance and erroneous measurements	114
IV.2.3 The load pressure sensors of the Inria Nancy – Grand Est platform	115
IV.2.4 IMU and load pressure sensors data fusion – Problem formulation	115
IV.2.4.1 Prediction step using an evolution model	116
IV.2.4.2 Correction step using an observation model	118
IV.2.5 Fault detection and exclusion using informational framework.....	124
IV.2.5.1 Fault detection.....	124
IV.2.5.2 Fault isolation.....	125
IV.2.6 Experimentation and validation of results.....	127
Conclusion	131

Chapter V - Conclusion and future works	134
V.1 Conclusion.....	134
V.2 Future works.....	135

Acronyms

AP	Access Points
AAL	Ambient Assisted Living
AmI	Ambient intelligence
ADL	Activities of Daily Living
AUC	Area Under Curve
AI	Artificial Intelligence
ARBFNN	Augmented Radial Basis Function Neural Network
BBM	Best Beacon Match
BLE	Bluetooth Low Energy
BOCDA	Brillouin Optical Correlation Domain Analysis
BPNN	Back Propagation Neural Network
CDC	Centers for Disease Control and Prevention
DFS	Depth-First Search
DFA	Detrended Fluctuation Analysis
DSP	Digital Signal Processor
DWT	Discrete Wavelet Transform
EMFi	Electro Mechanical Film
EIF	Extended Information Filter
EKF	Extended Kalman Filter
FSR	Force Sensing Resistors
GKLD	Global Kullback-Leibler Divergence
PKLD	Partiel Kullback-Leibler Divergence
EIF	Extended Information Filter
FDE	Fault Detection and Exclusion
FD	Fall Detection
FP	Fall Prevention
FPR	False Positive Ratio.
FN	False Negative
FPGA	Field-Programmable Gate Array
FSR	Force Sensing Resistor
FPS	Frames Per Second
GLONASS	GLObal NAVigation Satellite System
GNSS	Global Navigation Satellite System
GPS	Global Positioning System
HMM	Hidden Markov Model
HCM	Histogram Comparison Method
IMU	Inertial Measurement Unit
IF	Information Filter.
INS	Inertial Navigation System
KF	Kalman Filter
KLD	Kullback-Leibler Divergence
KNN	K-Nearest Neighbor
LE	Lyapunov Exponent
LLR	Log Likelihood Ratio

MPF	Mean Power Frequency
MC	Monte Carlo
MLP	Multi-Layer Perceptron
NFFT	Nonequispaced Fast Fourier Transform
PAL	Personally Assisted Living
PF	Peak Frequency
PLS	Personal Localization System
PSD	Power Spectral Density
PDA	Probability Data Association
RFID	Radio-frequency identification
ROC	Receiver Operating Characteristic
RSS	Received Signal Strength
RSSI	Receive Signal Strength indicator
ROS	Robot Operating System
TR	Time Reversibility
TPR	True Positive Ratio
TN	True Negative
SE	Sample Entropy
SFS	Sequential Forward Selection
SDE	Spectral Density Estimation
SVM	Sum Vector Magnitude
SoC	System on Chip
WMR	Wheeled Mobile Robot

Chapter I - Introduction

I.1 Ambient Intelligence (AmI)

Ambient intelligence (AmI) refers to electronic environments that are sensitive and responsive to the presence of people inside delimited environments. One of the AmI systems is the elderly assisted living system that enable elderly people to live in an intelligent and pro-active environment. It is charged with the supervision and control of the entrusted space, monitoring events and human well-being, recognizing human activities through a network of heterogeneous sensors, and providing support through its robotic actuators. In an ambient intelligence world, devices work in concert to support people in carrying out their everyday life activities, tasks and rituals in an easy, natural way using information and intelligence that is hidden in the network connecting these devices. In other words, AmI aims to enhance the way people interact with their environment to promote safety and to enrich their lives.

Among the various types of sensors employed in the perception of the environment, load sensors can measure the load pressure exerted by humans and objects on their surroundings.

This thesis will explore the capabilities of such load sensing floors to locate and track people, recognize their activities of daily living (ADLs) by determining their postures (walking, sitting, standing, lying down, and the transitions between them), as well as detect the falling down cases.

I.2 AmI System Flow

A typical AmI system needs sensors and devices to surround occupants of an environment (interactors) with technology that provide accurate data to the system. The information collected has to be transmitted by a network and pre-processed by what is called middleware, which collates and harmonizes data from different devices. The system has a higher layer of reasoning that accomplishes diagnosis and assists humans, and finally makes decision easier and more beneficial to the occupants of the environment. The high layer “Decision Making” process includes a “Knowledge Repository” where the events are collected and an “Artificial Intelligence Reasoner” (AI Reasoner), which will apply for example spatio-temporal reasoning to take decisions [1]. For

instance, a decision could be to perform some action in the environment and this is enabled via “Actuators”. Machine learning techniques and pattern recognition learn from the acquired information in order to update the AI Reasoner [2]. The “Figure 1.1” shows a representative information flow for AmI systems.

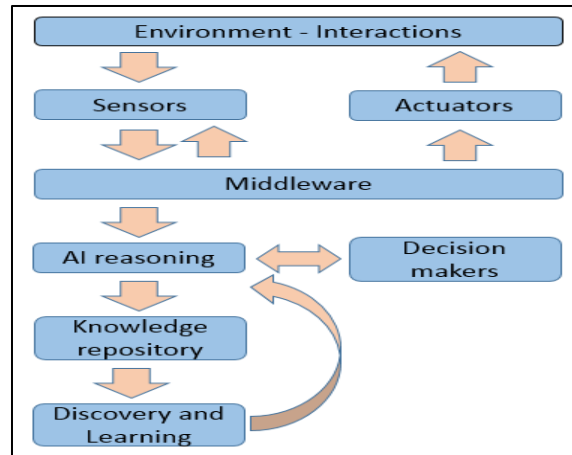


Figure 1.1 - Information flow in AmI system.

In this project, environment is the Inria Nancy - Grand Est platform with furniture, specific elements of the chamber like a chair, a kitchen and a toilet. Interactors in this environment will be the elder person, relatives and caregivers (e.g., nurses and physicians). The used sensors are the load sensors and the 3-axis accelerometers concealed under tiles as well as a simulated inertial measurement unit (IMU) assumed to be held by the elder. These sensors are used for tracking elders, identifying their ADLs and detecting the falling down cases. Actuators can be alert messages sent by communication system to notify a fall-alarm. Contexts of interest can be “the elder has fallen down and has remained down after 30 seconds”. Interaction rules can consider, for example, that “if elder status indicates that he/she is falling down caregivers should be notified”.

I.3 Aging population

Nowadays, aging population shows a drastic increasing substantially in the recent years and that growth is projected to accelerate in coming decades. It’s one of the greatest social and economic challenges of the 21st century [3]. Driven by falling fertility rates and a sustained increase in overall longevity of people resulting of advances in medicine and public health services, many countries; especially in the developed world; are now bracing themselves for the fact that their fastest-growing demographic is the over 80 years old. Moreover, the linear trend that life expectancies have followed for over a century is set to continue. People aged 65 years or more, here referred to

as elder people, are estimated to represent around 30% of the population in the next 30 years [4]. The “Figure 1.2” illustrates the world age population structure in 1950, 2010, 2050, and 2100.

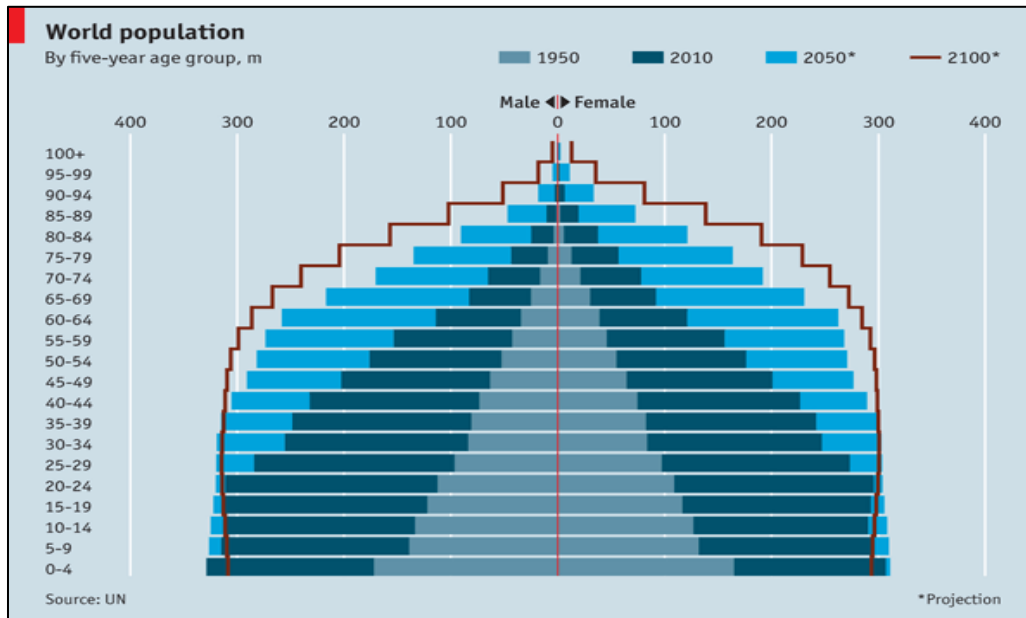


Figure 1.2 - Age structure in 1950, 2010, 2050, and 2100 according to United Nations study in 2015.

This demographic shift is not evenly distributed between all world regions. In the developed America and Europe, the ageing of the population is sudden compared to Africa. Ageing in the Middle East is expected to growth rapidly over the next 35 years. In Asia, due to the country’s lower mortality rate and the one-child policy that the Chinese government enforces, the population is aging quickly [5]. The percentage of elderly to young people in the Middle East is low compared to western countries. The “Figure 1.3” shows the number of persons aged 65 years or over, per hundred children under 15 years in different regions between 1950 and 2050.

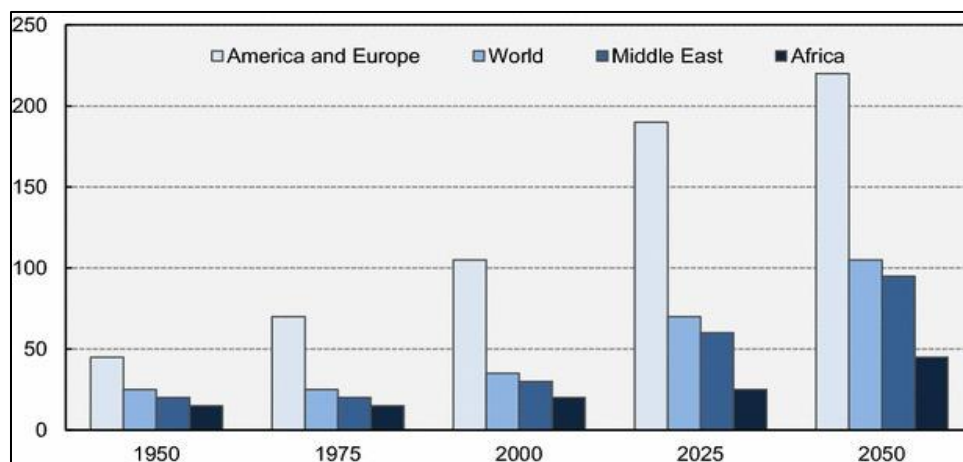


Figure 1.3 - Number of persons aged 65 years or over, per hundred children under 15 years.

In France, the National Institute for Statistics and Economic Studies (INSEE) predicts that the number of people over 60 years will increase by 10.4 million between 2007 and 2060 to reach the number of 23.6 million people in 2060, an increase of 80% in 53 years. The number of people over the age 75 will increase from 5.2 million in 2007 to 11.9 million in 2060 and from 1.3 to 5.4 million for people over 85 years. These numbers are shown in the “Figure 1.4”.

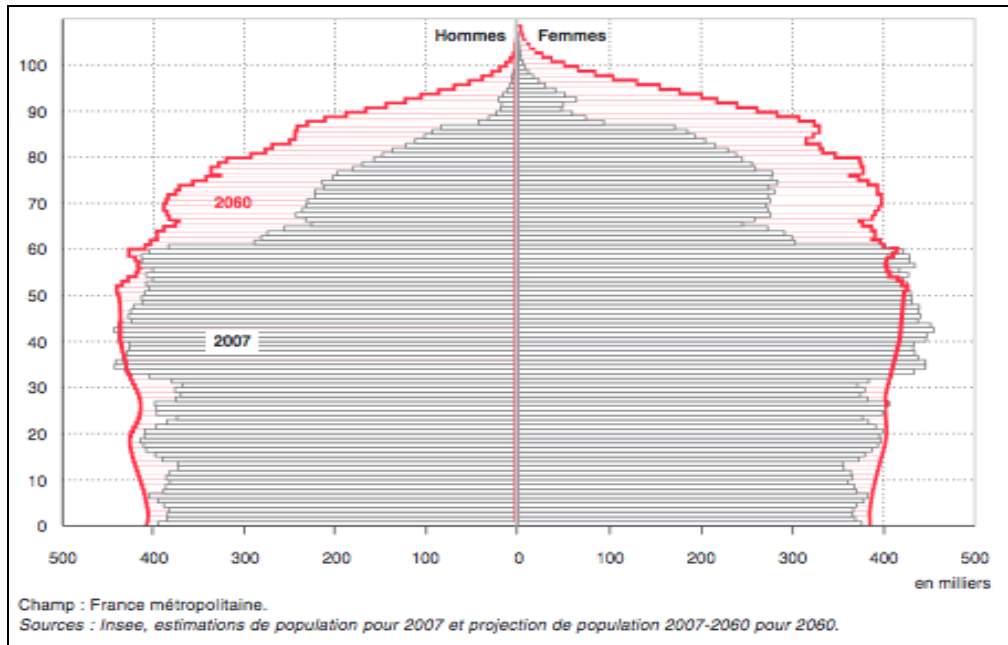


Figure 1.4 - Age structure in 2007 and 2060 according to INSEE study in 2010.

I.4 Elderly falls in aging population

Elderly falling down problem is one of the most serious life-threatening events that can occur, especially in the population aged 65 and over. This age group suffers from falls on a yearly basis and half of these elderly do fall repeatedly that also have dramatic psychological, medical and social consequences [6]. Most of these falls are associated with one or more identifiable risk factors (e.g. weakness, unsteady gait, confusion and certain medications), and research has shown that attention to these risk factors can significantly reduce rates of falling. According to the statistics of the Centers for Disease Control and Prevention (CDC), one out of three adults age 65 and older falls each year in the United States, and 61% of these falls occur at homes that cause around 10,000 deaths. However, obtaining a quick assistance after a fall reduces the risk of hospitalization by 26% and the death by 80% [7].

I.5 Causes of elderly falls

There are several causes for elderly falls. Some reasons such as age, gender, being unconscious, or suffering from chronic neurological or mental problems, cannot be controlled. Whereas other reasons; such as medications side effects, insufficient vision, poor hearing, or muscle weakness can be controlled or modified. Moreover, the factors associated with falls are classified as personal factors (physiological and neurological functions changes, Alzheimer’s diseases, etc.) and environment factors (loose carpets, wet or slippery floors, poorly constructed steps, etc.). The “Figure 1.5” classifies the most common reasons causing elderly falls according to their origin (environmental or personal) and controllability [8,9]. The presence of more than one cause of falling is common, and several studies have shown that the risk of falling increases dramatically as the number of causes increases.

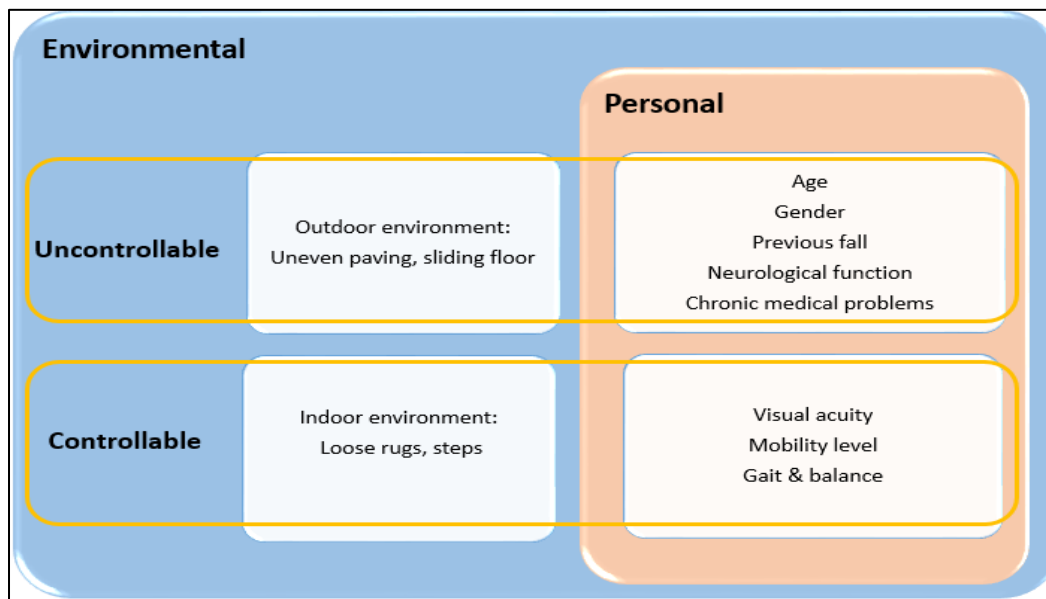


Figure 1.5 - Categories of common reasons causing falls.

I.6 Consequences of elderly falls

Falls in the elderly may cause adverse physical, psychological, social, financial and medical, as well as governmental and community consequences [10]. The “Figure 1.6” shows the main consequences related to elderly falling.

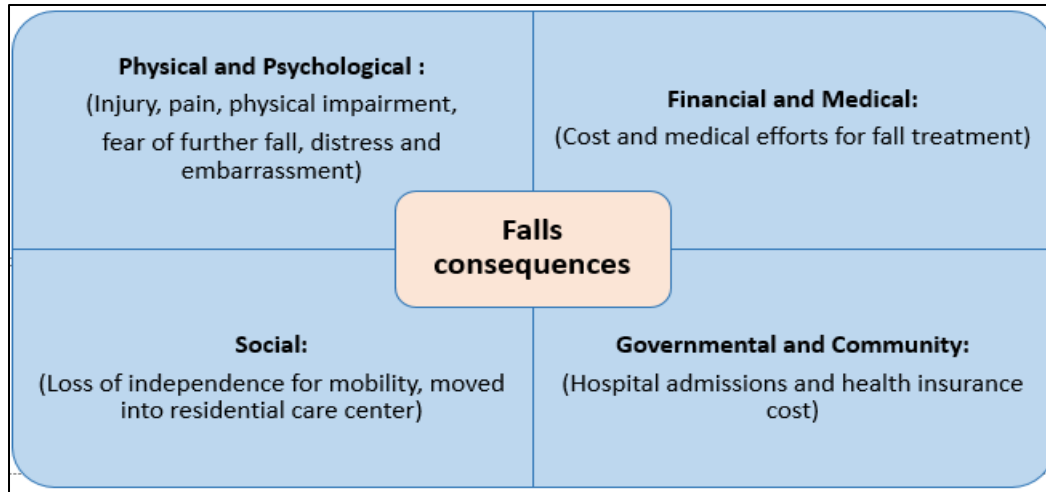


Figure 1.6 - The main consequences related to elderly falling.

- **Physical consequences:** are exemplified in possible injury i.e. broken bone or soft tissue injury, pain and discomfort, reduced mobility and possible long-term disability, and most of the time lead to increase the loss of independence and the ability to look after himself/herself.
- **Psychological consequences:** lead to loss of confidence when walking and moving due to the increased fear of repeated falling, fear and anxiety, in addition to distress, and embarrassment.
- **Social consequences:** are represented in curtailment of possible routine social activities, loss of independence and a reliance on family, friends or possible move into aging residential or nursing care center.
- **Financial and medical consequences:** imply the direct costs of medical care associated with injuries represented in increased costs to the statutory services such as physiotherapy rehabilitation, hospital care, and social care [11].
- **Governmental and community economic consequences:** designate the fact that falls can have devastating effects on people's health and that falls greatly contribute to the level of hospital admissions and health insurance costs. Consequently, governments are incited to improve both the prevention and treatment of falls and these are most effective when social care and the government work together. Furthermore, as the population gets older, it has to be recognized that community health and social care organizations need to work more closely to set up effective falls prevention programs and to consider this as even more of a priority. That is, for little initial investment patients are getting better care, more falls are being

prevented, and money is being saved. According to a 2013 report made by the National Center for Health Statistics, the annual expenditures for long-term care services in the United States of America are estimated to be between \$210.9 billion and \$306 billion [12]. In the European Union, according to a 2008 report by Ernst & Young, the public expenses on senior housing equaled €8.7 billion in Italy (2005), €10.3 billion in the United Kingdom (2004), €7.6 billion in Germany, and €1.32 billion in Belgium (2003). In France, the market size of the personal assistance services was evaluated at €12 billion in 2007 [13].

I.7 Advances in AmI as a driver for seniors independent living

Advances in AmI can deliver key skills remotely and enable home-based care. Technology will play an increasingly active role in providing care to ageing populations. For example, the automatic detection of falls would help reducing the time of arrival of medical caregiver, and accordingly reducing the mortality rate [14]. Accordingly, in order to achieve a good degree of fall prevention for elderly people, many supportive systems have been developed to track and monitor elderly ADLs at home in order to assist their independent living and reduce the cost of premature institutionalization. But generally, all of these systems are relying on only one data provider (movement-sensor, camera, or accelerometer, etc.) that have their own limitations and do not ensure 100% reliability [15]. Moreover, there still is a lack in experience and systematic knowledge to intelligently assemble the components into a robust, user-friendly and effective system, making no false alarm and detecting each fall case, without affecting elderly daily living patterns [16].

I.8 Existing AmI projects

Several projects are developed around the world on the topic of Personally Assisted Living (PAL) as AmI applications that aim to monitor and assist elders and chronic or Alzheimer's disease patients, and to form habitats with home automation. Some examples of projects are listed below.

In France, The Inria Nancy Research Center has been supporting since 2010 the design and the construction of an innovative platform for favoring research in assistance for elderly people at home [17-21]. The Tissad project was developed by Thomesse that defines a generic architecture for remote monitoring systems. The Casper project has the objective to follow the domestic activities of elderly or handicapped people using specific autonomous sensors in order to provide

solutions that would improve their life at home [22]. The Actidom project aims to measure the activity of fragile elderly persons in their daily life, so as to determine the evolution of their state of dependence [23]. The Gerhome [24], CIU-santé (CIU-health) [25,26], Sweethome [27], and ParaChute [28] projects have also tackled the problem of an automated, objective evaluation of the frailty of elderly persons, using fixed cameras and experimental sensors.

In the United States of America, the University of Colorado at Boulder has developed the Adaptive Control of Home Environments (ACHE) project [29] to automatically control the temperature, heating and the lighting levels inside a building. The projects Gator Tech Smart House of the University of Florida [30], MavHome [31] of the University of Arlington, Aware Home Research [32] of the Georgia Institute of Technology are similar projects having the objective to optimize the comfort and security of elderly people at home.

SELF (Sensorized Environment for LiFe) [33] developed at the University of Ibaraki in Japan that aims to supervise the state of health of persons, by analyzing several physiological criteria. The systems developed by the University of Tokyo [34] and the intelligent house of Osaka [35] are other Japanese examples of intelligent homes similar to SELF. The CarerNet system aims to offer several healthcare services at home, such as the alarm, tracking of health procedures, and e-health [36]. A platform for domestic medical care has been developed in Spain, to assist patients suffering from specific pathologies to live inside their homes. The platform was composed of two parts: a client application for the local processing of data, and a medical call-center [37].

Moreover, Microsoft has also proposed a system that uses cameras coupled to movement detectors placed on the walls for tracking and locating humans through image processing techniques. It was developed for the EasyLiving project [38].

One can see that AmI systems have been attracted significant attention although the area is very new. As a result of its spreading, there are many projects, scientific events, books published, commercial exhibitions and governmental projects being launched every year. AmI has a strong emphasis on forcing computing to make an effort to reach and serve humans. The technological infrastructure seems to be continuously evolving in that direction, and there is a fruitful atmosphere on all sides involved: normal users/consumers of technology, technology generators, technology providers and governmental institutions, that this paradigm shift is needed and feasible.

Finally, the studies focus nowadays on integrating AmI solutions into habitats to design and build a smart home equipped with an AmI system, exploiting complementary technologies like non-intrusive sensing floors, depth cameras, and mobile assistant robots.

I.9 Background of the thesis

This thesis is placed in the domestic AmI context settings. The large scale of PAL that proposes technological solutions to improve the quality of life of frail people. These solutions come in the form of smart sensors, robotics, and home automation systems. They aim to improve the security, safety and the autonomy of elderly, allow them to remain in their own homes, and to preserve or restore their daily-life necessary functions.

This work describes a novel approach of personal localization system (PLS), ADLs recognition and automatic fall detection system using multi-data providers that aim to provide more accuracy, precision and efficiency. Yet the main sources of data are the ground sensors network within the Inria Nancy - Grand Est platform that will be presented in details in the “Chapter II, Section 3”, and the simulated IMU described in “Chapter IV, Section 2”.

I.10 Objectives and structure of the thesis

The objective of this thesis is to explore the abilities of the Inria Nancy – Grand Est sensing floor as an AmI smart home to offer localization and tracking of elderly in their independent living senior apartments, (ADLs) recognition, and automatic fall detection system, using a non-intrusive sensors network (load pressure sensors and accelerometers) concealed under tiles.

Indeed, most of the work on load pressure data was interesting, unless the fall detection accuracy was unfortunate due to false alarms coming from falling down and lying down's postures. This result leads to conclude that by using load pressure sensors alone, we cannot distinguish between these two postures. To solve this issue, we propose merging between the load pressure sensor measurements and the accelerometer sensor decisions.

Moreover, we take in consideration the erroneous or noisy sensors measurements that can affect the system accuracy. In this way, the importance and necessity of a step of diagnosis of sensor defects is absolutely essential. Therefore, we present a generic and accurate method for PLS with tolerance to sensor defects in a distributed system. It allows to detect and exclude any faulty measurement from any used sensor.

Furthermore, this original method will open the gate to track an unlimited number of people simultaneously and to use an adaptive or automatic thresholding method for classifying.

As a consequence, the system accuracy is satisfactory and the results show that the proposed methods are efficient, and they can be easily used in a real elder tracking and fall detection system.

This thesis, which constitutes this scientific exploration, is structured in five chapters organized as follows.

- Chapter I provides a synopsis of the AmI systems, the ageing population, the causes and the implications of elderly falls, the PAL systems as AmI applications, and finally the background and the contributions of the work in this thesis.
- Chapter II is dedicated to a general presentation of both existing fall detection systems and sensing floors including the Inria Nancy sensing floor prototype. It is divided into three main sections:
 - Section 1 gives an overview of the existing fall detection systems,
 - Section 2 offers a panorama about sensing floors, and of the methods developed for person localization and tracking and ADLs recognition,
 - Section 3 presents the sensing floor prototype developed at Inria research center in Nancy Grand Est, which is used throughout this thesis.
- Chapter III presents the contributions of using the Inria Nancy sensing floor as PAL system that provides elderly localization and tracking, ADLs recognition, and automatic fall detection. It is also divided into three main sections:
 - Section 1 introduces a new technique for scanning the pressure distributions on tiles that are used to locate and track people, recognize their main ADLs and the transitions between them,
 - Section 2 presents the methodology of accelerometer data collection, features extraction, features selection, signal changing detection, and classification methods that are used to detect falling cases,
 - Section 3 presents the merging between the load pressure sensors results and the accelerometers results to provide more accuracy in ADLs recognition and fall detection.
- Chapter IV presents the application of an informational framework for a fault-tolerant PLS using multi-sensors data fusion with fault detection and exclusion algorithm.

- Chapter V provides a general conclusion together with perspectives for future researches.

I.12 Key contributions of this thesis

This thesis provides several contributions, which consist in a general overview of the existing fall detection systems and sensing floors. Moreover, we develop new techniques, some inspired from the field of signal processing and computer vision, for user perceiving, ADLs recognition and fall detection using a user-friendly and non-intrusive sensing floor. Another main contribution of this work consists in PLS using an informational framework. We use in this part the informational form of a Kalman Filter (KF) called Information Filter (IF) for a distributed information fusion architecture, and a Fault Detection and Exclusion (FDE) method to ensure the system reliability.

More precisely, the contributions of the work in this thesis are:

- A general overview of the existing fall detection systems (Chapter II, Section 1) and the sensing floors (Chapter II, Section 2),
- An algorithm for elderly localization and ADLs recognition using simple load pressure sensors (Chapter III, Section 1),
- A new Filter method for selecting pertinent features that discriminate between falling and non-falling states, as well as a method to detect the signal changing when a person falls down (Chapter III, Section 2),
- A technic to enhance ADLs recognition and fall detection accuracy results using fusion between load pressure sensors and accelerometers decisions (Chapter III, Section 3),
- Developing a method able simultaneously to localize people in addition to detecting and excluding the faulty sensors and erroneous measurements (Chapter IV),
- Detecting and isolating the sensors defaults through a distributed architecture (Chapter IV),
- Using an informational metrics in the synthesis of a residual test based on the Kullback-Leibler Divergence (KLD) (Chapter IV).

I.13 Publication list

This thesis contains parts that have been published in international journals, or presented at international conferences, as well as extracts from yet unpublished, ongoing work.

Journal articles

- M. Daher, M. El Badaoui El Najjar, A. Diab, M. Khalil, and F. Charpillet. "Elder Tracking and Fall Detection System using Smart Tiles". *IEEE Sensors Journal*, vol. PP 99 (2016): 1-1.
- M. Daher, M. El Badaoui El Najjar, A. Diab, M. Khalil, and F. Charpillet. " Automatic Fall Detection System using Sensing Floors". *Int. J. Comput. Inform. Sci* 12 (2016): 75.

Conference articles

- M. Daher, M. El Badaoui El Najjar, A. Diab, M. Khalil, and F. Charpillet. "Towards a usable and an efficient elder fall detection system". In *Advances in Biomedical Engineering (ICABME), 2015 International Conference on*, pp. 93-96. IEEE, 2015.
- M. Daher, A. Dib, M. El Badaoui El Najjar, A. Diab, M. Khalil, and F. Charpillet. "Ambient Assistive Living System Using RGB-D Camera". Accepted to be published in *Advances in Biomedical Engineering (ICABME), 2017 International Conference*. IEEE, 2017.

Papers in preparation

- M. Daher, J. Al Hage, M. El Badaoui El Najjar, A. Diab, M. Khalil, and F. Charpillet. "High Integrity Personal Localization System Based on Informational Formalism".
- M. Daher, M. El Badaoui El Najjar, A. Diab, M. Khalil, and F. Charpillet. "Ambient Assistive Living System for Elderly In-home Staying".

Chapter II - Fall detection systems and sensing floors: existing prototypes and related works

Overview

This chapter contains a general presentation of both existing fall detection systems and sensing floors including performance and accuracy evaluations. The Inria Nancy smart apartment and its sensing floor prototype have been also presented as a research center favoring such systems.

The chapter is divided into three main sections and a general conclusion of the chapter.

- Section 1 gives an overview of the existing fall detection systems,
- Section 2 offers a panorama about sensing floors and the methods developed for user localization and tracking as well as for ADLs recognition,
- Section 3 presents the sensing floor prototype developed at Inria Research Center in Nancy Grand Est, which is used throughout this thesis,
- General conclusion recapitulates all the three previous sections, and shows the importance and the necessity of this work.

Section 1: Fall detection systems

II.1.1 Introduction

According to nihseniorhealth.gov (a website for older adults), falling represents a great threat as people get older, and providing mechanisms to detect and prevent falls is critical to improve people's lives. Over 1.6 million U.S. adults are treated for fall-related injuries in emergency rooms every year suffering fractures, loss of independence, and even death.

Using pervasive technology to help and enhance elderly people living alone at home has become an emerging research area in AmI. Consequently, there has been significant interest in fall detection (FD) and fall prevention (FP) both from a research and commercial perspective for decades. Many approaches have been taken technologically towards falls detection with varying degrees of accuracy. A large number of efforts have been made to monitor not only falls, but also to generally monitor daily activities, and then to prevent falls accordingly. The "Figure 2.1" shows the interest on fall detection from 2002 to 2012.

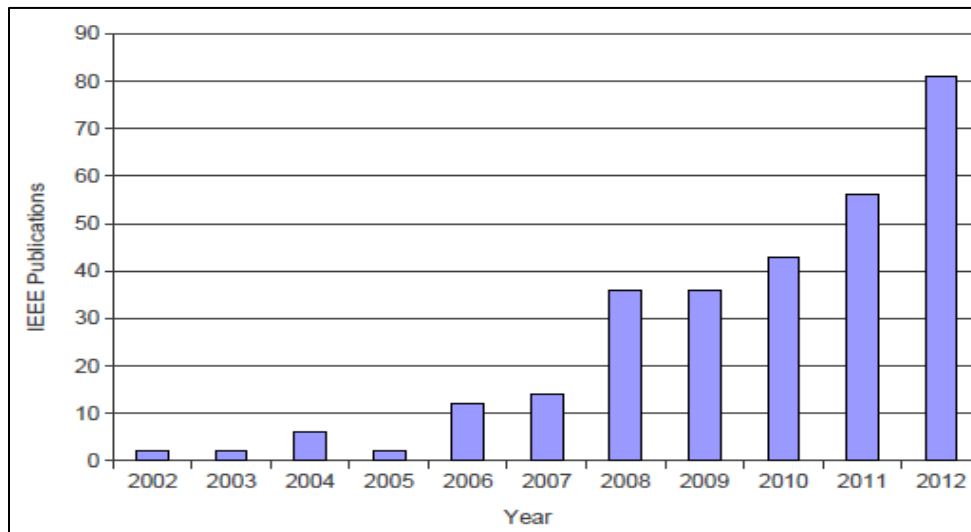


Figure 2.1 - Interest on fall detection.

However, there still isn't a 100% reliable algorithm that catches all falls with no false alarms. Also there are difficulties in properly defining people's daily living pattern without intrusiveness and privacy invasion.

This section presents a detailed review of research work achieved in FD systems as part of AmI systems, including qualitative comparisons among various studies and the different types of

sensors. This review aims to highlight the various solutions proposed for tackling the problem of fall detection from different perspectives.

II.1.2 Fall detection system framework

There have been a lot of fall detection techniques proposed since the early 1990s. It can be said that most fall detection systems runs on the same mechanism. The “Figure 2.2” shows the general framework of a fall detection system [39].

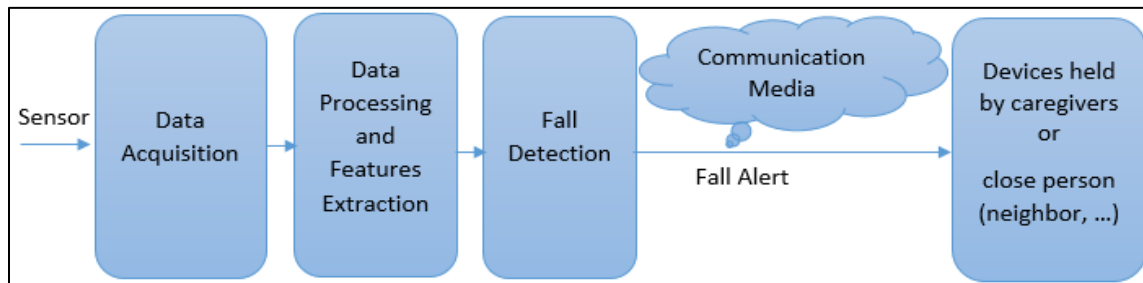


Figure 2.2 - General framework of a fall detection system.

From the research made through the fall detection systems that consist of prototype system, approaches or proposals, it can be categorized into three main categories. The first category of fall detection system involves wearable devices. The next category is fall detection involving ambient analyzer. The last category of fall detection involves motion detection (camera-based). Each system has its own working methodology that has pros and cons regarding the usability, accuracy, privacy, etc. The “Figure 2.3” shows the three categories of fall detection systems.

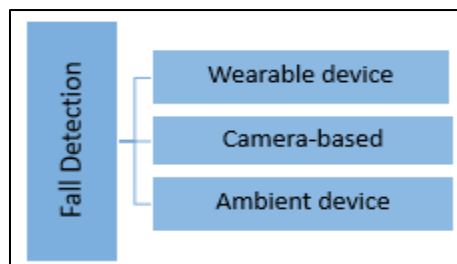


Figure 2.3 - Categories of fall detection systems.

II.1.2.1 Wearable sensors

Wearable sensors are electronic devices that are worn by (or implanted in) a person, which are designed to collect biomedical, physiological and activity data [40]. These sensors are typically cheap and small in size making them an attractive solution to low-budget projects. They can be

worn on different parts of the body or can be embedded in other devices such as watches, shoes, belts, etc. The main disadvantage of wearable sensors is their high level of obtrusiveness.

Accelerometers are a type of wearable sensors that are widely used in fall detection systems that use threshold-based algorithms to detect fall-related events. A threshold is a limit that when surpassed generates an action in the system (e.g., a fall is detected—caregiver is informed). The most common threshold used with the accelerometer data is the sum vector magnitude of acceleration and the rotation angle information [41]. When a real fall happens, collision between human's body and ground will produce obvious peak value at the acceleration sum “**a**” which has magnitude given by the Equation (2.1).

$$a = \sqrt{a_x^2 + a_y^2 + a_z^2} \quad (2.1)$$

Where a_x , a_y , and a_z present accelerometer measurements of three axes. The system uses the acceleration sum as the first step to distinguish high intensity movements from others. But normal motions such as jumping or sitting also produce peak values, which mean that additional detection features are required.

The second feature used here is an angle calculated based on acceleration measurements. As human's motion has low acceleration, it is feasible to get gravity component in each axis by using a low pass filter. If gravity components could be separated before and after human's fall, then it is possible to calculate the rotation angle of accelerometer coordinate in 3D space, which is also equivalent to the rotation angle of gravity vector relative to fixed coordinate [42]. Coordinate constructed by the accelerometer and the gravity vector is shown in the “Figure 2.4”. The rotation of gravity vector in fixed coordinate is shown in the “Figure 2.5”.

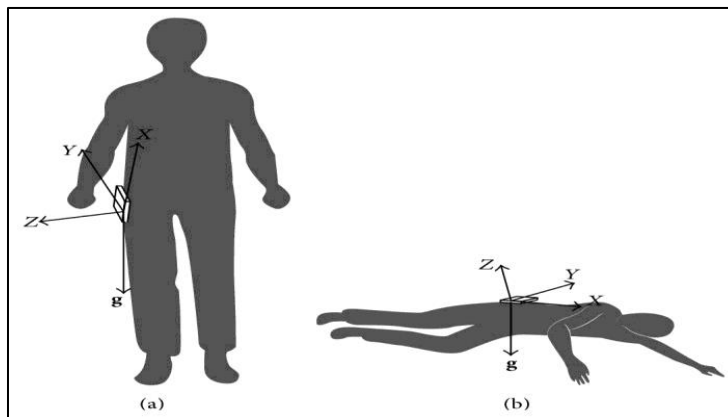


Figure 2.4 - Coordinate and gravity before and after falling. (a) Before falling. (b) After falling.

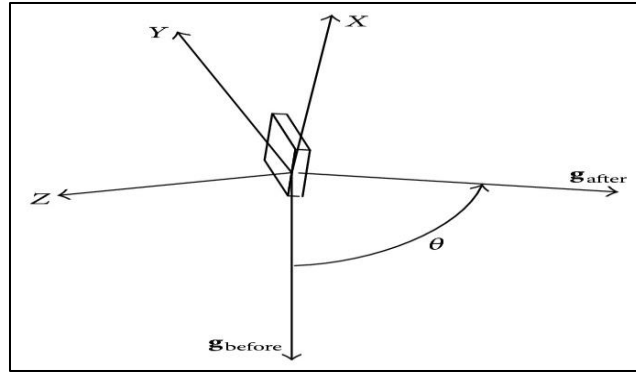


Figure 2.5 - Rotation of gravity relative to fixed coordinate.

II.1.2.2 Camera-Based sensing

In the past 10 years, there have been great advances in computer vision and video cameras. It opens up a new branch of methods for fall detection. Indeed, the posture and shape of the faller change drastically in fractions of seconds during a fall [43]. These rapid changes are used to determine if a fall happened. Camera-based systems benefit from these patterns by monitoring the subject's posture and shape during and after a fall. They use different approaches to detect falls such as monitoring human skeleton. They are robust solutions but their computational cost is unattractive for real time applications. Others systems that are based on simpler features (e.g., the falling angle, vertical projection histogram) are not computationally intensive as the human skeleton based systems but they suffer from a high false alarm rate [44,45].

Privacy issues are one of the biggest worries for camera-based systems, and few solutions to alleviate this problem are known such as sending subjects' images when an alarm is triggered only. Other possible solutions use deep and infrared cameras [46,47].

II.1.2.3 Ambient sensing

Ambient sensors are installed in or around the house, appliances and furniture, which are designed to collect different types of data, providing information on the patient's environment and activities.

Pressure sensors are often used because of their non-obtrusiveness and their low cost. The fundamental principle is that the pressure changes regarding the distance between the user and the sensor; the closer the user is to the sensor the higher the pressure is. The low fall detection accuracy (below 90%) is the main disadvantage of these sensors [41].

The rest of this section summarizes the proposed fall detection approaches, the contributions, and the drawbacks/challenges for each research work surveyed in this review.

II.1.3 System evaluation

The results showing the evaluation of a system are usually stored in an (2x2) array known as confusion matrix (see Figure 2.6).

		prediction outcome		total
		<i>p</i>	<i>n</i>	
actual value	<i>p'</i>	True Positive	False Negative	<i>P'</i>
	<i>n'</i>	False Positive	True Negative	<i>N'</i>
total		<i>P</i>	<i>N</i>	

Figure 2.6. Confusion matrix example.

- True Positives (TP): number of positive instances that were classified as positive.
- True Negatives (TN): number of negative instances that were classified as negative.
- False Positives (FP): number of negative instances that were classified as positive.
- False Negatives (FN): number of positive instances that were classified as negative.

Many performance indicators are used to evaluate the efficiency in classification problems such as:

- Accuracy: is the number of correctly classified instances over the number of all instances. It is the most widely used, and it is defined as follows:

$$Accuracy = \frac{TP + TN}{TP + TN + FP + FN} \times 100\% \quad (2.2)$$

- Sensitivity (or recall): is the number of the correctly classified positive instances over the number of all positive instances, and it is defined as follows:

$$Sensitivity = \frac{TP}{TP + FN} \times 100\% \quad (2.3)$$

- Precision: is the number of the correctly classified positive instances over the number of positive predicted instances, and it is defined as follows:

$$Precision = \frac{TP}{TP + FP} \times 100\% \quad (2.4)$$

II.1.4 Existing prototypes

The first fall monitoring system was developed in the early 1970s. It requires the user intervention by pressing a remote transmitter button to send out an alert message to caregivers [48]. On the other hand, automatic fall monitoring research has been conducted since 1990s. The most relevant studies on fall detection systems are described next.

Bilgin et al.

This system was talented to detect falls using a data mining approach [49]. It only employs the accelerometer placed on the waist of the subject, and it is only capable of detecting a fall when a person is standing. It uses a k-NN approach to detect if a fall has occurred. The acquired results show an accuracy of 89.4% with a recall of 100%.

Ozcan et al.

The proposed project aims to create an autonomous system that is able to provide quick and accurate real-time responses to critical events like a fall, while preserving computational resources [50]. Besides its ability to detect falls, the system also classifies non-critical events such as sitting and lying down. It uses a Microsoft LifeCam camera mounted on the center of the elder's pelvis that captures images. When a fall occurs edge orientations in a frame vary drastically and extremely fast, as a result of this subsequent frames get distorted. A dissimilarity distance is computed between two frames, and if it is greater than a predefined threshold a fall is detected. The lack of auto exposure adjustment in the camera was the most drawback of the system. False alarms may be raised if the scenery changes.

Bashir et al.

The proposed system is based on a wireless body area network that uses a tri-axial accelerometer, and a tri-axial gyroscope embedded in a necklace-like sensor [51]. Three stages are used to determine human status namely, fall, activity, and sleep. The information is sent to a base station that receives and stores the data. The system uses simple threshold-based algorithms that employs the posture angle, angular velocity, and acceleration to detect fall events. The experiments' results show an accuracy of 100% for ADLs, while the overall recall was 81.6%.

SmartFall

SmartFall is an automatic fall detection system built on top of the SmartCane [52]. The goal of this system is to automatically alert the caregivers or emergency service when the cane user falls. SmartFall is the first fall detection system in its class that employs subsequence matching algorithm, instead of the commonly used thresholding-based method. The sensors onboard the SmartCane system includes a tri- axial accelerometer, three signal-axis gyroscopes, and two pressure sensors. The results have indicated that the algorithm is able to detect almost all cases of falling in the experiment while achieving extremely low false-positive rates for most non-falling activities.

Almeida et al.

In 2007, Almeida et al. presented a walking stick with a gyroscope embedded at its base for detecting fall and measuring walking pace [53]. A fall was detected based on the magnitude of the resultant angular velocity along sideward and forward axes. The pace was derived from the summation of angular velocity between two adjacent peaks divided by the time interval between the two peaks. Warnings were given when a user walks faster than his/her normal speed.

eHome

Werner et al. created in 2011 a prototype named eHome representing an ambient assisted living system (AAL) that prospers for giving elderly the feeling of security in their homes [54]. The system provides a home user with a set of non-intrusive wireless sensors to collect elder behavioral data when faced to a life-threatening situation such as a fall. The system uses floor-mounted accelerometers to collect vibration patterns of an individual that are sent wirelessly to a base station. The fall detection process is based on the belief that distinctive impact vibrations. A threshold is used to identify if a fall event occurred based on the vibrations levels that propagate through the floor. In such case, the user is asked if he/she is ok or not. Care givers are notified by alarm triggering when the user does not respond within a predefined period. The recall and specificity in the experiments were 87% and 97%, respectively.

Sengto et al.

In 2012, Sengto et al. proposed a fall detection system algorithm based on a back propagation neural network (BPNN) that utilizes a tri-axial accelerometer mounted on the user's waist [55].

ADLs are divided in three groups: falling activities, slow motion activities (walking, getting up from bed, flopping), and sudden motion activities (running, jumping). An acceleration threshold is set to distinguish between slow motion activities and other activities. Falling and sudden motion have similar acceleration signal patterns. Therefore, Falls are detected if the threshold is surpassed a BPNN. The system specificity was 99.5%, while the overall recall was 96.25%.

Chen et al.

Chen et al. introduce a human fall detection system using a computer vision approach that detects fall events in real time using skeleton features and human shape variations [56]. The system is able to extract the human posture using a 2D model. The human contour is partitioned into triangular meshes by using the constrained Delaunay triangulation algorithm. The skeleton (a spanning tree) is acquired by running the well-known graph traversal algorithm Depth-first search (DFS) on the center of the triangular meshes. A distance map is used to calculate the distance between two skeletons. If the user's motion does not change within a certain period of time, a fall is detected. The system accuracy was 90.9% while maintaining a low false alarm rate.

Sorvala et al.

Sorvala et al. developed a fall detection algorithm that aims to reduce false alarms that represent a major problem for caregivers using two thresholds [57]. The system uses a tri-axial accelerometer, a tri-axial gyroscope (both mounted on the pelvis of the patient), and an ankle-worn tri-axial accelerometer. The solution distinguishes from falls, possible falls (where the subject gets up within a ten seconds after the detected impact), and ADLs. An impact is determined when the total sum vector magnitudes of both the acceleration and angular velocity exceeds their fixed thresholds. If the subject does not recover within the specified time an alarm will be sent to a predefined person (nurse, doctor, relative). The sensitivity of the algorithm is 95.6% and the specificity is 99.6%.

Humenberger et al.

Humenberger et al. proposed in 2012 a bio-inspired stereo vision fall detection system. It uses two optical detector chips, a digital signal processor (DSP), a field-programmable gate array (FPGA), and a wireless communication module [58,59]. The optical chips capture video frames. The FPGA creates the input data for the DSP by calculating 3D representations of the environment.

The DSP is loaded with a neural network that is used for classification purposes. Falls are divided into 4 states or phases pre-fall, critical, post-fall, and recovery phase. The system was mounted on the top corners of a room in order to monitor the subjects. The acquired results show 90% accuracy of fall detection.

Chen et al.

A wireless fall detector system using accelerometers was introduced by Chen et al. [60]. It consists of two modules that communicate with each other through wireless communication. The first module is a fall detection terminal that employs an inertial sensor (an accelerometer), a microcontroller and wireless SoC (System on Chip), and the second is a remote terminal that used to receive and store kinematic characteristics and raise alarms. The system uses a threshold-based algorithm to detect falls. Five tests were performed: forward fall (FF), backward fall (BF), left-side fall (LF), right-side fall (RF), and ADLs. The overall recall was 97% while the specificity was 100%.

Yuwono et al.

Yuwono et al. proposed a system a fall detection system using 3D accelerometer mounted on the user's waist that collect data and send it to a receiver board [61]. If the acceleration magnitude surpasses a predefined threshold the input signal is fed into a multilayer perceptron (MLP) neural network and an augmented radial basis function neural network (ARBFNN) to detect falls. A discrete wavelet transform (DWT) is employed to filter the acceleration signal and reduce the sampling signal rate; decreasing complexity and improving classifier generalization. The results of the experiment yield a recall of 97.65% and an ADL specificity of 99.33%.

SAFE

A fall detection system using wearable sensors was introduced by Ojetola et al. in 2011 [62]. The system uses a wireless sensor platform known as SHIMMER (Sensing Health with Intelligence, Modularity, Mobility and Experimental Reusability) [63]. The system utilizes two SHIMMER nodes: one in the chest and the other one in the subject's right thigh. Every node is equipped with a tri-axial accelerometer and tri-axial gyroscope, a Bluetooth device and a microcontroller device. The acceleration and angular velocity magnitudes were calculated to be

used as input features for a decision tree. Falls and ADLs were identified with a precision of up to 81% and recall of 92%. The accuracy ranged from 98.5% to 99.45%.

Shoaib et al.

In 2010, Shoaib et al. proposed a context-based method that exploits computer vision techniques in order to build a context model for detecting falls based on the position of the head from the floor [64]. The head location, the feet location, and the vertical distance of the head from the head centroid mean are used to detect a fall. A combination of ellipse matching and skin color matching is used to detect the head of the subject in a video clip frames that are divided into three blocks, namely head, floor and neutral blocks. Once the head has been located, the feet area is found using the medial axis. Six fall types are considered, backward, forward, lateral (right and left), syncope (fainting) and neutral. The reported system accuracy was 96% after was tested using twenty six video clips recorded in real home environments.

Amandine et al. (Inria Nancy - Grand East)

In 2014, Amandine et al. propose a simple system based on the Microsoft RGB-Depth Camera to promote home support for the elderly [65]. It is based on the analysis of the parameters extracted from the depth of images provided by the camera (the center of the mass of the person and the vertical distribution of the points of the silhouette). From these indicators, it is possible to secure a person's environment by detecting falls and dangerous behavior, and assess elder degree of fragility by analyzing the gait progress and activities.

Recently, fall detection based on tri-axial accelerometers embedded in smart phones has become increasingly popular. The advantage of using a smart phone for fall detection is that it can also be used to send out warning messages and/or track the location of a faller.

PerFallID

In 2010, Dai et al. introduced a fall detection system named PerFallID using android-based smartphone [66]. It takes advantage of the communication technologies embedded in a smartphone and the sensors (e.g., accelerometer, gyroscope, etc.) to detect falls and send alerts automatically when a patient is not responsive within a pre-specified time after a fall. The acceleration and angular data are used to set thresholds that determine if a fall has occurred. PerFallID represents a user-friendly fall detection system for elderly.

iFall

Another Android Application for smartphone-based using tri-axial accelerometer to detect falls is iFall (Android Application for Fall Monitoring and Response) [67], which is available at Google Play Store. Data from the accelerometer is evaluated with several adaptive threshold based algorithms and position data to determine a fall. The theoretical basis for the employed detection algorithm is similar to those of PerFallD, as the utilized algorithm is also grounded on the same acceleration threshold technique. Unlike PerFallD, the fall detection criterion considered by iFall uniquely depends on the global acceleration.

uCare

In 2012, Shi et al. proposed a fall detection system based on an android-based smartphone named uCare [68]. It detects fall events using the acceleration data from the phone's accelerometer. A threshold is used to trigger five states (normal, unstable, free fall, adjustment, and motionless). Normal refers to ADLs, unstable is related with the moment prior the fall, free fall is experimented when falling, adjustment deals with the impact of the fall, and motionless is the period of time after the fall when the subject is not moving. The data collection and experiments were conducted in a lab environment using a Google Nexus S phone and MATLAB. The precision obtained on the conducted experiments was 95.7% and the recall was 90%.

Wu and Tsai

In 2014, Wu and Tsai proposed a system which utilizing mobile phones as a detector to detect the falling [69]. The proposed system is composed of a server (computer that calculate the value of accelerometers) and a client (mobile phone containing 3 tri-axial accelerometers). The data of the 3 tri-axial accelerometers are converted to Sum Vector Magnitude (SVM) and transformed with the GPS location of the mobile phone to server that judges the falling case or not based on an adaptive threshold including height, weight and gender. An automatic text message will be send to caregivers and an alarm sound will trigger from the mobile phone alerting a fall event. Experimental results show that this method can detect the falls effectively.

Fall Detect

In 2014, Aguiar et al. proposed a smartphone-based fall detection named "Fall Detect" with the purposes to identify risky fall events and consequently alert emergency contacts when the user

does not recover [70]. The fall detection algorithm developed continuously screens the data from the smartphone built-in accelerometer when the phone is in the user's belt or pocket. Upon the detection of a fall event, the user's location is tracked and SMS and email notifications are sent to a set of contacts. The accuracy of the fall detection algorithm proposed was 97.5%.

II.1.5 Commercially available fall detection systems

There exist several fall detection products currently available in the market. Most of them are wearable devices with ease-of-use designs. The most common device placement position is the waist, but some devices are designed to be placed on the wrist, or around the neck. Most products use an acceleration sensor and lithium battery, which has a maximum lifetime of up to 2 years. They usually come with an alarm button allowing a manual call for help when a fall is not automatically detected.

Some fall detection systems are already commercially available today. Products like the *Vigi'Fall* [71], FATE [72], SensorBand [73], VitalBase [74], and others are being commercialized by companies mainly for the senior care industry.

Vigi'Fall

Vigi'Fall was created in collaboration of VIGILIO TeleMedical Company with Pr. Norbert Noury (INL Lyon), and it came on the market in November 2012 [71]. It is the first domotized fall detector maintained directly on the human body via a patch that can be worn by the user in a non-intrusive, permanent manner. The *Vigi'Fall* is based on a sensor system. A biosensor is worn by the user that gives the person's movements and the cardiac rhythm, while a number of other sensors are wirelessly attached to walls around the home. If the user suffers a fall, in addition to the fall signal emitted by the biosensor, the wall-mounted sensors detect the absence of movement and wirelessly relay a signal to a central control box, also located within the home. The system send the person's movements and the cardiac rhythm to a monitoring box (see Figure 2.7). The control box connects automatically, via telephone, to a nurse or to a call center if the fall occurs in the user's own home. In order to distinguish between real falls and false alarms, the device is equipped with data-fusion software which allows it to analyze the nature of the fall (with or without impact) and the resulting posture of the patient. *Vigi'Fall* has been successfully tested and the trials

demonstrated a 90% successful detection in real-world environments with false alarms practically eliminated.



Figure 2.7 – The Vigi'Fall system.

FATE

The European Commission and the Competitiveness Innovation framework Program (CIP) support the project named FALL DeTECTOR for the Elderly (FATE) with the main objective of fall detection and prevention [72]. FATE has been designed to be comfortable to wear, easy to use, and non-invasive. It was deployed in June 2015 with the focus on improving the elder's quality of life by an accurate detection of falls in ageing people, both at home and outdoors. This has been done by implementing an accurate, portable and usable fall detector incorporating accelerometer that runs a complex and specific algorithm to accurately detect falls, and a robust and reliable telecommunications layer based in ZigBee and Bluetooth technologies, capable of sending alarms when the user is both inside and outside the home. The system is complemented by secondary elements such as a bed presence sensor or the i-Walker, an intelligent robotic walker, with the entire system ensuring successful prevention and detection of falls in all circumstances.

II.1.6 Conclusion

This section presents a detailed review of research work achieved in the fall detection systems domain. Different approaches are thoroughly reviewed and qualitatively compared regarding the performance and the precision. Also, the most important aspects that need to be considered when designing FD systems are described (obtrusiveness, occlusion, multiple people in the scene, privacy, computational cost, energy consumption, noise, etc.).

However, all fall detection and prevention systems relying on only one data provider (movement-sensor, camera, accelerometer, etc.) have their own limitations and do not ensure

100% reliability [75]. Additionally, there still is a lack in experience and systematic knowledge to intelligently assemble the components into a robust, user-friendly and effective system, making no false alarm and detecting each fall case, without affecting elderly daily living patterns [76].

Multi-sensors data fusion is the area focusing on creating multi-modal systems, which receive data from several providers and perform correlation or fusion upon it in order to increase the accuracy and reliability of the proposed systems. Moreover, a combination of movement sensors and signal-processing technologies can provide more accurate and precise fall detection and prevention approaches.

Section 2: Sensing floors

II.2.1 Introduction

Sensing floors are floors equipped with sensors for various ambient intelligence applications, like human tracking, ADLs recognition, perception of the environment, e-health, etc. They offer many advantages in terms of privacy, perception and non-intrusive for users. They could also provide many useful parameters extracted from human ADL (velocity of walking, stride length and cadence, number and type of interactions with objects, etc.). These parameters serve as medical indicators of the state of human gait that can serve for both fall detection and fall prevention systems. Two types of a sensing floor were identified: modular floors (e.g. tiled floors), and monolithic sensors (e.g. carpets). The installation of monolithic sensors is quick, as they have to be simply unrolled onto the floor and plugged. In comparison, the installation of modular floors is more complex, as each component needs to be installed and connected separately. On the other hand, modular floors offer many advantages concerning the maintenance part: module breakdowns can be easily localized to be replaced or fixed. Regarding sensing capabilities, the smaller the floor tiles are, the higher is the sensing resolution, and the better is the segmentation of objects on the floor.

Different projects using the sensing floors in ambient intelligence contexts since 1990, for instance, the Oracle Research Laboratory (ORL) Active Floor by Addlesee et al. [77], the MagicCarpet by Paradiso et al. [78], the LiteFoot by Fernstrom and Griffith [79] and the Smart floor by Orr and Abowd [80]. These floors provided information for reasoning about the observed space, and were later on integrated into smart environments, aimed at delivering assistance services to users. These smart environments also integrated assistive robotic technologies with sensing networks like the Gator Tech Smart House made by the University of Florida [81], the Aware Home introduced by the Georgia Institute of Technology [82], the RoboticRoom system developed by the University of Tokyo [83,84], and the ActiSen activity-aware sensor network jointly developed by researchers from several US universities [85]. Additional improvements were brought by research on human footprint biometrics [86,87], which allowed sensing floors to identify humans by extracting features from human gait and footprints.

This following section shows an overview of existing floor prototypes, their strengths, weaknesses and their practical applications.

II.2.2 Existing prototypes

In this section, we present the prevailing sensing floor prototypes in chronological order, subdividing them into monolithic and modular prototypes with the capacity to measure the intensity of the applied pressure. We also present the floors on which more advanced applications have been developed, such as multi-target tracking and human recognition, together with the features they extract and the methods they employ for human and object recognition.

II.2.2.1 Monolithic pressure-sensing floors

MagicCarpet

In 1997, Atlantic Paradiso et al. developed the MagicCarpet, a pressure-sensing floor that detect human's footsteps in terms of position and impact force as an interface for a musical instrument [78]. It uses a pair of Doppler radars to measure upper-body kinematics (velocity, direction of motion, amount of motion) and a grid of piezoelectric wires. The MagicCarpet is rectangular, (3m x 1.8m) and is easy to transport as it can be rolled up like a normal carpet.

LiteFoot

In 1998, Fernstrom and Griffish developed the LiteFoot, a floor slab with embedded sensors that detected human's foot movements. The system is based on infrared optical proximity sensors placed approximately 40mm apart in a grid in a floor space (2m x 2m) to detect objects [79]. LiteFoot is a rigid floor slab weighting around 100 kg, so it is not easily transportable.

Schmidt et al.

In 2002, Schmidt et al. developed a monolithic pressure-sensing surface [88], (2.4m x 1.8m) in size, mounted on 4 load cells located in the corners (see Figure 2.8). The system permits to locate and track a single person in the environment, identify the addition and removal of single objects from the scene, as well as recognize when objects were being knocked over.

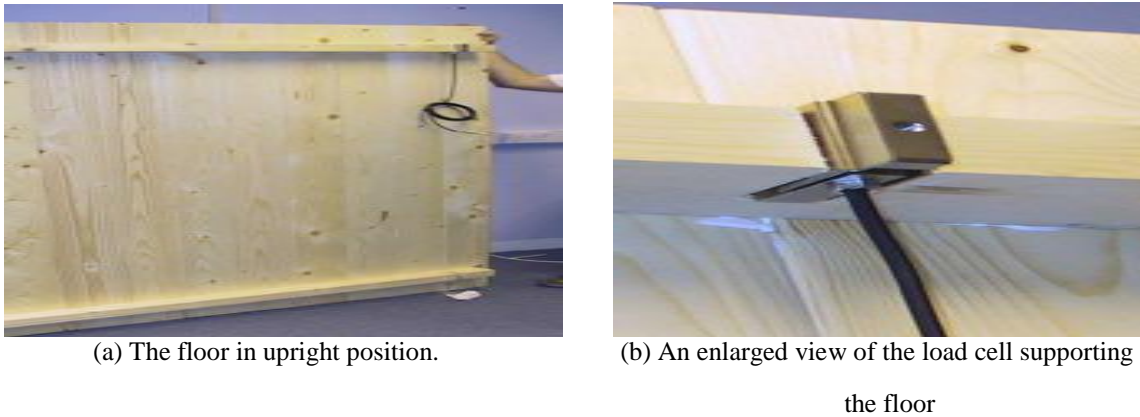


Figure 2.8 – The monolithic sensing floor presented by Schmidt et al.

Alwan et al.

In 2006, Alwan et al. designed a fall detection system based on floor vibration using a piezoelectric sensor [89]. The performance of the detector is evaluated by conducting controlled laboratory tests using anthropomorphic dummies. The results showed 100% fall detection rate with minimum potential for false alarms.

Glaser et al.

The developed system is a textile-based large-area sensor network, integrated into a carpet of size (2.4m x 2m). Flexible textile-based conductive material (Microprocessor modules integrated into a fabric with interwoven silver-plated copper wires) is shaped into (15cm x 15cm) constructions (see Figure 2.9).



Figure 2.9 - The sensing carpet presented by Glaser et al.

This system is used for detecting footsteps and calculating user trajectories [90,91]. A light will be switched on automatically if a person presses the carpet. If a person falls down on the carpet and doesn't move for a time period, or the person didn't leave the bed for a certain time, then an emergency call will be activated. Such functionality would give elderly or handicapped persons a chance to live a self-determined life, without feeling abandoned. The “Figure 2.10” shows the sensor signals derived from the smart carpet with a person lying on the floor as depicted.

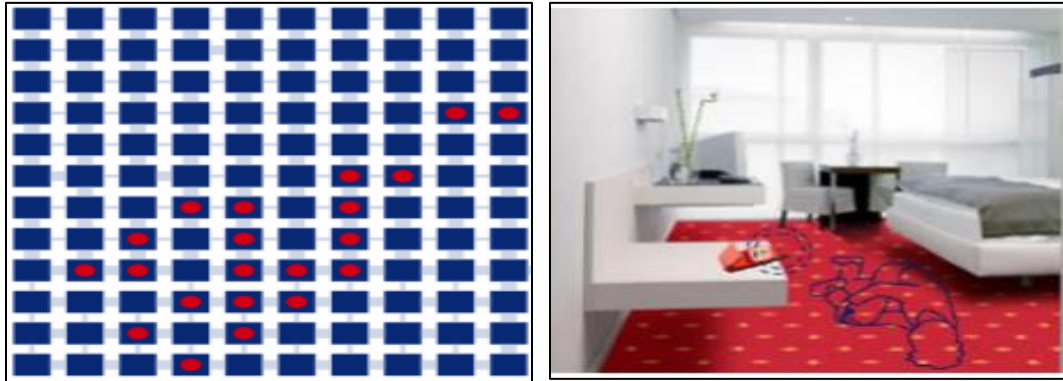


Figure 2.10 - Sensor signals (left) derived from a person that lies on the smart carpet prototype like depicted in the right picture.

Shen and Shin

Shen and Shin designed a sensing floor using an optical fiber sensor [92]. The system is based on Brillouin optical correlation domain analysis (BOCDA) to detect the strain deviation along a fiber caused by pressure events (see Figure 2.11). A 40m fiber was embedded between two layers of soft material, forming a sensing surface of size 1.6m by 4m. The floor was divided into 160 blocks, each of size (20cm x 20cm). The floor was able to detect and track human occupants by applying suitable data-processing algorithms. The success rate of location detection was 96%, and the estimation error for the weight of the occupant was ± 5 kg.

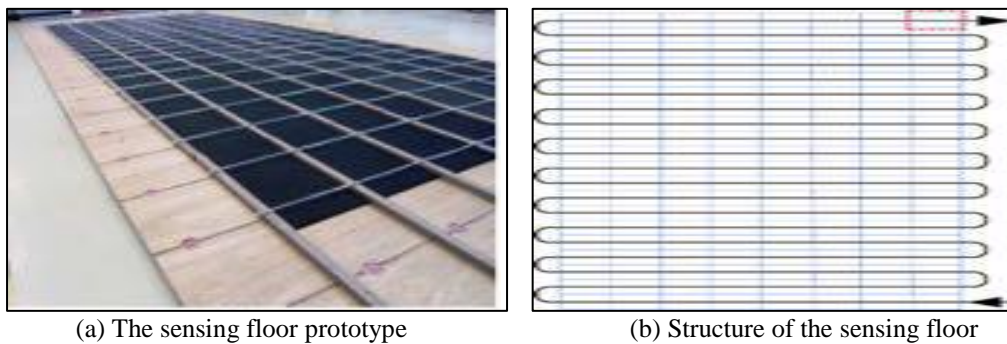


Figure 2.11 – The sensing floor which employs BOCDA technology.

II.2.2.2 Modular pressure-sensing floors

Reilly et al.

In 1991, Reilly et al. developed a clinical walkway for imaging foot placement with high resolution that is capable of sensing foot-to-ground contact for gait analysis. The system uses magnetostrictive delay lines that were originally developed for memory storage in early computers [93]. The prototype was a modular floor, consisting of panels 0.32m by 0.64m, assembled into a 2.5m by 0.64m walkway.

Morishita et al.

A modular floor sensor with high resolution, composed of 0.5m square tiles was proposed by Morishita et al. [94]. Each equipped with 4096 pressure switches in a 64x64 array, which provided about the presence or absence of load on them. The system allows obtaining sharp images of the surfaces in contact with the floor such as footprints or shoe and unconstrained measurement of the locations of humans, robots and objects.

Yun et al.

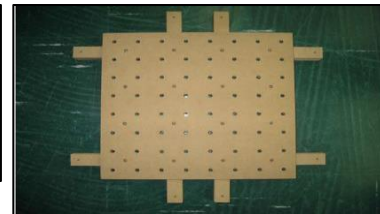
Yun et al. worked on several sensing floor prototypes. Their first prototype, the UbiFloorI [95] consisted of 144 ON/OFF switch sensors fitted onto a cushioned carpet, with a walking area of 3m by 1m (see Figure 2.12 (a)). The UbiFloorII [96] was a (12x2) array of wooden tiles, each measuring (30cm x 30cm) and each containing 64 uniformly distributed photo-interrupter sensors (see Figure 2.12 (b)). The system was used to identify users based on their stepping pattern (gait length, foot angle, heel strike time, etc.), while tracking the user's location with the ON/OFF switch sensors. The system can provide the natural interface since it does not require users to carry sensors and to pay attention to anything. Experimental results show that the proposed system can recognize the registered users at the rate of 92%.



(a) UbiFloorI, presented by Yun et al.



(b) The UbiFloorII presented by Yun et al. in [19,20]



(c) A close-up of a tile

Figure 2.12 – The UbiFloor series of prototypes presented by *Yun et al.*

Addlesee et al.

Addlesee et al. developed the ORL active floor, which is a modular sensing floor made of tiles with load cells in the corners. The tiles are (0.5m x 0.5m) in size, rigid, being made of 18mm thick plywood with a 3mm mild steel plate on top (see Figure 2.13). The system uses the Hidden Markov Models (HMMs) to classify the detected footstep traces, in order to recognize the walking persons [77].

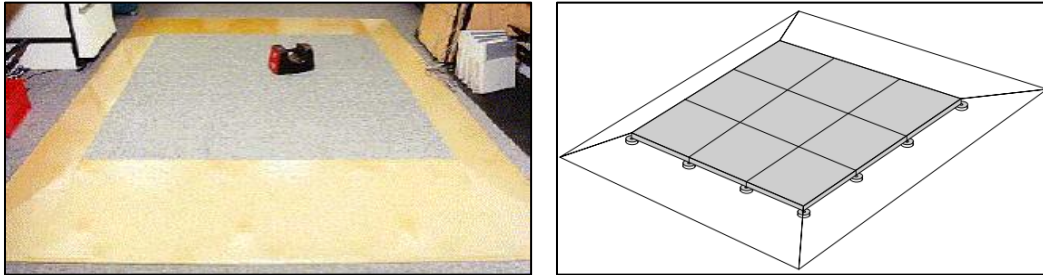


Figure 2.13 - Prototype Active Floor with test weight developed by Addlesee et al.

Pirttikangas et al.

Pirttikangas et al. designed a pressure-sensitive floor as part of a smart living room at the University of Oulu [97]. A 100 square meter floor was made of stripes of Electro Mechanical Film (EMFi) material (30 vertical and 34 horizontal stripes, each 30 cm wide), which make up a (30x34) matrix of cells of size (30 cm x 30 cm), with a sampling rate of 100Hz (see Figure 2.14). The system is used for the automatic human recognition using their gait pressure pattern and the discrete HMMs. The results are promising (78% overall success rate of footstep identification), but the problem of identification will be more difficult with several persons walking in the room at the same time.



Figure 2.14 – The sensing floor composed of EMFi stripes presented by Pirttikangas et al.

Gouwanda and Senanayake

Gouwanda and Senanayake present a real time force-sensing instrument that is designed for human gait analysis purposes [98]. The system uses force-sensing mat that contains 144 Force Sensing Resistors (FSR) which are distributed evenly over a 0.48m x 0.54m acrylic board (see Figure 2.15). It is capable of recording and monitoring ground reaction forces exerted by human foot during various activities such as walking, running and jumping in real time.

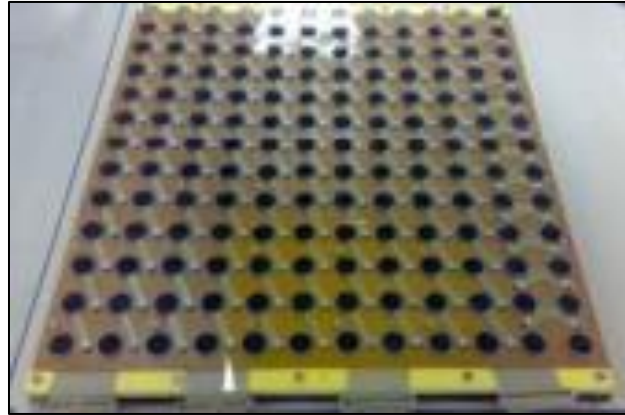


Figure 2.15 – The structure of the FSR floor presented by Gouwanda and Senanayake.

Richardson et al.

Richardson et al. developed a modular floor composed of a tessellation of interlocking tiles connected together to create a pressure-sensitive area of varying size and shape, giving it the potential to be integrated into an interactive environment [99]. The floor space uses an array of force-sensitive resistors on each node to detect pressure, and that pressure information is output by way of a self-organized network formed by the floor nodes (see Figure 2.16).



Figure 2.16 – Prototype tiles in a small Z-Tiles floorspace presented by Richardson et al.

Rangarajan et al.

In 2007, Rangarajan et al. developed floor consisting of 96 networked pressure-sensing mats, arranged in a rectangular matrix of (12x8), covering a surface of 16 m² nearly, and with a sampling frequency of 43Hz [100]. Each sensing mat is (0.48m x 0.43m) in size, and is embedded with 2016 FSRs (see Figure 2.17). The floor has a high sensing resolution that allows the direct detection of the heel and toes. The system was later used by Qian et al. [101,102] to identify humans based on their gait features.

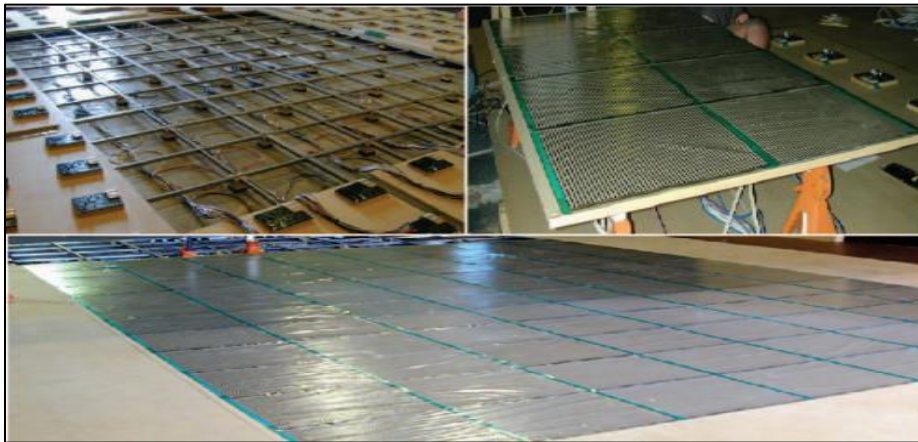


Figure 2.17 – The Sub-floor steel framework (top left), the surface floor wooden framework (top right), the complete view of AME Floor-III after assembly (bottom).

Liau et al.

In 2008, Wen-Hau et al. developed a floor containing 25 sensing tiles (60cm x 60cm) of size, with a spacing of 20 cm between neighboring tiles, and with a single load sensor under each tile [103]. This spacing left blanks in the sensing surface of the floor. To counter this, tracking of the inhabitants was performed using an algorithm called Probability Data Association (PDA), which is based on the Kalman filter. The system was able to track humans with a [0-28] cm error between their estimated and real location, also it cannot differentiate different persons having close weight.

Bose and Helal

Bose and Helal presented a tiled floor for detecting humans and analyzing their gait [104], developed for the Gator Tech Smart House [81]. The floor had piezoelectric force sensors embedded under the tiles and attached to their central support (see Figure 2.18).

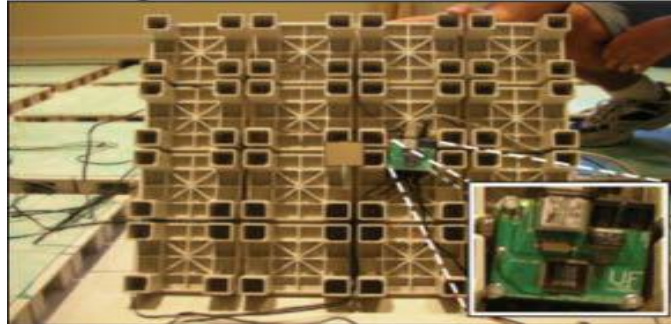


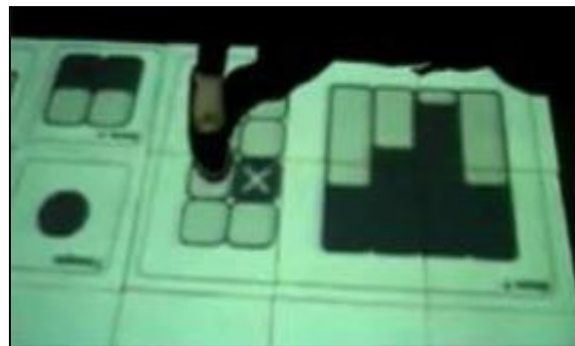
Figure 2.18 – The pressure-sensing tile presented by Bose and Helal.

Rajalingham et al.

A tiled load-sensing floor that acts as a human-computer interface was developed by Rajalingham et al. where an image of the interface is overlaid on the floor, on which users can press virtual buttons with their feet (see Figure 2.19). The floor was composed of 36 tiles, each (0.3m x 0.3m) in size, equipped by 4 force-sensing resistor (FSR) sensors in the corners of the tile and by vibro-tactile actuators beneath the plate, which could provide feedback to the users. The system was used for three dimensions human posture tracking using Bayesian filters [105].



(a) The floor pressure-sensing interface.



(b) A user interacting with floor-based interface widgets.

Figure 2.19 – The sensing floor presented by Visell et al.

Rimminen et al.

In 2010, Rimminen et al. presented the use of near-field imaging floor sensors for fall detection [106]. Fall classification was performed using a two-state Markov chain and pose estimation based on Bayesian filtering.

Tzeng et al.

Tzeng et al. used a floor pressure sensor for detecting high impact on the floor and an infrared camera to identify subject's actions [107].

Lombardi et al.

Lombardi et al. developed a (0.6m x 0.6m x 4.5mm) tiled sensing floor, where each tile contains sensing stripes [108] (see Figure 2.20). The system uses Randomized Tree classifiers to discriminate between the presence of an object and a human on a tile, as well as between human postures (standing, walking, jumping, lying), based on the matrix of pressures sensed by the tile, the mean pressure value and its variance over a temporal interval, and the barycenter's movement.



(a) The installed floor prototype

(b) The contact-sensing stripes

Figure 2.20 – The sensing floor presented by Lombardi et al. in [85].

Smartfloor

In 2014, Heller et al. developed the Smartfloor, a modular sensing floor consisting of 36 interconnected force-sensing wooden tiles (0.5m x 0.5m) [109], with strain gauge single axis load cells in each of the 4 corners (see Figure 2.21). A short throw projector was used to project a visual interface on the surface of the floor. The system was used basically to study and train the dynamic balance of athletes. Interactive applications were also developed to fight child obesity, and to help rehabilitate elderly people for preventing falls.

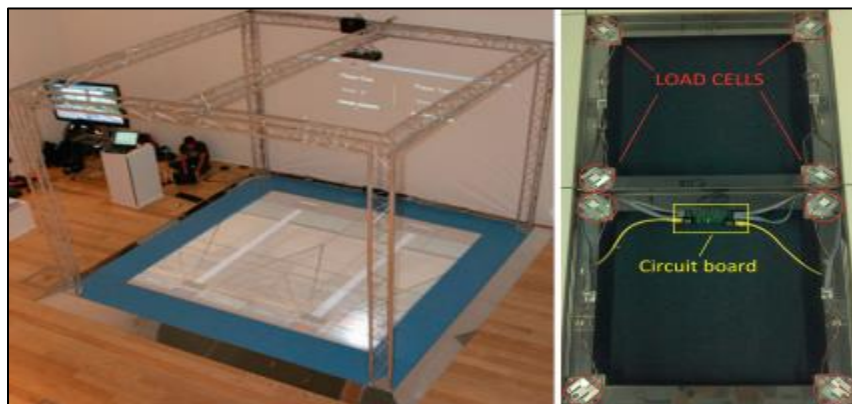


Figure 2.21 - The complete Smartfloor and detail of a pair of tiles.

Inria SmartTiles

In 2015, Andries et al. presented the Inria SmartTiles sensing floor for tracking and recognizing people and objects in the environment using the weight information provided by pressure sensing floors [18]. The system can record the pressure profiles of static and dynamic entities (objects and people) evolving on the floor. The pressure profiles allow tracking, localizing and recognizing these entities. The system also aid to robotic navigation, by generating and providing the safest navigation paths through the environment.

II.2.3 Commercially available sensing floors

There exist several sensing floors products commercially available today. Products like the SensFloor [110,111], a floor network of capacitive proximity sensors, and FloorInMotion [112] by Tarkett are being commercialized by companies mainly for the senior care industry.

SensFloor

In Germany, the enterprise Future Shape offers sensor floor system called “SensFloor” in the fields of Ambient Assisted Living (AAL) and Smart Home [110,111]. It is a textile-based underlay with integrated microelectronics and proximity sensors that can be installed underneath practically any type of floor covering (see Figure 2.22 (a)). Whenever a person walks across the floor, the integrated sensors in the sensor underlay are activated and a sequence of location- and time-specific sensor events is sent to the central control unit (see Figure 2.22 (b)). With the aid of pattern recognition and computation, these signal patterns can be used to identify different types of events. It is possible to detect the presence of people, the direction of their movement, and to recognize a person lying on the floor after a fall. The SensFloor system is suitable for various comfort, safety and security applications such as switching of orientation lights, controlling of automatic doors, fall detection, intrusion alarm, activity monitoring, leakage water detection as well as presence recognition. In production areas the sensitive floor supports the interaction of humans and machines by detecting the exact location of people and uses this to control the robots.

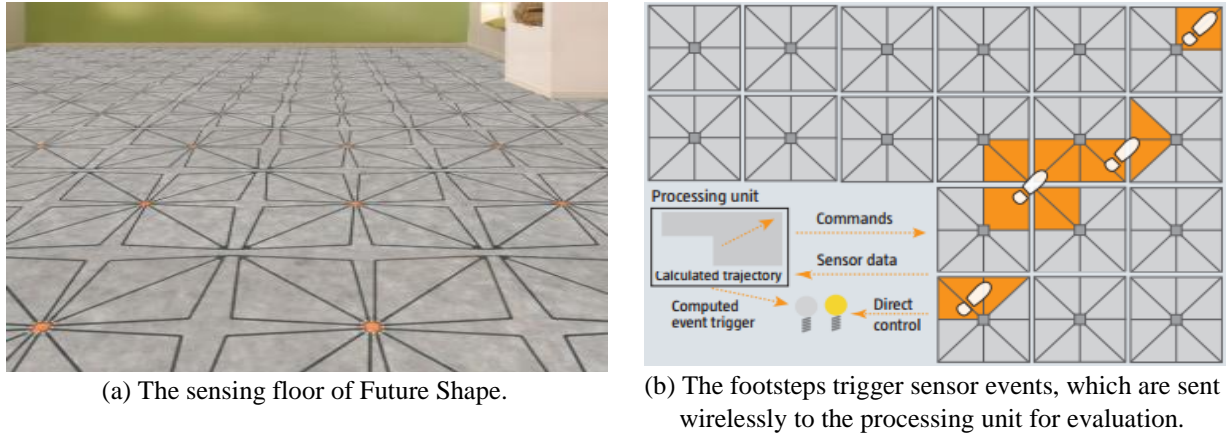


Figure 2.22 – The SensFloor, presented by Lauterbach et al.

FloorInMotion

In France, the company Tarkett offers an intelligent and connected floor, coupled with an alert service and monitoring of abnormal situations called "FloorInMotion" [112]. Due to its knowledge of the healthcare market, Tarkett has developed an innovative solution that detects abnormal situations or unusual behavior of elderly people or residents of healthcare institutions. This major innovation is the result of studies carried out among experts in this sector, and listening to the needs of patients, families and professionals. The system provides caregivers with a 24-hour real-time information service on residents' activity in their connected living space. In addition to its function of alerting in case of incident (fall, exit, intrusion), FloorInMotion Care, by the relevance of the information transmitted, participates in a proactive support oriented towards the well-being of the resident.

II.2.4 Conclusion

The domain of sensing floors has been in rapid expansion in the last twenty years, with applications evolving from entertainment to health monitoring and surveillance. They offer many advantages compared to other types of sensors, in terms of privacy, perception, and non-intrusive due to their invisibility to users. Although existing floors have limited capabilities, being able to detect people lying on the ground and tracking those walking in the environment, they have the potential to become a versatile sensor for AmI. They can provide space occupancy information for robot navigation, data on human localization, and derivate analytics like activity monitoring, and health diagnosis for the continuous supervision of human.

This section presents a detailed review of research work achieved in the sensing floor systems domain, including descriptions of the sensors they use and their modularity. The “Section 3” will introduce the sensing floor prototype designed by the research team at Inria, developed both for the perception and analysis of human activities, and for interaction with robots in their navigation and exploration tasks. This floor is used for all the applications presented in this thesis.

Section 3: The Inria Nancy – Grand Est sensing floor prototype

II.3.1 Introduction

We have surveyed the states of the arts on existing fall detection systems and sensing floor prototypes in the two previous sections. We will introduce now the Inria Smart apartment and its sensing floor prototype developed by LARSEN Team at Inria Nancy – Grand Est, which will be used throughout this thesis.

II.3.2 Origins of the Project

The Inria Nancy Research Center has been supporting since 2010 the design and the construction of an innovative platform for favoring research in indoor assistance for elderly. This artificial apartment platform has been funded by the CPER - MISN¹ (Contrat de Projet Etat-Région 2007-2013 - Modélisation, Informations et Système Numérique) of the Lorraine region, with the project Info-Situ (2010-2013). It consists of a standard apartment (kitchen, bathroom, bedroom and living room), with several smart and connected devices as sensor networks. A schematic view of this apartment composed of smart tiles is showed in the “Figure 2.23 (left)”.

The platform has been designed to make technical experimentations easier in an environment, which is as close as possible to reality. Many technical developments have been done during the IPL - PAL (Inria Project Teams - Personally Assisted Living). In particular, the team led by F. Charpillat has been working both (1) on the development of new algorithms to exploit/connect the sensors and the devices, and (2) on the effective deployment of different kind of connected devices:

- A network of depth cameras. These depth cameras are either fixed on the wall or are placed on-board wheeled mobile robots. One important achievement has been to connect these cameras to the Ethernet network, each camera being considered as a Robot Operating System (ROS²) node with computation capabilities. Another achievement has concerned the automatic calibration of these cameras. Today eight infrared cameras and one RGB-D Kinect camera cover completely the main living and kitchen area of the sensorized “smart” apartment. A network of Qualisys motion capture cameras is also covering the apartment to

¹ <http://www.enseignementsup-recherche.gouv.fr/cid65962/contrat-de-projet-etat-region-2007-2013-en-region-lorraine.html#c2007>

² www.ros.org/

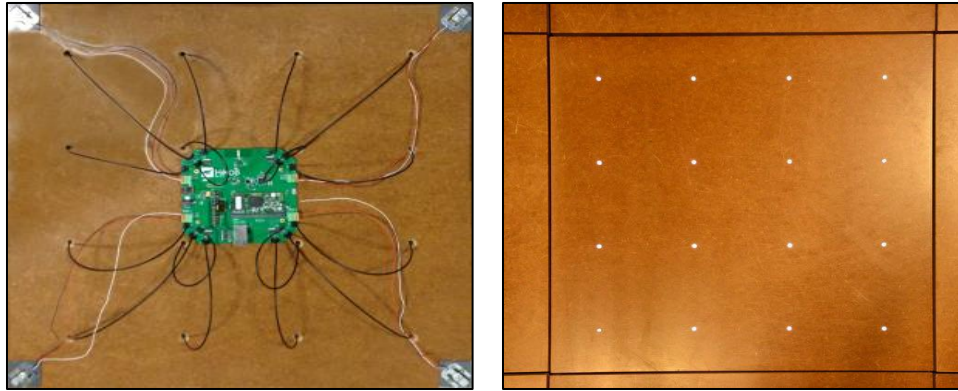
provide ground truth and precise robot and human tracking. The Qualisys system works at 300 frames per second (FPS) and with a millimeter precision, which will enable us to obtain with a high precision the 3D position of the joints of the person we will use as a ground truth to evaluate our approach. The frame rate of the Kinect cam is 30 FPS. The location of the Qualisys and the Kinect cameras are shown in the “Figure 2.23 (right)”.



Figure 2.23 - The Inria Nancy smart apartment (left), the location of the 8 cameras of the Qualisys system and the Kinect camera (right).

- Smart tiles composed of 104 rigid tiles (60*60 cm) representing a sensing floor prototype. Each tile is equipped with an accelerometer, a magnetometer, and four load sensors positioned at each corner “Figure 2.24”. They have been designed by Charpillet’s team in cooperation with Hikob³ and the Inria SED (Services d'Expérimentation et de Développement) of Grenoble during the PAL evaluation period. The pressure sensors employed (strain gauge load cells) measure the load forces exerted on the floor. The embedded accelerometers detect shocks that can be caused by objects or human’s falling on the ground. The magnetometers serve to detect metallic masses located on the tiles, such as robots. Each tile also has 16 light-emitting diodes that provide visual feedback. The sensors are queried periodically for measurement data, with a frequency of 50 Hz.

³ <http://www.hikob.com/>



(a) Smart tile bottom view

(b) Smart tile top view

Figure 2.24 – The smart tiles. The bottom view (a) shows the pressure sensors located in the corners, as well as the accelerometer and the CPU visible in the center. The black cables feed 16 light emitting diodes (LEDs) that are used for providing visual feedback and shown in top view (b).

Cartography of this apartment composed of smart tiles with their identifiers is showed in the “Figure 2.25”. The red dots in the corners of tiles indicate the positions of the pressure sensors. The walls are shown in black. The tiles under the furniture in the sleeping room (top left room), under the toilet in the bathroom (top middle room), and under the kitchen furniture (top right room) have been left unequipped with sensors, and are shown here in grey.

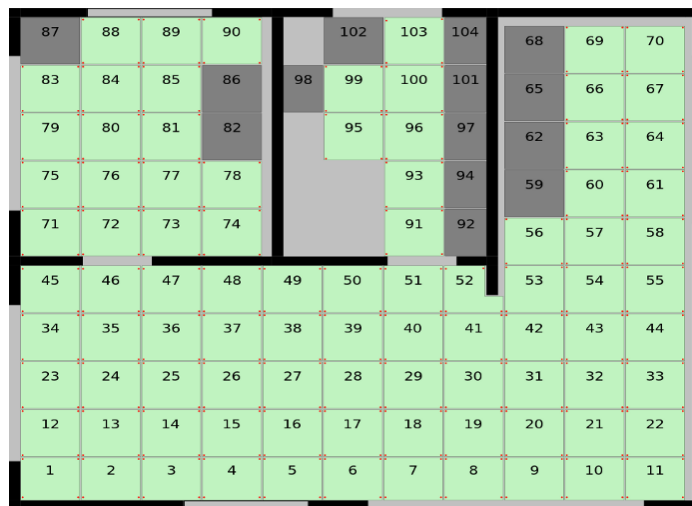


Figure 2.25 - Cartography of the tiles composing the sensing floor, with their identifiers.

II.3.3 Research projects of the Inria Nancy – Grand Est research center

The Inria Nancy - Grand Est center conducts sustained activity in the sector of information science and technologies, including computer science, applied mathematics, control engineering and multidiscipline themes situated at the crossroads between information science and

technologies and other scientific areas, including life sciences, physics and human and social sciences.

Many research projects have been achieved in partnership with the French National Centre for Scientific Research, the University of Lorraine, the University of Strasbourg and the University of Franche Comté.

- Living Assistant Robot (LAR) (2014-2016): The goal of LAR is to design a mobile assistant robot to improve the autonomy and quality of life for elderly and fragile persons at home. The LARSEN team is contributing to the project studying the robot navigation, perception and interaction, user modeling through machine learning, human tracking and human activity tracking and recognition.
- MUROTEX (2014-2015) (Multi-agent coordination in robotics exploration and reconnaissance missions): The main objective of the project is to develop a distributed planning framework for efficient task-allocation planning in exploration and reconnaissance missions by a group of mobile robots operating in an unknown environment, considering communication constraints and uncertainty in localization of the individual team members. One main challenge is to decentralize the decision, in order to scale up with a large fleet of robots (existing solutions are centralized or depend on full communication).
- ANDY (2017-2020) Advancing Anticipatory Behaviors in Dyadic Human-Robot Collaboration: AnDy influences the robotic technologies by providing robots with the ability to control physical collaboration through intentional interaction. This project relies on three technological and scientific breakthroughs. First, AnDy will innovate the way of measuring human whole-body motions by developing the wearable AnDySuit, which tracks motions and records forces. Second, AnDy will develop the AnDyModel, which combines ergonomic models with cognitive predictive models of human dynamic behavior in collaborative tasks, which are learned from data acquired with the AnDySuit. Third, AnDy will propose the AnDyControl, an innovative technology for assisting humans through predictive physical control, based on AnDyModel. AnDy paves the way for novel applications of physical human-robot collaboration in manufacturing, health-care, and assisted living.
- CoDyCo (2013-2017) Whole-Body Compliant Dynamical Contacts for Cognitive Humanoids: The CoDyCo project aims at advancing the current control and cognitive understanding about robust, goal- directed whole-body motion interaction with multiple

contacts. CoDyCo will go beyond traditional approaches: (1) proposing methodologies for performing coordinated interaction tasks with complex systems; (2) combining planning and compliance to deal with predictable and unpredictable events and contacts; (3) validating theoretical advances in real-world interaction scenarios with the iCub humanoid robot engaged in whole-body goal-directed tasks. The evaluations will show the iCub exploiting rigid supportive contacts, learning to compensate for compliant contacts, and utilizing assistive physical interaction.

- SATELOR (2014-2018) (Region Lorraine industry & research project): The aim of Satelor project is to develop services for maintaining safely elderly people with loss of autonomy at home or people with a chronic diseases. It works toward developing a technology for an augmented and sensorized environment (including a low-cost mobile robot) that can monitor the patient activity at home and inside public/private healthcare facilities, particularly to detect anomalies and discontinuities in the rhythm of daily activities, and to detect falls of elderly people.

More projects are also offered such as SCIARAT (2016-2018), PsyPhine (2015-2018) with details on <https://team.inria.fr/larsen/projects/> and RESIBOTS (2015-2020) with details on <http://www.resilient-robots.net>.

Additionally, many theses are also presented such as:

- Amandine Dubois uses Camera RGB-D in her thesis entitled "Fragility measurement and elderly fall detection system that can serve elders at home". She proposes a system to detect falls and prevent the frailty of the elderly [65].
- Mihai Andries works on the load sensors in his thesis entitled "Object and human tracking, and robot control through a load sensing floor". He succeeds to developed and introduce new techniques for tracking and recognizing people and objects in the environment, using the weight information provided by load-sensing floors [113].
- Abdallah Dib proposes in his doctoral thesis a system for capturing human movement in 3D for a mobile robot evolving in a crowded environment [114]. The proposed system uses a low-cost RGB-D camera being able to be embarked on a mobile robot capable of locating and following the person in motion and of estimating its posture even when the person being followed is partially obscured by objects.

This thesis will explore and analyze the capabilities of such sensing floor. More formally, it will explore the paradigms applicable for the analysis of sensing information coming from an omnipresent floor-pressure sensor, located inside a delimited physical space. As domain of application, we will focus on assisted living facilities for elderly people by detecting elders' falls, locating and tracking them, as well as recognizing their main ADLs. The purpose is to allow elders to age comfortably at home, and also to reduce the workload of the medical personnel in hospitals, retirement homes and similar facilities. The main sensors used in this work are the Gauge pressure sensors and LSM 3-axis accelerometers concealed under intelligent tiles.

II.3.4 Intra and inter tiles communications

Besides being equipped with a set of sensors, each tile also has an on-board processing unit, as well as a ZigBee wireless technology (IEEE802.15.4 based) and wired connection, which also provides electric power and supports a real-time process communication with its neighbors and any agent laid on it [115]. Moreover, nodes use the ROS for intercommunication between multi-agent models to provide for instance, a navigation system for mobile robots (see Figure 2.26) [17].



Figure 2.26 – PeKeeII robot communicating with an interactive sensing floor.

II.3.5 Inria sensing floor capabilities

The main objective of our research on this floor sensor is locating and tracking elders at home, recognizing their main ADLs, as well as detecting falling down cases. Yet, a large number of applications have already been implemented including mobile objects localization, footsteps extraction and tracking, human frailty evaluation, weight measurement, visual guidance, breathing tracking, as well as games entertainment [113].

II.3.6 Conclusion

We have presented in this section, the sensing floor prototype developed at Inria Nancy - Grand Est. Compared to the previous sensing floor prototypes, it requires a lower number of sensors per piece, and have additional capacity to store information and perform distributed computations on the tiles of this modular floor.

We also provided an overview of the preliminary applications already implemented in this platform. Supplementary advanced applications developed on this floor during this thesis will be presented later, together with directions for future work.

General conclusion

This chapter surveys the state of the art of FD systems and sensing floors domain, including performance and accuracy evaluations for several studies. It aims to serve as a point of reference on elderly fall-related and assistive living systems.

Many supportive technologies and systems have been developed to track and monitor elderly ADLs in order to assist their independent living and reduce the cost of premature institutionalization. However, most of these systems are relying on only one data provider (movement-sensor, camera, or accelerometer, etc.) that have their own limitations and do not ensure 100% reliability. Additionally, there is always a lack of experience and systematic knowledge to intelligently assemble the components into a robust, user-friendly and effective system, making no false alarm and detecting each fall case without affecting elderly daily living patterns.

Consequently, this work is geared towards offering a novel system for elderly tracking, ADLs recognition, and fall detection, using a set of non-intrusive sensors networks that provides more accuracy, reliability and efficiency, as well as system fault tolerance.

In the next chapter, we will explore the Inria Nancy - Grand Est sensing floor as an innovative smart home for favoring research in PAL domain as an AmI application.

Chapter III - Processing and simulating data from the Inria Nancy – Grand Est sensing floor

Overview

This chapter focuses on processing and simulating data collected from the Inria Nancy – Grand Est sensing floor. The aim is to explore the abilities of such floor to serve as a smart home in the AmI domain that offers localization and tracking of elderly, ADLs recognition, and automatic FD system, using a non-intrusive sensors network (load pressure sensors and accelerometers) concealed under tiles.

The chapter is composed of three main sections and a general conclusion.

- Section 1 introduces the technique for scanning the load pressure distributions on tiles that are used to locate and track elders as well as recognize their main ADL's,
- Section 2 presents the methodology of accelerometer data collection, features extraction, features selection, signal changing detection, and classification methods that are used to detect falling cases,
- Section 3 shows how can the merging between the load pressure sensors results and the accelerometers decisions serve to enhance the system accuracy,
- General conclusion recapitulates all the three previous sections.

Section 1: Processing and simulating data from the load sensing floor

III.1.1 Introduction

This section describes the ongoing work of human localization and tracking, activities recognition, and fall detection in independent living senior apartments using load pressure sensors and 3-axis accelerometers concealed under intelligent tiles. The load pressure sensors permit to locate and track elders as well as recognize some ADLs. However, the fall detection accuracy on real data contains false alarms coming from lying down postures. To solve this issue, we propose merging between the load pressure sensors measurements and the accelerometers decisions. As a consequence, the system accuracy is satisfactory and the results show that the proposed methods are efficient and can be integrated in a real PAL system.

III.1.2 The load pressure sensors of the Inria Nancy – Grand Est platform

As mentioned in the “Chapter II-Section 3”, each tile is equipped with four load pressure sensors located at the corners and concealed under the tiles (see Figure 3.1). These load sensors of the brand SparkFun SEN-10245⁴ measure the load forces exerted on the floor. The specification of the sensors is shown in the “Figure 3.2”.

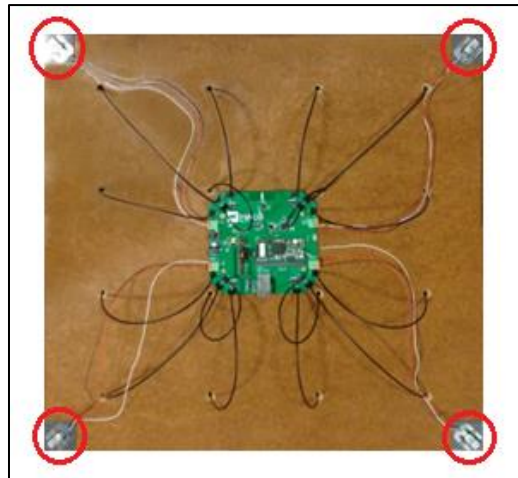


Figure 3.1 – The smart tiles. The bottom view shows the pressure sensors located in the corners.

⁴ <https://www.sparkfun.com/products/10245>.

Capacity	kg	40-50
Comprehensive Error	mv/v	0.05
Output Sensitivity	mv/v	1.0±0.1
Nonlinearity	%FS	0.03
Repeatability	%FS	0.03
Hysteresis	%FS	0.03
Creep	(3min)%FS	0.03
Zero Drift	(1min)%FS	0.03
Temp. Effect on Zero	%FS/10°C	1
Temp. Effect on Output	%FS/10°C	0.05
Zero Output	mV/V	±0.1
Input Resistance	Ω	1000±20
Output Resistance	Ω	1000±20
Insulation Resistance	MΩ	≥5000
Excitation Voltage	V	≤10
Operation Temp. Range	°C	0--+50
Overload Capacity	%FS	150



Figure 3.2 – Specifications and image of the SparkFun SEN-10245 load sensor.

III.1.2.1 Load frequency distribution and sensors calibration

The load frequency distribution measured by the sensors seems non-Gaussian for each sensor individually, while it has approximately normal distribution shape for the combined 4 sensors. Moreover the sensor has a randomly offset when no pressure is existed. To make the values more comprehensible, a calibration of the load sensors has to be performed and a function converting arbitrary sensor units to newton must be determined. Two calibration values are needed to determine the linear function of data conversion on each tile: the first is gotten by measuring the pressure when there is nothing on the floor, where the second will be calculated after placing a known weight on each tile. This function showed a linear correspondence between the measured and real values with a slope of 0.1335 (i.e. 1 pressure unit measured by the load sensor corresponds to 0.1335 kg or 133.5 g) (see Figure 3.3). These measures were obtained with a combined noise ratio of the four sensors nearly ± 2 kg. To obtain maximum precision, each sensor should be calibrated separately, which makes this procedure long. Supposing that all tiles have the same

slope of their conversion functions, a faster joint calibration method of the 4 sensors of a tile can be easily made [113].

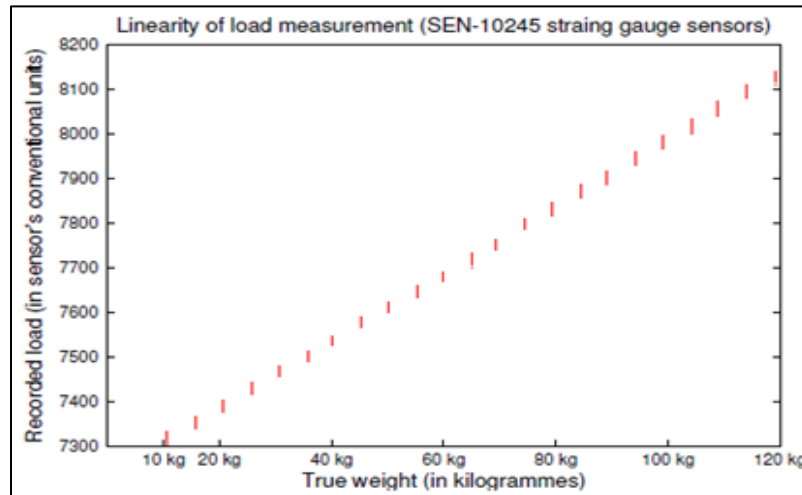


Figure 3.3 – The load measure linearity for a tile. The intervals that can be seen instead of expected dots are due to measurement noise.

III.1.3 Load data collection

The data collection is in charge of recording specific variables in a methodical method that ensure the accuracy and validity of the collected information [116]. This procedure starts by identifying the variables needed and determining where and how this data can be gathered. Data can be compiled in different ways such as measuring items, weighing items or observing changes. Meaningless information or noise is removed from the data and only useful values are used to form the final output database. These values have to be normalized before being used. Attributes are adjusted to share a common measurement scale.

During this work, six different volunteers - at the ages of 28, 30, 39, 42, 44 and 60 - were participated to make ten different scenarios repeated five times. System test contains four kinds of the main ADLs (i.e., walking, sitting, standing, and lying down) and diverse kinds of fallings. Activities were made with different ways like soft and hard falls, fast and slow walking, falling from sitting and falling from walking, etc. Some scenarios contain 1 subject and others contain 2 different subjects. From the signals generated by the load sensors and the accelerometers under the tiles, a raw database was built to be used in this work. In this chapter, we will proceed with the load data to track and recognize elder ADLs.

The data generated by the load sensing floor can be passed to a data processing software either as a recorded .txt file, or through a ROS publisher/listener interface by publishing it on the corresponding topic. The software treats the data packets sent regularly by the tiles every 20 milliseconds. Data is finally converted to .mat file (which is readable by Matlab) and has the following format:

Gauge [IP/ID] [msg_ID] [Timestamp] [ValA] [ValB] [ValC] [ValD]

Where

- *Gauge* is the type of sensor sending these data,
- *[IP/ID]* is the IP/ID address of the tile,
- *[msg_ID]* is the identification number of the message,
- *[Timestamp]* is the timestamp (in milliseconds) of recording,
- *[ValA]* is the value for the first gauge sensor (arbitrary units) (force),
- *[ValB]* is the value for the second gauge sensor (arbitrary units) (force),
- *[ValC]* is the value for the third gauge sensor (arbitrary units) (force),
- *[ValD]* is the value for the fourth gauge sensor (arbitrary units) (force).

One can see the format of the data sent by the load sensors in the “Table 3.1”.

Information				Load Data			
Sensor type	IP/ID	msg_ID	Timestamp	ValA	ValB	ValC	ValD
Gauge	192.168.1.40	4648	1.455E+12	1920	1919	2174	1212

Table 3.1 – Format of data package containing pressure measurements.

III.1.4 Elder tracking and ADLs recognition using the load data

The load sensors measure the load forces exerted on the floor that can be used to determine, for example, where you are stood on the floors surface and the way you are stood. In addition, we will proceed in this work to determine the posture of the monitored person (walking, sitting, standing, lying down, falling down, etc.) by combining the pressure amount, the pressure duration on a tile, and the tiles proximity (the floor surface exerted by load forces) using a relatively simple algorithm that represents one of the contributions of this thesis. As a result, one can recognize the main elderly ADLs, localize and track them, as well as detect their falls. Consequently, tiles can be

exploited to extend agents' perceptions and communications (of human or robot) to offer a quick assistance after fall detection alert [117,118].

III.1.4.1 ADLs definition

ADLs are routine activities that people tend to do every day without needing assistance. The main ADLs studied in this work are: walking, sitting, standing and lying down. This work aims to recognize each activity and equally the transitions between them by determining the posture of the monitored person, as well as detect falling down cases. The following diagram shows the main ADLs and falling states, as well as the transitions among them (see Figure 3.4).

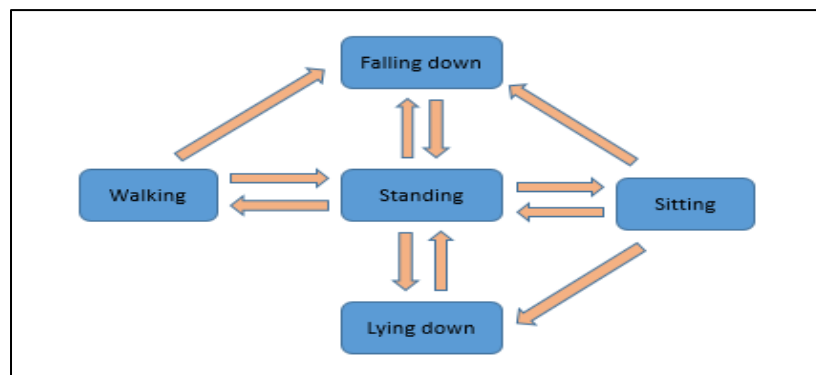


Figure 3.4 - State diagram of the main ADL with the transitions among them.

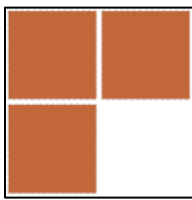
III.1.4.2 Characteristics of all postures

In this section, the characteristics of different kinds of posture were defined based on the load forces exerted on the floor and other information (the tiles proximities and the duration). Based on the scenarios of all occurrences, we experimentally identified the characteristics of each activity and we can note the following:

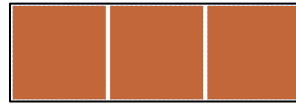
- Walking: the load forces exerted on the floor are high and move on neighbor tiles within a short time period.
- Standing: the load forces exerted on the floor are high and they are fixed on the same tiles for a time period.
- Sitting: the load forces exerted on the floor are split between less than 2 linear tiles and they are fixed on the same tiles for a time period.
- Lying down: the load forces exerted on the floor are split among at least 3 linear tiles and they remain on the same tiles for a time period.

- Falling down: this posture has the same characteristics of the lying down one regarding the load forces exerted on the floor.
- Unknown: we also take in consideration the situation where the person is going outside or existing in an area that is unequipped with sensors (i.e. taking a bath or a shower in the bathroom), and the case where there is a sensor defect. In such cases, there is no load force exerted on tiles, and they are denoted as “*Unknown*”.

Note that the number of linear tiles is the number of tiles in a same row or in a same column (straight line).



Number of linear tiles = 2



Number of linear tiles = 3



Number of linear tiles = 3

III.1.4.3 Load data processing

From the gauge database tables, we obtain 4 matrices ($n \times m$) where their values correspond to the load forces exerted on the 4 load pressure sensors of each tile. The matrix dimensions n and m correspond to the number of tiles per row and per column respectively of the platform. Also we calculate another matrix ($n \times m$) where their values correspond to the mean load forces exerted on the 4 force sensors of each tile. The load forces were calculated after being normalized and filtered from noise, and they were reset to zero where no person exists on the tiles. The algorithm searches the maximal value of the mean load forced exerted on each tile and then compare this value with two predefined thresholds. The first (threshold1) can distinguish the walking/standing postures from the sitting/falling/lying-down/unknown ones. Then the proposed method differentiates between walking and standing up postures regarding the duration of load force exerted on a tile using its identifier and comparing it with the previous one. On the other hand, the second threshold (threshold2) distinguishes between the unknown posture and the sitting/falling/lying down. Then, the sitting was differenced from falling/lying down based on the number of linear tiles exerted by load forces (tiles' proximity) [19]. See the characteristics of all postures defined in the previous paragraph.

The threshold1 and the threshold2 are estimated to 3/4 and 1/4, respectively, of the maximum value of the load forces exerted on tiles. Since, we found when observing the forces exerted on the tiles that the maximal values were obtained when the person is walking or standing up, so we choose the threshold 75%. Whereas these values are lower in other postures because the load force is distributed on different tiles, so we choose the threshold 25%. The detailed flow chart of the algorithm is shown in the “Figure 3.5”.

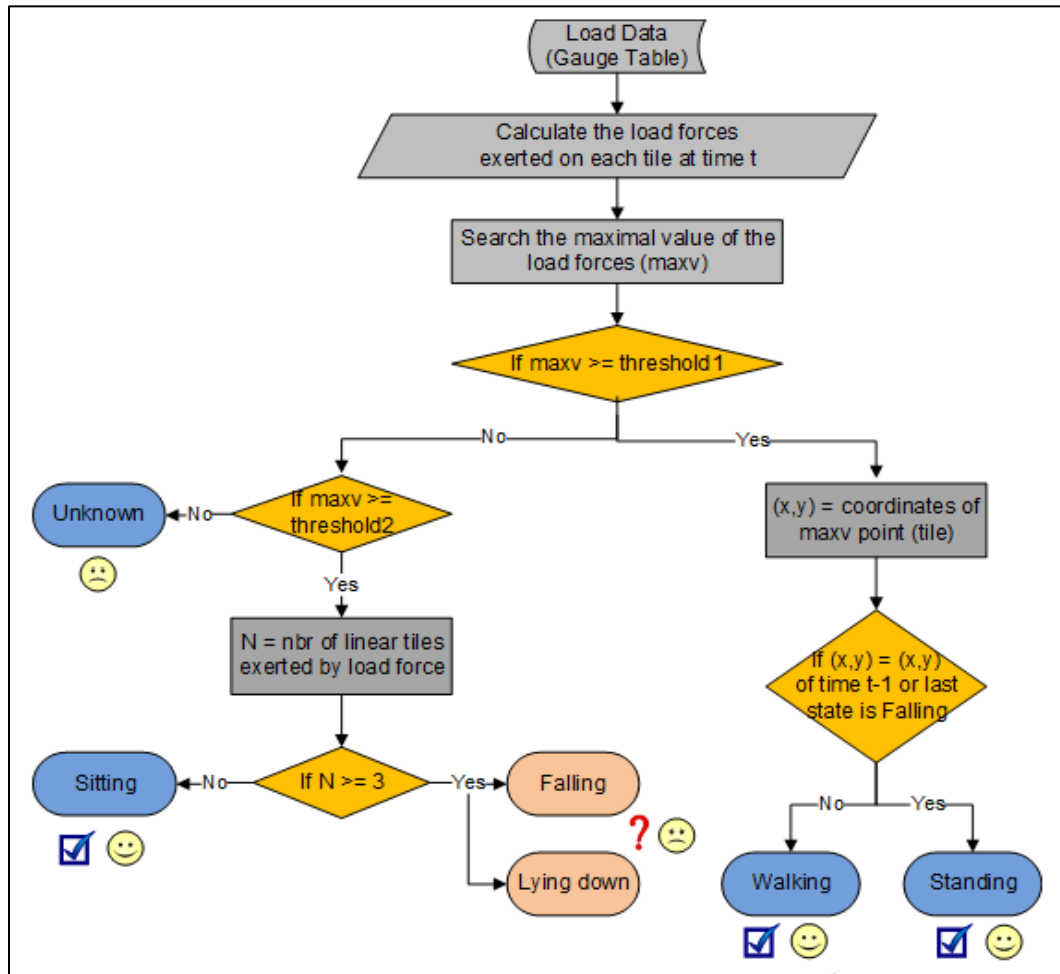


Figure 3.5 - Flow chart diagram of the algorithm.

This system has shown high accuracy to locate elder and estimate the main Activities Daily Living (ADL). Unfortunately, the pressure sensor is insensitive to lying down posture, and it generate a false alarm of falling since more than three linear tiles are exerted by load forces for the both postures. An alarm from the force sensor will signify that someone was falling; even the person was lying down.

III.1.4.4 Experiments and results

To illustrate this procedure, a program was developed using Matlab, which shows the different information and decisions depending on the video sequence (several sequences have been processed but only one is presented here). Results show that our proposed system can differentiate among the different ADL postures with a good accuracy, unless the cases of falling and lying down. Six postures are shown in the six figures “Figures 3.7 - 3.12” below. The unknown posture means that there is no person on the floor.

Each figure contains four pictures that represent:

- (a): the video snapshot taken from an RGB-D cameras fixed on the wall.
- (b): the exerted force on a tile for a period of time. Zero level of exerted force indicates that there is no person and denoted as unknown posture. High level of exerted force for a short time on a specific tile indicates a walking posture. High level of exerted force for a long time on a specific tile indicates a standing posture. Moderate or low level on less than three linear tiles indicates a sitting posture. Moderate or low level on more than three linear tiles indicates a lying down or falling posture.
- (c): the cartography of the apartment represented as image. Similarities can be identified between the pressure sensing and imaging domains. The pressure perceived by a load-sensing surface is analogous to the amount of light perceived by an image-recording sensor. Both in imaging and pressure sensing, the sensor can be shifted by less than a pixel width to register a slightly different part of the incoming light or pressure. In this work, the dark cells have identified as free (due to the absence of pressure on the tile), while the white cells are cells that are identified as occupied (see Figure 3.6).
- (d): the posture estimated by our system (as a caption for the picture in red color) with the trajectory followed by the person (content of the picture).

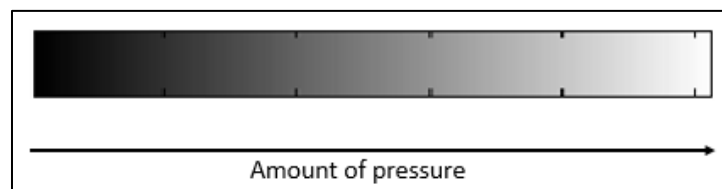


Figure 3.6 – Amount of pressure representation.

One can see the estimated postures of different ADLs with the human movement tracking in the “Figures 3.7 - 3.12”.

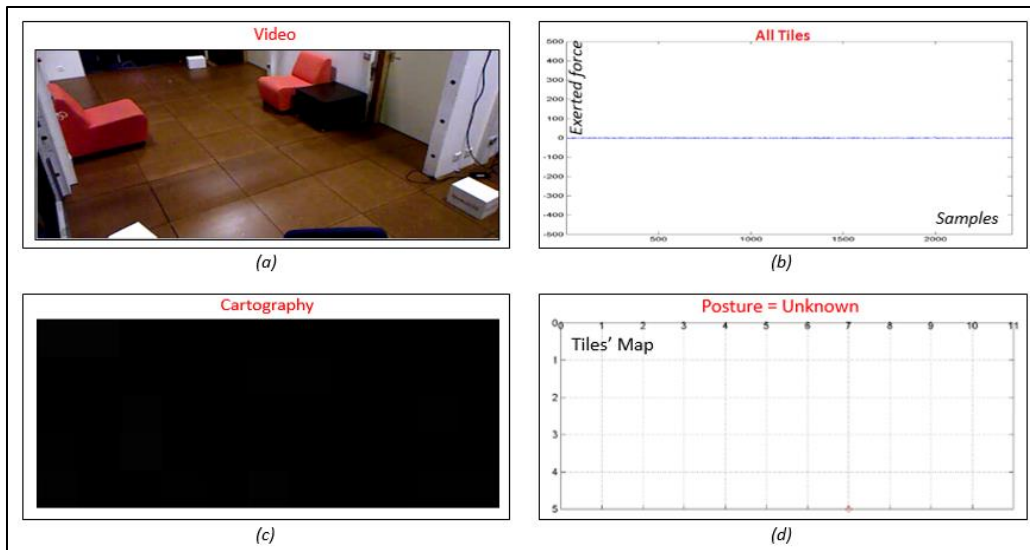


Figure 3.7 - Unknown posture.

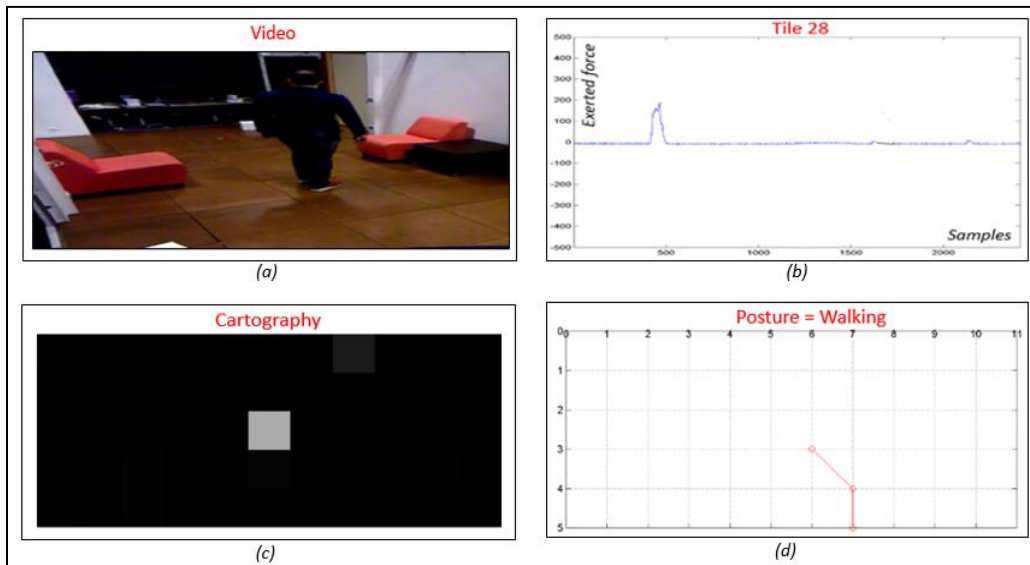


Figure 3.8 - Walking posture.

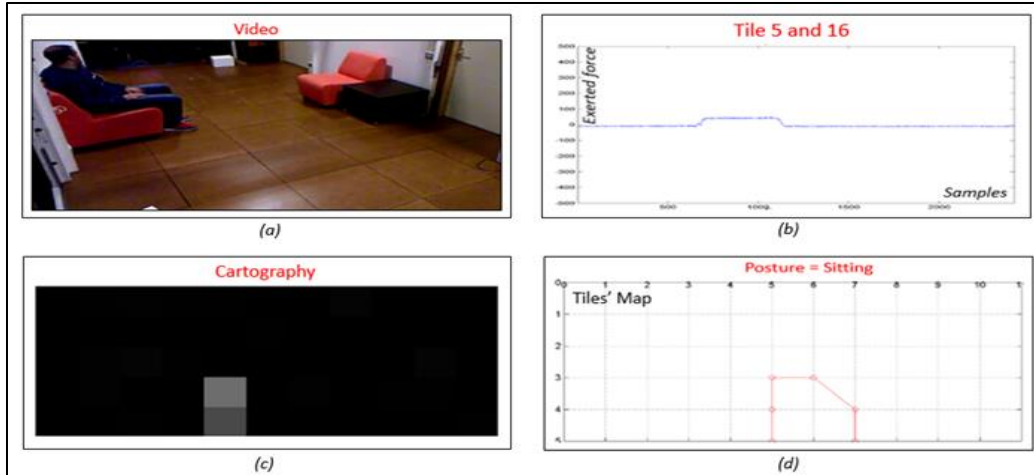


Figure 3.9 - Sitting posture.

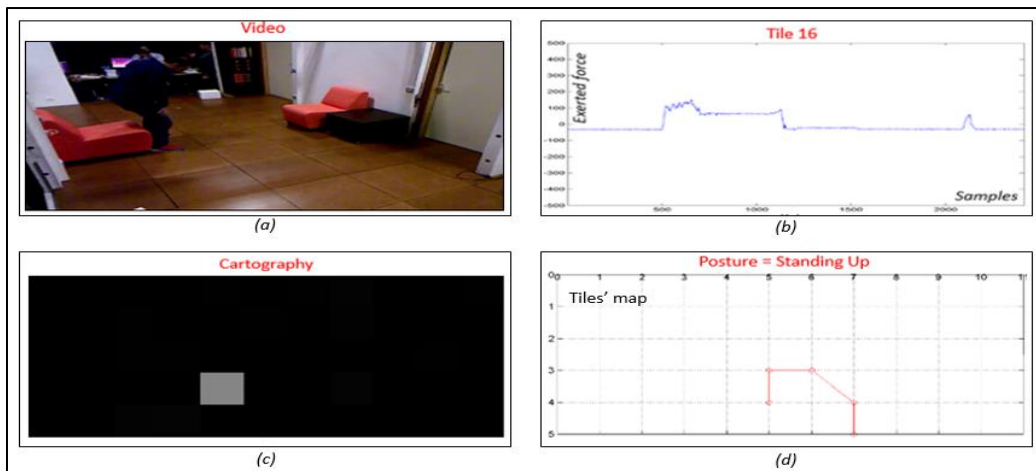


Figure 3.10 - Standing up posture.

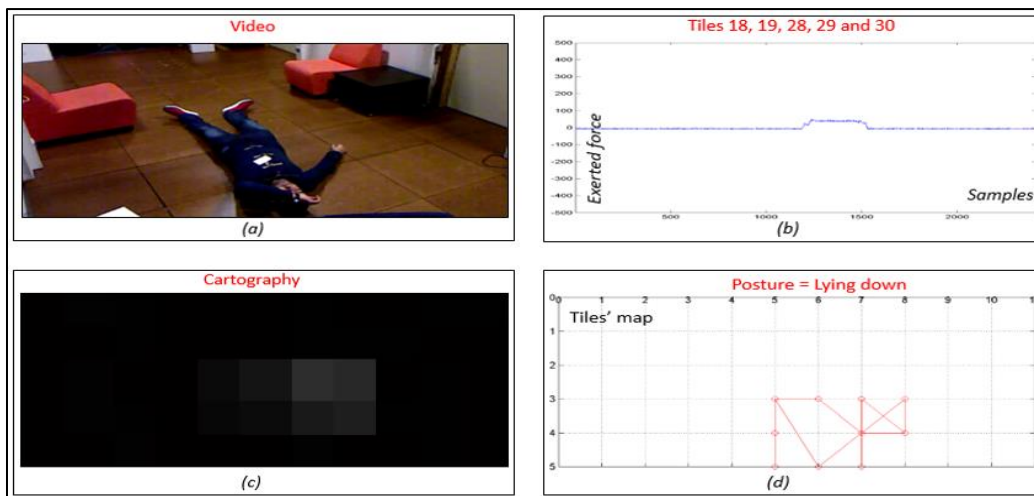


Figure 3.11 - Lying down posture.

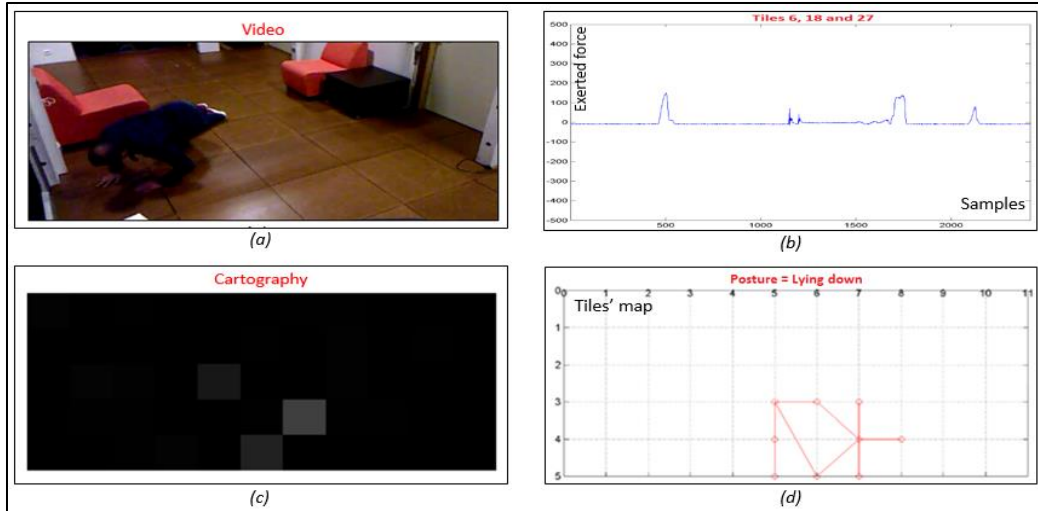


Figure 3.12 - Falling posture.

One can see obviously that in the “Figures (3.7-5.11)”, the estimated posture in picture (d) is the same as the real posture shown in the picture (a), and this result validates the proposed approach for ADLs recognition using the load sensors. On the other hand, it is clear that in the “Figure 3.12”, the real posture is “Falling” (see picture (a)) while the estimated posture is “Lying down” (see picture (d)). Thus, one can see that the proposed methods are accurate to recognize ADLs. To prove this accuracy, the mass center localization extracted from a Kinect camera fixed on the wall of a subject playing a sequence of (walking–sitting–falling–standing–walking) is drawn in the “Figure 3.13” to validate the estimated postures [119].

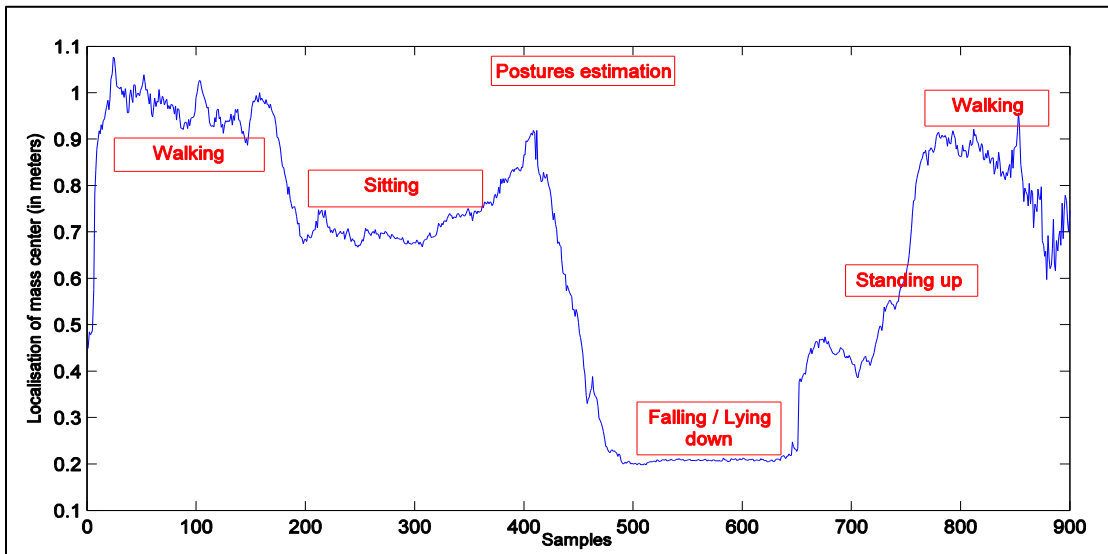


Figure 3.13 - Localization of the mass center of a subject with the estimated postures results.

To generalize this result, ten different sequences with six different subjects were tested to show the accuracy and the efficiency of the proposed system. “Table 3.2” shows the sensitivity results of ADLs’ postures estimations.

Real postures	Estimated postures	Sensitivity
60 Unknown	60 Unknown	100%
150 Walking	148 Walking + 2 Standing Up	98.7%
65 Standing Up	60 Standing Up + 3 Sitting + 2 Unknown	92.3%
42 Sitting	40 Sitting + 2 Unknown	95.2%
20 Lying down	19 Lying down + 1 Sitting	95%
34 Falling down	32 Lying down + 2 Sitting	0%

Table 3.2 – Sensitivity of ADLs’ postures estimations.

The first column describes the real postures of the six subjects in the ten sequences. The second column shows the estimated postures of the proposed methods. The third column shows the sensitivity or the True Positive Ratio ($TPR = TP / (TP+FN)$) of the proposed system, where TP and FN are respectively the numbers of valid and invalid estimated postures, 100% indicating that all real postures were truly estimated.

III.1.5 Conclusion

In this section, we have seen how a network of load pressure sensors can be exploited to perform ADLs recognition and human movement tracking. One can see by using the load sensors concealed under tiles, we can track humans and distinguish between the main ADLs postures defined above (unknown, walking, standing, sitting, and lying down) with a high accuracy, but it is impossible to detect the falling down cases and they are estimated as “Lying down” postures (see Figure 3.14).

Therefore, we propose the usage of the 3-axis accelerometer measurements with threshold-based algorithm to detect falls since they are widely used in fall detection systems.

Section 2 will present how to process the accelerometer data to distinguish between lying down postures and falling down cases.

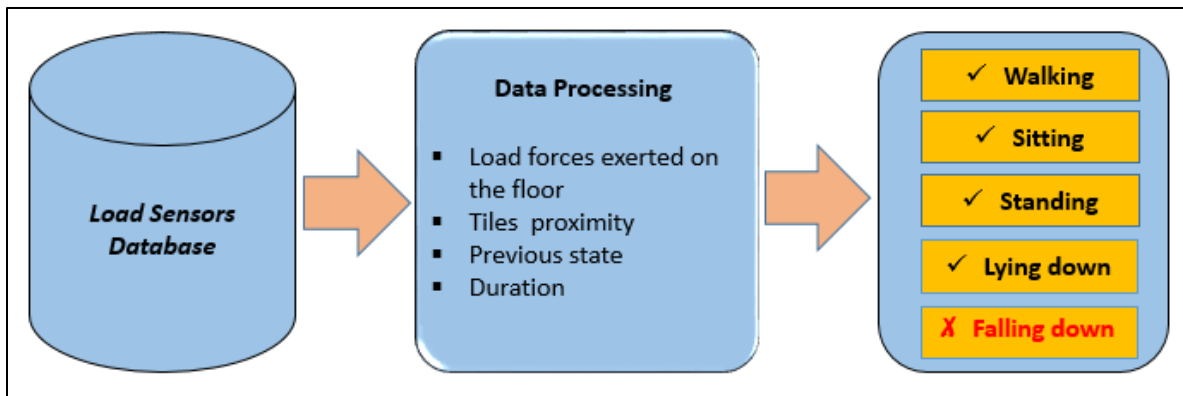


Figure 3.14 - ADLs recognition using simple pressure sensors.

Section 2: Processing and simulating data from the accelerometers

III.2.1 Introduction

In the previous section, we have seen how a network of simple load sensors can be exploited to perform elder tracking and ADLs recognition. However, results contain false alarms coming from elder fall cases that are estimated as lying down postures. These results prove that load sensors cannot distinguish between lying down and fall postures.

On the other hand, automatic fall detection is a major issue in PAL and has the potential of increasing autonomy and independence while minimizing the risks of living alone.

Consequently, to provide reliable system with minimum false alarms rate in ADLs recognition and detect each case of fall, we propose the use of the accelerometers especially that they are usually used to detect elderly falls.

This section describes a novel approach of detecting elderly falls in independent living apartments using accelerometer concealed under tiles.

III.2.2 The accelerometers of the Inria Nancy – Grand Est platform

Each tile of the Inria platform is equipped with an LSM 3-axis accelerometer of the brand LSM303⁵ that measure the acceleration of a moving or vibrating body in the X, Y and Z axis. Centrally located and concealed under the smart tiles as shown in the “Figure 3.15”, the accelerometers can detect impacts with the floor (e.g., falls, ball bounces) using threshold-based algorithms. The LSM303 breakout board combines a magnetometer/compass module with a triple-axis accelerometer to make a compact navigation subsystem. The I2C interface is compatible with both 3.3v and 5v processors and the two pins can be shared by other I2C devices. The cables are as small as possible to minimize the effect of the cable’s capacitance noise, and devices are shielded to reduce the noise generated by external signals. The specification of this sensor is shown in the “Figure 3.16”.

⁵ <https://learn.adafruit.com/lsm303-accelerometer-slash-compass-breakout>

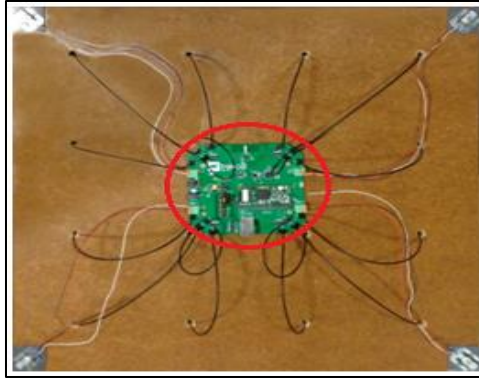


Figure 3.15 – The smart tiles. The bottom view shows the accelerometer and the CPU visible in the center.

- Analog supply voltage: 2.16 V to 3.6 V
- Digital supply voltage IOs: 1.8 V
- Power-down mode
- 3 magnetic field channels and 3 acceleration channels
- ± 1.3 to ± 8.1 gauss magnetic field full-scale
- ± 2 g/ ± 4 g/ ± 8 g dynamically selectable full-scale
- High performance g-sensor
- I²C serial interface
- 2 independent programmable interrupt generators for free-fall and motion detection
- Accelerometer sleep-to-wakeup function
- 6D orientation detection
- ECOPACK[®], RoHS, and “Green” compliant



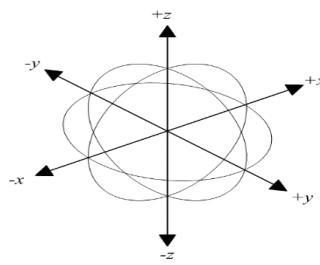


Figure 3.16 – Specifications and image of the LSM 3-axis accelerometer.

III.2.3 Accelerometer data collection

Every accelerometer generates data that can be passed to a data processing software either as a recorded .txt file, or through a ROS publisher/listener interface by publishing it on the corresponding topic. The accelerometers are queried for measurement data with a frequency around 50 Hz. The sampling frequency of 50 Hz was chosen because it has been shown to be high enough for acceleration data analysis in fall-related motions [120,121]. Data is finally converted to .mat file and follows the following format:

Lsm [IP] [msg_ID] [Timestamp] [AccelX] [AccelY] [AccelZ]

Where

- *Lsm* is the type of sensor sending these data,
- *[IP]* is the IP address of the tile sending these data,
- *[msg_ID]* is the identification number of the message,
- *[Timestamp]* is the timestamp (in milliseconds) of recording,
- *[AccelX]* is the X value of the tile accelerometer,
- *[AccelY]* is the Y value of the tile accelerometer,
- *[AccelZ]* is the Z value of the tile accelerometer.

One can see the format of the data sent by the accelerometers in the “Table 3.3”.

Information				Accelerometer Data		
Sensor type	Tile ID	msg_ID	Timestamp	X	Y	Z
Lsm	192.168.1.28	15786	1.45562E+12	46	18	-72

Table 3.3 – Format of a data package containing acceleration measurements.

III.2.4 Fall detection using the accelerometer data

The main objective of using accelerometer is to (1) detect human fall that are one of the major causes of morbidity and mortality in elderly population, and (2) enforce the accuracy of the proposed system by reducing the false alarms rate derived from falling cases estimated as lying down postures. Raw data collected from accelerometers concealed under tiles is proceeded by some processing tasks in order to obtain meaningful information to be used in fall detection. In this view, PAL would widely benefit from non-intrusive, reliable, efficient, and affordable system [20]. The accelerometer data processing steps is shown in the “Figure 3.17”.

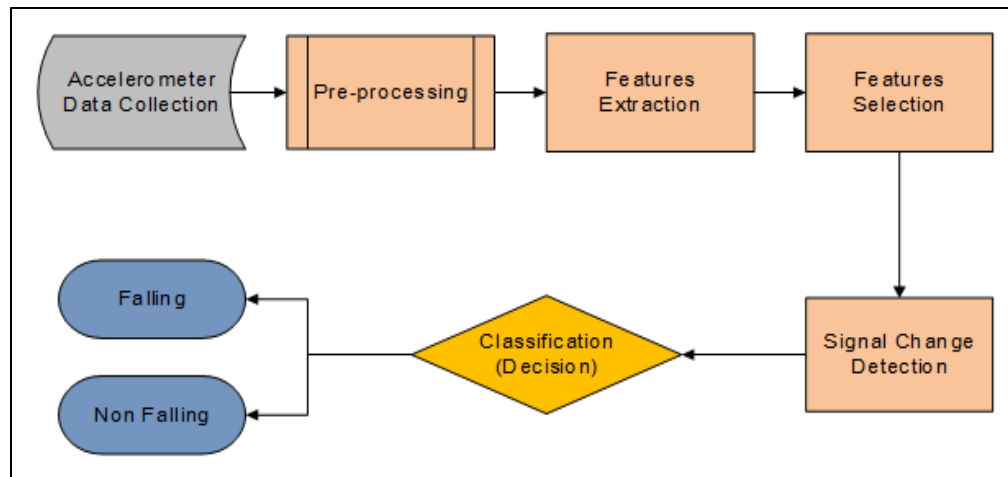


Figure 3.17 – The accelerometer data processing steps.

III.2.4.1 Accelerometer data preprocessing

After collecting data from the accelerometers, a preprocessing phase takes place. Meaningless information or noise is removed from the raw data and only useful values are used. These values are normalized to share a common measurement scale. After that, data tables are fragmented into fall and non-fall fragments to obtain two different classes, and then followed by windowing step.

III.2.4.1.1 Data fragmentation

The start and the end of each fall action have been annotated based on the pictures and the videos taken from RGB-D cameras fixed on the wall. Similarly, for each normal activity case, suitable start and end times have been chosen so that the delimited time span contains activities as similar as possible to falls, i.e. with highly varying signals.

III.2.4.1.2 Windowing

Each signal is divided into smaller time segments called windows of fixed length and with a fixed overlap. Overlap is normally used to avoid an arbitrary, rigid partitioning of the signal, which could result in sample boundaries cutting across important features. Good values for both window size and overlap have been found through preliminary experiments as 50 samples and 25 samples, which correspond to 1 second and 0.5 second respectively. The windowing process is shown in “Figure 3.18”.

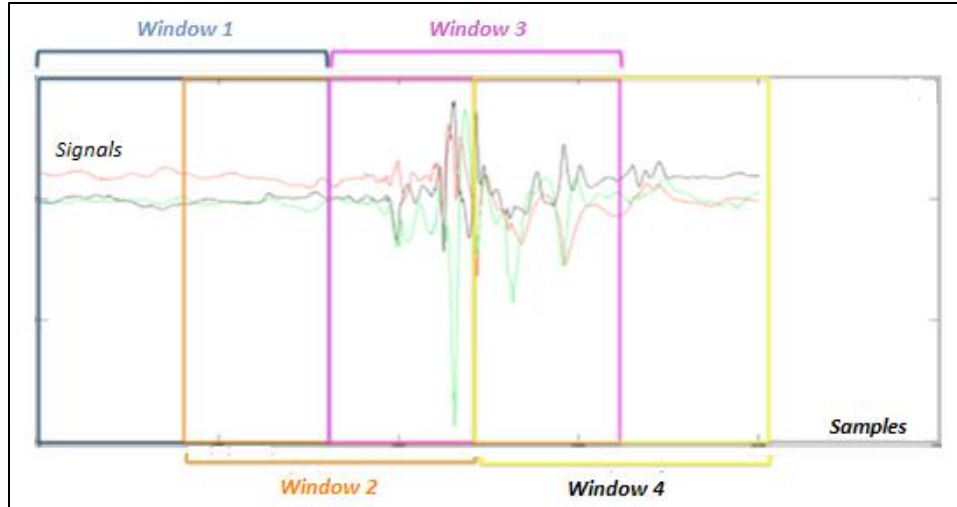


Figure 3.18 - Windowing process.

III.2.4.2 Features extraction

The number of features or parameters in a dataset has a direct impact on the dataset's descriptive power. The more features a dataset has, the more expressive it is. However, finding meaningful relationships among the instances and the class can be more difficult because the feature space grows exponentially with the number of features. Features extraction is the process by which relevant characteristics or attributes are identified from the collected data. It is also known as dimensionality reduction because only features that best describe the input data are selected from the raw data, and meaningless information or redundant features are discarded. Therefore, the size of the dataset is reduced, and this reduction usually lowers the work of the subsequent modules [122]. In this view, 20 features (16 linear and 4 nonlinear) are extracted from each window data. Features have been cautiously picked in order to get a more descriptive and smaller output dataset: Mean Power Frequency (MPF), Peak Frequency (PF), and Deciles which contain the Median Frequency D5, parameters extracted from the wavelet packet decomposition, Time Reversibility (TR), Detrended Fluctuation Analysis (DFA), Lyapunov Exponent (LE), and the Sample Entropy (SE).

III.2.4.2.1 Linear parameters

a) Parameters related to power spectral density

In statistical signal processing, the goal of the Spectral Density Estimation (SDE) is to estimate the power spectral density that characterizes the frequency content of the signal [123].

The Welch's method is used in this work. It is based on the concept of using periodogram spectrum estimates, which are the result of converting a signal from the time domain to the frequency domain. Welch's method is an improvement on the standard periodogram spectrum estimating method and on Bartlett's method, in that it reduces noise in the estimated power spectra in exchange for reducing the frequency resolution. This Welch Periodogram uses a window of type Nonequispaced Fast Fourier Transform (NFFT) with a size equal to the half of signal length and 50% overlap.

- Periodogram is the basic modulus-squared of the discrete Fourier transform.
- Bartlett's method is the average of the periodograms taken of multiple segments of the signal to reduce variance of the spectral density estimate.
- Welch's method is a windowed version of Bartlett's method that uses overlapping segments.

In our work, 11 frequency parameters are extracted from the power spectral density PSD: mean frequency MPF [124], peak frequency PF [125,126], deciles D1...D9 [127] that contain the median frequency D5 [126,127,128]. Deciles correspond to frequencies D1...D9 that divide the power spectral density into parts containing 10% of total energy.

$$\int_{D_{p-1}}^{D_p} S_x(f)df = 0.1 \int_0^{f_{max}} S_x(f)df \quad (3.1)$$

b) Parameters extracted from wavelet packet decomposition

The decomposition of signals into orthonormal bases (discrete wavelet transform) is based on the theory of multi-resolution analysis. This theory proves that we can analyze a signal by decomposing it into approximation and detail coefficients [129]. The wavelet packet transforms a signal from the time domain into time-frequency domain. Several families exist in wavelets such as Haar, Daubechies, and Symlets. Each window signal is split into an approximation and detail coefficients that are divided afresh into a second-level approximation coefficients and detail coefficients, and so on [130]. The approximations correspond to smoothed versions of the low-pass filtered signal, and the details contain only the information of high frequencies or discontinuities. As a final point, we calculate the variances on the following details levels 2, 3, 4, 5 and 6 (named W1, W2, W3, W4 and W5), which are used for classification as proposed by Diab et al. in [131] (see Figure 3.19).

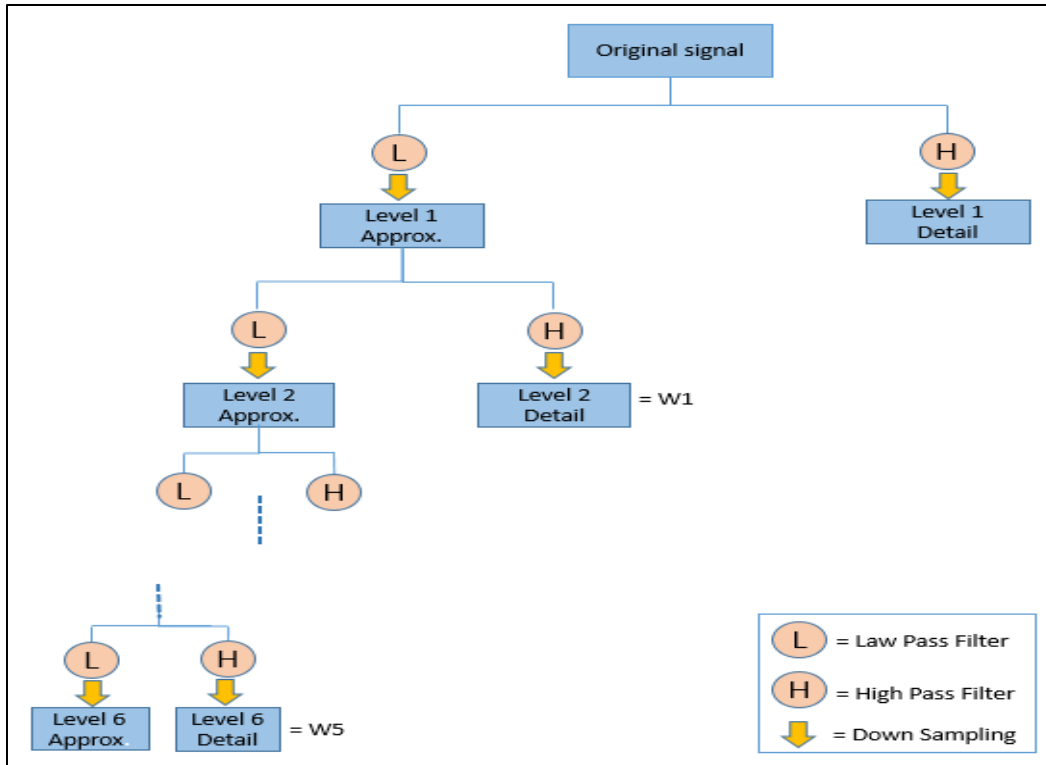


Figure 3.19 - Wavelet packet decomposition.

The sampling frequency used in our work is 25 Hz. Therefore the detail coefficients bandwidth are: Detail 2 [6.26 – 12.6 Hz], Detail 3 [3.13 – 6.26 Hz], Detail 4 [1.57 – 3.13 Hz], Detail 5 [0.79 – 1.57 Hz], and Detail 6 [0.4 – 0.79 Hz] (see Figure 3.20). These selected details contain more than 96% of the signal energy and cover the frequency band of interest.

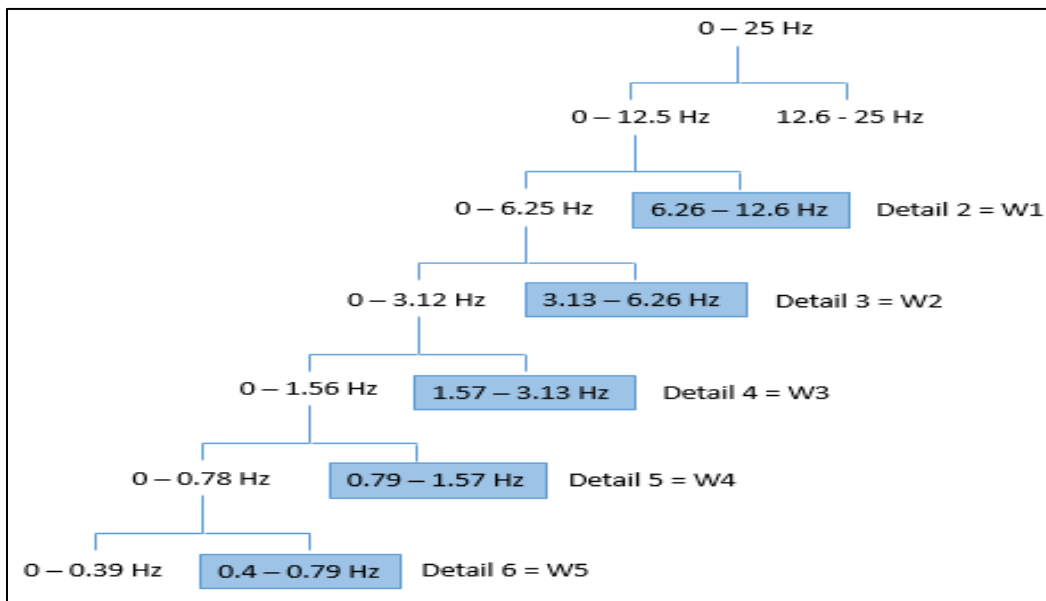


Figure 3.20 - Tree of the wavelet packet transform. The highlighted packets are the ones selected in this study.

III.2.4.2.2 Non-linear parameters**a) Time Reversibility (TR)**

TR tests if the process dynamics stay well defined when reversing the time-states' sequence. It is a good indication of nonlinearity. The TR characteristic of a signal x is then calculated as following:

$$Tr(\tau) = \frac{1}{N-\tau} \sum_{d=\tau+1}^N (x(d) - x(d - \tau))^3 \quad (3.2)$$

Where N is the signal length and τ is the time delay. For more details see [132].

b) Detrended Fluctuation Analysis (DFA)

DFA is an important method for measuring the autocorrelation of non-stationary signals by calculating the signal complexity using the fractal property [133]. It was first proposed by Peng et al. in 1995. This method is a modified root mean square method for the random walk. Mean square distance of the signal from the local trend line is analyzed as a function of scale parameter.

c) Lyapunov Exponent (LE)

LE studies the stability and the sensibility on initial conditions of the system. It measures the rate of trajectory separation between adjacent tracks in phase space [134,135]. In our study, we have used the equation (3) to calculate LE described in [134]:

$$\lambda = \lim_{t \rightarrow \infty} \lim_{\|\Delta_{d0}\| \rightarrow 0} \left(\frac{1}{t} \right) \log(\|\Delta_{dt}\| / \|\Delta_{d0}\|) \quad (3.3)$$

Where $\|\Delta_{d0}\|$ represents the Euclidean distance between two states of the system to an arbitrary time t_0 , and $\|\Delta_{dt}\|$ corresponds to the Euclidean distance between the two states of the system at a time later t .

d) Sample Entropy (SE)

SE is used to identify the regularity of signals. In our work, we have used the Sample Entropy described in [135]. They indicated that a least predictable time series have higher sample entropy. Considering a time series x which represents a signal of length N and patterns $aj(0, \dots, m - 1)$ of length m , with $m < N$, and $aj(i) = x(i + j)$; ($i = 0, \dots, m - 1$; $j = 0, \dots, N - m$). The time series x in a time $t = ts, x(ts, \dots, ts+m-1)$ as a match for a given pattern aj , if $|x(ts + i) - aj(i)| \leq r$ for each $0 \leq i < m$. Sample Entropy is then computed as follows:

$$SE_{m,r}(x) = \begin{cases} -\log\left(\frac{C_m}{C_{(m-1)}}\right): C_m \neq 0 \wedge C_{(m-1)} \neq 0 \\ -\log\left(\frac{N-m}{N-m-1}\right): C_m = 0 \vee C_{(m-1)} = 0 \end{cases} \quad (3.4)$$

Where the four parameters N , m , r and C_m represent, respectively, the length of the time series, the length of sequences to be compared, the tolerance for accepting, and the number of pattern matches (within a margin for r) that is constructed for each m . The value of r equals 0.2 according to the literature and m is determined by the method of the false nearest neighbors (FNN) [128].

III.2.4.2.3 Results of features extraction

As mentioned above, 20 parameters have been extracted from the original signals that can be used in order to improve the performance. The extracted parameters are shown in the “Figure 3.21.” in function of the number of windows. This signal is normalized before being drawn.

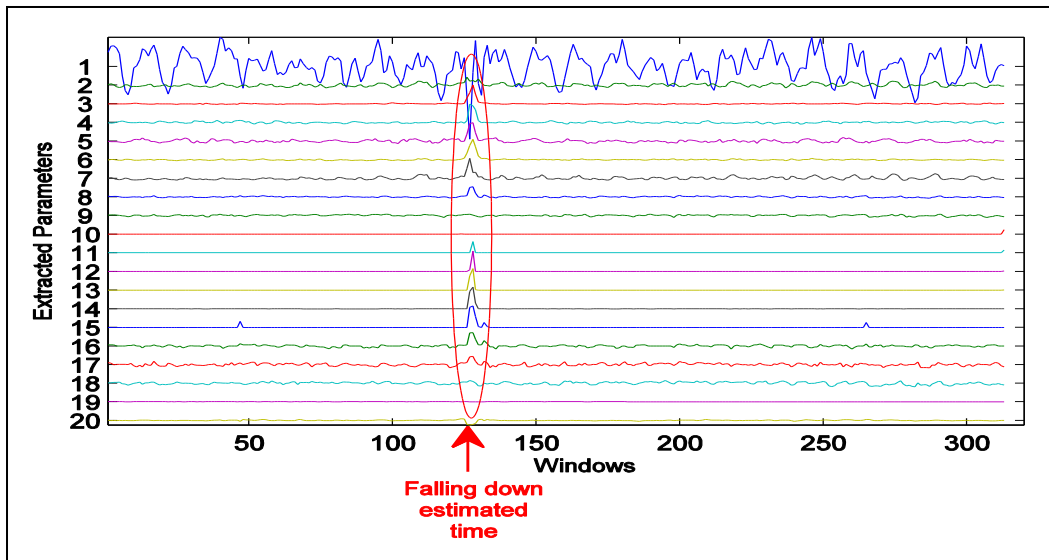


Figure 3.21 - Some Extracted Parameters (1: TR, 2: DFA, 3-7: Wavelet Packet decomposition parameters, 8: MPF, 9-18 Decil, 19: SE, and 20: LE).

It is clear that most of extracted parameters have a high peak in case of fall. So, the new target is now to select the most relevant one that separates between falling and non-falling case and then detect the modification on the signals when fall took places.

III.2.4.3 Feature selection

The number of parameters in a dataset has a direct impact on the dataset’s descriptive power. The more features a dataset has, the more expressive it is. However, finding meaningful

relationships among the instances and the class can be more difficult because the feature space grows exponentially with the number of features that causes problems in pattern recognition and classification techniques. On the other hand, by selecting only the features that best describe the input data and discarding redundant and noisy features, the size of the dataset is reduced and it is very helpful in improving the performance of learning algorithms regarding the speed of learning and the predictive accuracy [136].

In other words, feature selection is generally defined as a search process that is used to find a "relevant" subset of features F_{Best} from those of the starting subset of features F (see Figure 3.22). The notion of relevance of a chosen subset of features always depends on the objective function that evaluates applicant subsets and returns a measure of their “goodness”. This measure is used by the search strategy to select new applicants.

Assume that $F = \{ f_1, f_2, \dots, f_i, \dots, f_m \}$ is a set of features of size m , where m represents the total number of original features and $i=1$ to m . J is an evaluation function of a chosen subset of features. We assume that the greatest value of J will be obtained for the best subset of features.

The aim of the selection is to find a subset $F_{Best} = \{ f_{s1}, f_{s2}, \dots, f_{sj}, \dots, f_{sp} \}$ of size p ($p < m$), $s_j \in \{1 \dots m\}$, and $F_{Best} \subseteq F$ such as :

$$(F_{Best}) = \text{Max} (SC) \tag{3.5}$$

Where SC is a candidate subset of features, $SC \subseteq F$ and the size of SC can be a number, either already defined by the user, or controlled by one of the generation methods of subsets which will be described in the next section.

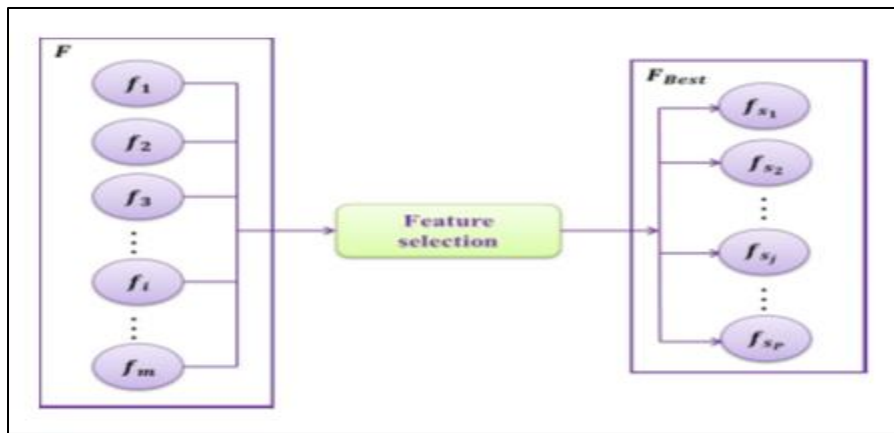


Figure 3.22 - Feature selection technique.

III.2.4.3.1 Feature selection process

The general process for a feature selection method is composed of four steps: subset generation, subset evaluation, stopping criterion, and result validation.

The subset generation is a research strategy that is used to select candidate feature subsets for evaluation [137]. Then, an evaluation criterion measures the goodness of this candidate subset, and then compares it with the previous best one in order to determine whether this subset is suitable or not. If the new candidate subset is found to be better, it replaces the previous best subset. These two processes are repeated until a given stopping criterion is satisfied. Finally, a validation part is used in order to check the validity of the selected best subset [138] (see Figure 3.23).

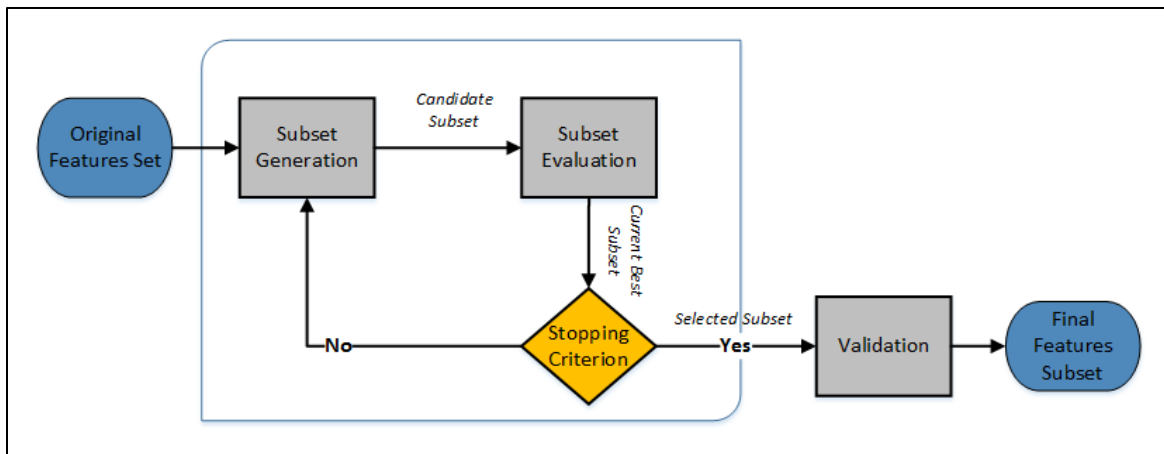


Figure 3.23 - Feature selection process.

a) Subset generation

The subset generation step in feature selection process usually falls into three categories [135]:

- *Exhaustive or complete search:* In this approach, a complete research on all subsets of features is performed to select the "best" subset of features. This research strategy ensures to find the optimal subset. The main problem of this approach is that the number of the possible subsets increases exponentially with the number of features, so it requires too much computing and time.
- *Heuristic search:* In this category, a heuristic approach to guide research is used. The algorithms that use this approach are usually iterative algorithms which each iteration allows selecting or rejecting one or more characteristics. Therefore, search can start with an empty set and successively add features (i.e., sequential forward selection), or start with a full set and successively remove features (i.e., sequential backward selection), or start with both ends

and add and remove features simultaneously (i.e., bidirectional selection or stepwise). Algorithms based on heuristic search are simple to implement and fast in producing results but they can complete the process with some risks of losing optimal subsets.

- *Random search:* The procedure of random search (also called stochastic or non-deterministic) is to randomly generate a finite number of sub-features sets to select the best. In addition, random search strategies converge quickly to a general "semi-optimal" solution, which is preferable to avoid the phenomenon of over-learning.

b) Subset evaluation

The methods used to evaluate a subset of features in the selection algorithms can be classified into three main categories: "filter", "wrapper" and "embedded".

i) Filter methods

The filter methods were first used for the features selection. In such methods, the subset selection procedure is independent of the learning algorithm and is generally a pre-processing step. The approaches that are based on this model often use a heuristic approach as a research strategy, and a feature relevance score is calculated to indicate the relevance [139]. The best subset of features obtained by this technique is presented as input to the classification algorithm. The main disadvantage of this method is that it disregards the influence of the selected feature on the performance of the classifier. Obviously, this leads to a faster learning pipeline but it is possible for the criterion used in the pre-processing step to result in a subset that may not work very well downstream in the learning algorithm [140,141,142]. The procedure of the filter model is illustrated in the "Figure 3.24".

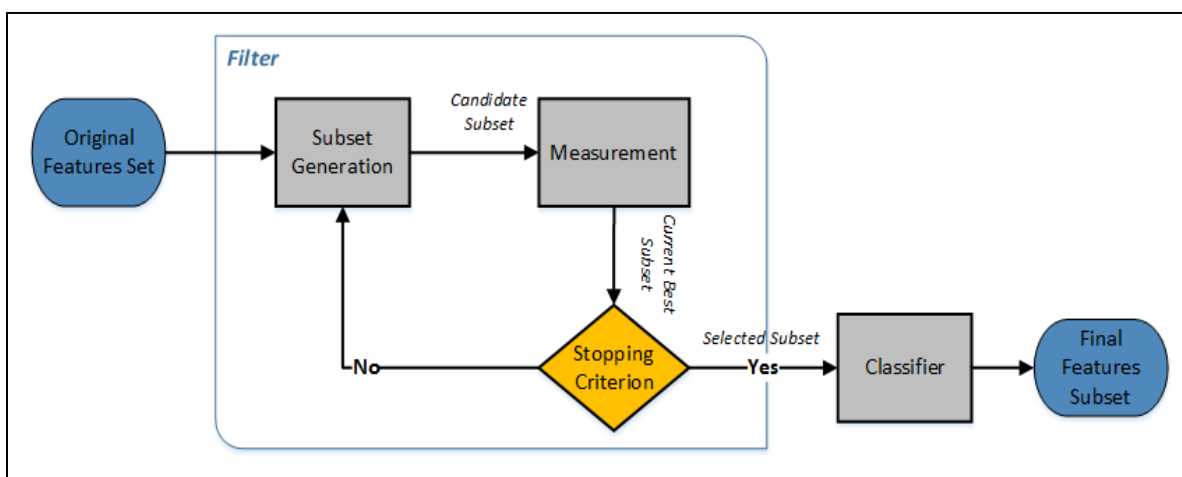


Figure 3.24 - Procedure of the filter model.

The most important measures used in the literature as score or evaluation criteria are:

- *Distance measures*: for a two-class classification problem, a feature f_1 is more relevant than another feature f_2 if f_1 leads to a greater difference between the conditional probabilities of the two classes than f_2 . Euclidean or other distances can be used here.
- *Information measures or entropy*: determine the information gain of a given feature. A feature f_1 is scored more than f_2 if the information gain is greater for f_1 than for f_2 .
- *Measures of dependences or correlations*: describe the ability to predict the value of a feature from another. In feature selection for classification, a feature f_1 is better than the feature f_2 if the correlation between the feature f_1 and class C is greater than the correlation of the feature f_2 and C .

ii) Wrapper methods

Unlike filter approaches, the subset selection takes place based on the learning algorithm used to train the model itself, and these methods allow detecting the possible interactions between features. The two main disadvantages of this method are the increasing of over-fitting risk when the number of observations is insufficient, and the significant computation time when the number of variables is large. Obviously, this means that computationally intensive learning algorithms cannot be used [143,144]. The procedure of the wrapper model is illustrated the “Figure 3.25”.

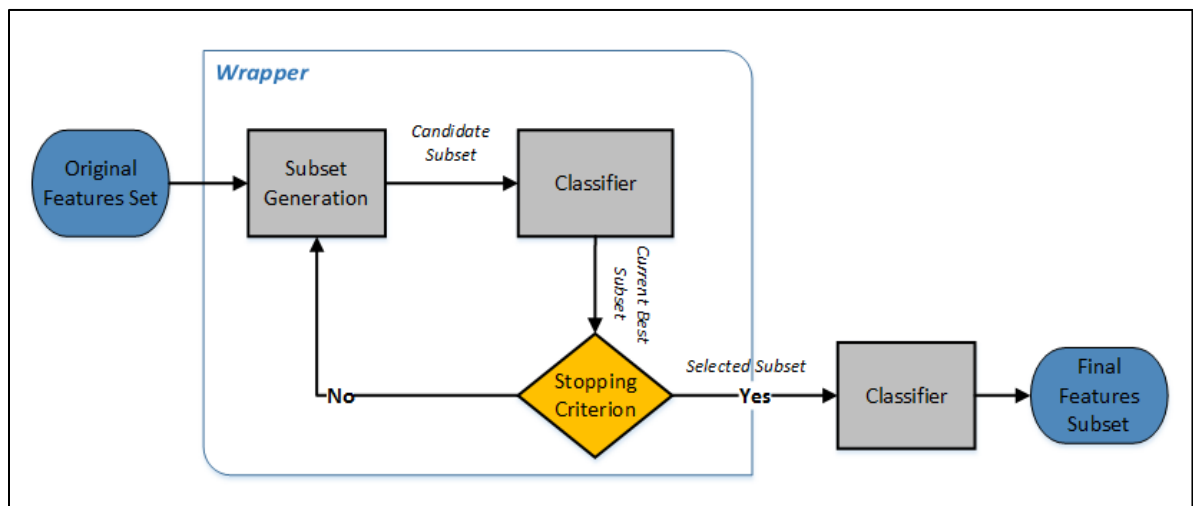


Figure 3.25 - Procedure of the wrapper model.

iii) Embedded methods

Recently, embedded methods have been proposed to reduce the classification of learning by combining the advantages of both previous methods. The search for an optimal subset of features

is included in the classifier construction and can be regarded as a search in the combined space of feature subsets and assumptions [145].

In this work, several wrapper and filter methods were used. The “Table 3.4” presents the advantages and disadvantages of these two techniques.

Method	Advantages	Disadvantages
Filter	Fast, Independent of classifier, Better computational complexity	Ignores interaction with classifier
Wrapper	Simple, Interacts with classifier, Models feature dependencies, Good classification accuracy	Computationally intensive, slow execution, risk of overfitting

Table 3.4 - Advantages and disadvantages of the filter and wrapper methods.

c) Stopping criteria

Some criteria must be defined to stop the search process such as:

- The search is completed
- A threshold is reached, like good rate of classification, minimum number of features or maximum number of iterations.
- There is no possibility of finding a subset better than the current subset.

d) Validation

A simple way for result validation is to directly measure the result using prior knowledge about the data. As in the case of synthetic data where the relevant features are known in advance, we can directly compare this known set of features with the selected features. However, in real-world applications where no prior knowledge are existed, we have to rely on some indirect methods by monitoring the change of mining performance with the change of features. For example, for a selected feature subset, if we use the classification error rate as a performance indicator, we can simply conduct the before and the after experiments to compare the error rate of the classifier learned on the full set of features and that learned on the selected subset [139].

III.2.4.3.2 Review of a few selection methods

In this part, we present some features selection methods of literature used in this work. We chose to present methods based on different research techniques defined previously as well as different techniques of evaluation. We also develop and theoretically examine a new method called Histogram Comparison Method (HCM), and a combination of this method with another well-known method called Sequential Forward Selection (SFS); HCM combined to SFS (HCM-SFS), these two methods are considered as contributions to this thesis.

a) Sequential Forward Selection (SFS)

SFS is the first method proposed in 1963 by Marill and Green for features selection. SFS starts with an empty data set and proceeds by expanding the data set with the feature, of which addition to the data set boosts the wrapped model performance most. The algorithm adds features in such manner recursively until stopping criteria is met [146]. The pseudo code of this method is presented in the “Algorithm 3.1”.

Algorithm 3.1: SFS

1. Input:
 $F = \{ f_1, f_2, \dots, f_i, \dots, f_m \}$, m : size of features, f_i is a vector of values for feature i of all observations O
 $C = \{ c_1, \dots, c_O \}$, C is vector of classes corresponding to each observation

2. Output:
 $F_{Best} = \{ f_{s1}, \dots, f_{sj}, \dots, f_{sP} \}$, P : size of features selected, ($P < m$), $sj \in \{1 \dots m\}$

3. Initialization:
 Start with an empty set of features $F_{Best} = \emptyset$, $Y = \emptyset$, $E = \emptyset$

4. While $|Y| \leq m$ $f_{add} = \arg \max_{f \notin Y} J(Y \cup f)$
 $E = E \cup \{J(Y \cup f_{add})\}$
 $Y = Y \cup f_{add}$
 End while

F_{Best} is the subset corresponding to $\min(E)$

5. Return F_{Best}

Starting with an empty subset, the value of the criterion function (J) is calculated for each feature by using a classifier. The feature presenting the best classification performance is selected (f_{add}) and then added to the subset (Y). The next step consists of adding sequentially the feature f_{add} that has the highest criterion function ($Y \cup f_{add}$) when combined with the set of features Y that has already been selected. In this work, SFS is implemented starting from a single parameter subset to the full parameters set in order to plot and analyze the classification error along the

complete procedure. Finally, the combination of features that have the minimum classification error is chosen.

b) Relief

Relief is a feature selection algorithm used in binary classification proposed by Kira et al in 1992 [147]. This method can estimate the quality of features through a type of nearest neighbor algorithm that selects neighbors (instances) from the same class and from the different classes. From the whole instances, a random sample (NS) is firstly chosen. An instance lj is selected randomly. "Near Hit" and "Near Miss" of the instance lj are calculated using the measure of Euclidean distance. "Near Hit (H)" is the nearest instance that belongs to the same class of the selected instance (having the minimum Euclidean distance with this instance). "Near Miss (M)" is the nearest instance that belongs to a different class of the selected instance. Therefore, weights (W) for each feature (fi) are estimated based on these Near Hits, and the Near Misses according to the following equation:

$$W_i = W_i - \frac{diff(f_{l,i}, f_{H,i})^2}{NS} + \frac{diff(f_{l,i}, f_{M,i})^2}{NS} \quad (3.6)$$

Where:

$f_{l,i}$ is the value of the feature fi for the instance l

$f_{H,i}$, $f_{M,i}$ are the neighborhoods H and M for the feature fi

If fi is:

- Nominal, $diff(f_{l,i}, I_{i,t}) = \begin{cases} 0 & \text{if value of } f_{l,i} \text{ and } I_{i,t} \text{ are equal} \\ 1 & \text{if the values are different} \end{cases}$
- Numerical, $diff(f_{l,i}, I_{i,t}) = \frac{val(f_{l,i}) - val(I_{i,t})}{\max(fi) - \min(fi)}$

Where $\max(fi)$ is the maximum value of the feature fi and $Val(fl,)$ is the value of the feature fi for the instance l .

This adjustment process of weights is repeated for NS instances. The Relief algorithm produces weights for each feature, and selected only the features having weights greater than or equal to a threshold. The Relief pseudo code is presented below in the "Algorithm 3.2".

Algorithm 3.2: Relief

1. Input:
 $F = \{ f_1, f_2, \dots, f_i, \dots, f_m \}$, m : size of features, f_i is a vector of values for feature i of all observations O
 $C = \{ c_1, c_2 \}$, C is vector of classes corresponding to each observation
 NS = Number of sample by default equal to 0

2. Output:
 $F_{Best} = \{ fs_1, \dots, fs_j, \dots, fs_p \}$, p : size of features selected, ($p < m$), $s_j \in \{1 \dots m\}$

3. Initialization:
Start with an empty set of features $F_{Best} = \emptyset$
Initialize all weights $W_i = 0$

4. for $j=1:NS$
Randomly selecting an instance (observation) l_j of the set of observations
Find their Near Hit (H) and Near Miss (M)
for $i=1:m$

$$W_i = W_i - \frac{\text{diff}(f_{L,i}, f_{H,i})^2}{NS} + \frac{\text{diff}(f_{L,i}, f_{M,i})^2}{NS}$$

end for
end for $W = \{ W_1, \dots, W_i, \dots, W_m \}$
for $i=1:m$
if $W_i > \text{Threshold}$
Add features f_i to F_{Best}
end if
end for

5. Return F_{Best}

c) ReliefF

Kononenko et al. propose a number of updates to Relief method, which works only with the two-class problems to the multiple-class problems. It aims to estimate the quality of features according to how well their values separate the instances according to their distance in the problem space. Given randomly selected instances, the algorithm searches for the k nearest neighbors from the same class and k nearest neighbors from each of the other possible classes. Based on which class do the neighbors belong to, the algorithm updates the feature quality information by increasing its value if the feature separates instances with different classes well and by decreasing its value in the opposite scenario. The process of random instance selection is repeated for several times, where the number of iterations is pre-chosen by the user [147]. The pseudo code of this method is presented in the “Algorithm 3.3”. In this work, we selected the features with weight value larger than the average value of all weights after being obtained.

Algorithm 3.3: ReliefF

1. Input
 $F = \{ f_1, f_2, \dots, f_i, \dots, f_m \}$, m : size of features, f_i is a vector of values for feature i of all observation O
 $C = \{ c_1, \dots, c_0 \}$, C is vector of classes corresponding to each observation
 NS = Number of sample by default equal to 0

2. Output:
 $F_{Best} = \{ f_{s1}, \dots, f_{sj}, \dots, f_{sp} \}$, p : size of features selected, ($p < m$), $s_j \in \{1 \dots m\}$

3. Initialization:
 Start with an empty set of features $F_{Best} = \emptyset$
 Initialize all weights $W_i = 0$

4. for $j=1:NS$
 Randomly selecting an instance l_j of the set of observations
 Find their q Near Hit $H = \{ H_1, H_2, \dots, H_t, \dots, H_q \}$
 and their q Near Miss $M = \{ M_1, M_2, \dots, M_t, \dots, M_q \}$
 for $i = 1 : m$

$$W_i = W_i - \sum_{t=1}^q \frac{\text{diff}(f_{l,i}, f_{H_t,i})^2}{NS * q} + \sum_{C \neq \text{class}(l_j)} \frac{\frac{P(C)}{1 - P(\text{class}(l_j))} \sum_{t=1}^q \frac{\text{diff}(f_{l,i}, f_{M_t,i})^2}{NS}}{NS * q}$$

% $P(C)$ is the probability of the class C which belongs to the “near miss” $f_{M_t,i}$
 end for
 end for
 $W = \{ W_1, \dots, W_i, \dots, W_m \}$
 for $i = 1 : m$
 if $W_i > \text{Threshold}$
 Add features f_i to F_{Best}
 end if
 end for

5. Return F_{Best}

d) F-score

F-score is a simple and effective criterion to measure the discrimination of each feature. Based on statistic characteristics, it is independent of the classifiers. F-score is given by the following equation:

$$F\text{-score}(i) = \frac{(\bar{X}_i^{(+)} - \bar{X}_i)^2 + (\bar{X}_i^{(-)} - \bar{X}_i)^2}{\frac{1}{n_+ - 1} \sum_{k=1}^{n_+} (X_{k,i}^{(+)} - \bar{X}_i^{(+)})^2 + \frac{1}{n_- - 1} \sum_{k=1}^{n_-} (X_{k,i}^{(-)} - \bar{X}_i^{(-)})^2} \quad (3.7)$$

Where $\bar{X}_i^{(+)}$, $\bar{X}_i^{(-)}$ and \bar{X}_i are the averages of the i th feature of the positive, negative and whole datasets; n_+ and n_- are the number of positive and negative instances respectively; and $X_{k,i}^{(+)}$ and $X_{k,i}^{(-)}$ are the i th feature of the k th positive instance and the i th feature of the k th negative instance. A larger F-score(i) indicates that the feature is more discriminative. A known deficiency of F-score is that it considers each feature separately and therefore cannot reveal mutual information between features. However, F-score is simple and generally quite effective [148]. In our work, we selected the feature with the highest F-score value. The pseudo code of this method is given in the “Algorithm 3.4”.

Algorithm 3.4: F-score

1. Input:
 $F = \{ f_1, f_2, \dots, f_i, \dots, f_m \}$, m : size of features, f_i is a vector of values for feature i of all observations O
 $C = \{ c_1, \dots, c_0 \}$, C is vector of classes corresponding to each observation

2. Output:
 $F_{Best} = \{ fs_1, \dots, fs_i, \dots, fs_p \}$, p : size of features selected, ($p < m$), $s_j \in \{1 \dots m\}$

3. Initialization:
Start with an empty set of features $F_{Best} = \emptyset$

4. for $i=1:m$

$$F\text{-score}(i) = \frac{(\bar{X}_i^{(+)} - \bar{X}_i)^2 + (\bar{X}_i^{(-)} - \bar{X}_i)^2}{\frac{1}{n_+ - 1} \sum_{k=1}^{n_+} (X_{k,i}^{(+)} - \bar{X}_i^{(+)})^2 + \frac{1}{n_- - 1} \sum_{k=1}^{n_-} (X_{k,i}^{(-)} - \bar{X}_i^{(-)})^2}$$

end for
 $F\text{-score} = \{ F\text{-score}(1), \dots, F\text{-score}(i), \dots, F\text{-score}(m) \}$
for $i=1:m$
if $F\text{-score}(i) > \text{Threshold}$
Add features f_i to F_{Best}
end if
end for

5. Return F_{Best}

e) Histogram Comparison Method (HCM)

The histogram is an important tool that represents the statistical characteristics of data. The histogram is used to represent the distribution of each feature extracted from the signal to be classified. HCM was proposed to measure similarity or dissimilarity for a given feature by comparing the distance of the two histograms. It is a novel filter model, which calculates the

discriminative ability of each feature separately. That is to say, features with higher distance have better separation ability in classification problems. The algorithm of HCM is defined as the following: We assume two-class classification problems. An instance is represented by a vector composed of m features values. For each feature f_i , we calculate the distance value (D_{f_i}) by going from the maximum value (Max_{f_i}) to the minimum value (Min_{f_i}) with a fixed threshold, and for each step, we count the difference between the numbers of instances of each class that are above the threshold (i.e. $d(f_i)$). Finally, we accumulate the differences denoted score value ($D_{f_i} = \sum d(f_i)$). The parameter that has the higher distance value is the most discriminant, and it was selected. HCM is computed as the follows:

$$D_{f_i} = \sum \sum_{threshold}^{Max_{f_i}} |N_i^+ - N_i^-| \quad (3.8)$$

Where N_i^+ and N_i^- are respectively the number of instances of the i th feature belong the first and the second class, that are above the threshold [21]. The pseudo code of this method is given in the “Algorithm 3.5”.

Algorithm 3.5: HCM

1. Input:

$F = \{ f_1, f_2, \dots, f_i, \dots, f_m \}$, m : size of features, f_i is a vector of values for feature i of all observations O

$C = \{ c_1, c_2 \}$, C is vector of classes corresponding to each observation

2. Output:

$F_{Best} = \{ f_{s1}, \dots, f_{sj}, \dots, f_{sp} \}$, p : size of features selected, ($p < m$), $sj \in \{1 \dots m\}$

3. Initialization:

Start with an empty set of features $F_{Best} = \emptyset$

4. for $i=1:m$

$$D_{f_i} = \sum \sum_{threshold}^{Max_{f_i}} |N_i^+ - N_i^-|$$

end for

$D = \{ D_{f_1}, \dots, D_{f_i}, \dots, D_{f_m} \}$

F_{Best} = the features having the most high values of D_f

5. Return F_{Best}

f) HCM-SFS

HCM can only examine the discriminative ability of each individual feature. Hence, features with low scores will be disregarded, even if they are complementary to the top features and might be very useful when they have combined with others parameters than were considered each one lonely. In the other hand, SFS yields the discriminative capacity of multiple features but it also suffers from the nesting effect; a parameter added in a given step cannot be removed during the next step. Hence, we introduce the HCM-SFS method, which combines the two previous methods HCM and SFS [21]. Relevant features selected by HCM are afresh passed to SFS for pick out the most pertinent features group of them. Consequently, we get rid from the problem of choosing features individually presented in HCM and also from nesting problem of SFS.

III.2.4.3.3 Results of feature selection

First, the developed HCM is tested to select the discriminative parameters on synthetic data and evaluate its efficiency compared to well-known methods in literature. Second, we will show the results of parameters' selection to select the most relevant parameters from the extracted set.

In this view, a synthetic database is generated with a Gaussian noise, composed of 200 observations that are divided into two classes each of 30 parameters around the value (0) for the first class, and around the value $(0 \pm \Delta)$ for the second class, where " Δ " is the difference between the two classes. Our aim is to test the efficiency of HCM regarding its accuracy to select relevant parameters and its time delay. Our method shows a good accuracy in relevant parameters selection. For a difference value between two classes (Δ) greater than 0.4, the error rate ratio is around 1% which is clearly lower than ReliefF (30%) and F-score (12%) as shown in the "Figure 3.26".

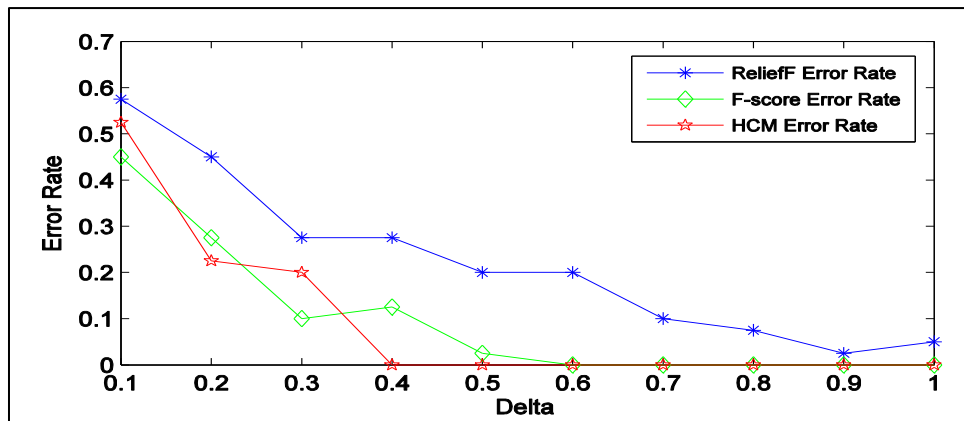


Figure 3.26 - Comparison of ReliefF, F-score, and HCM error rates.

We also have been noticed that the time latency of HCM (0.03s) is less than the ones of ReliefF (0.05s) and F-score (0.045s). This characteristic allows this method to be used in some applications where the time is critical. These results are taken from a machine with Intel® Core™ i5-3317U CPU @ 1.70GHz (4 CPUs), ~ 1.7GHz with 4GB RAM.

Since HCM identifies only the discriminative ability of individual feature, and SFS suffers from the nesting effect, we integrated the HCM-SFS method that determines the distinctive capacity of multiple features with better accuracy than SFS, especially for a low difference class's value ($\Delta < 0.4$). For example, the error rate ratio is decreasing from 72% to 28% for a ($\Delta = 0.1$) (see Figure 3.27).

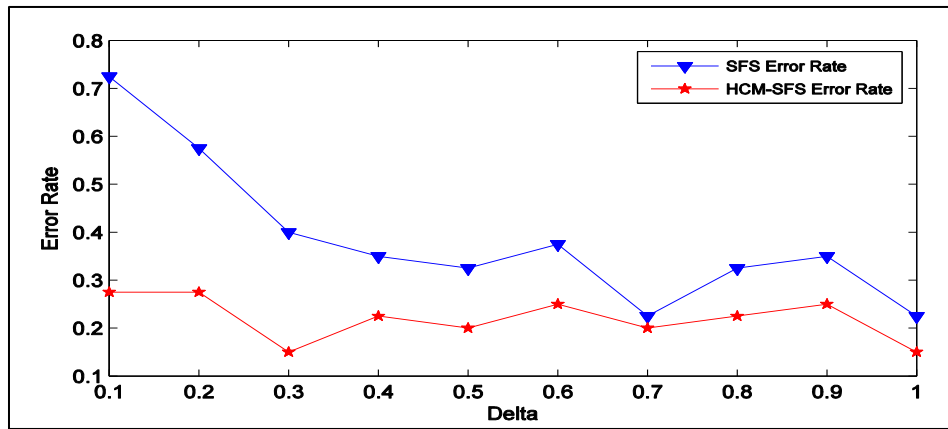


Figure 3.27 - Comparison of SFS and HCM-SFS error rates.

Thereafter, HCM is applied on the 20 extracted parameters to select the most relevant since it is more simple and fast. The “Figure 3.28” shows the relevance scale of the parameters.



Figure 2.28 - Relevance scale of the parameters.

Using one of the most three relevant parameters (D5, D6, and W3) instead of the original signals can reduce the dataset size and consequently improve the efficiency of our system. In this work, we choose the D5 as discriminative parameter to separate between falling and non-falling cases.

III.2.4.4 Signal change detection

Signal change detection is the ability to detect that a change occurred on the characteristics of a signal and making some inference about the actual time of change. Most detection algorithms are essentially based on the statistical theory of hypothesis testing that detects changes in the behavior of a stochastic process over time and makes some inference about the actual time of change [149]. The problem is to decide between two hypothesis (H_i) and (H_j) (see “Figure 3.29”). Identifying the likely time that a fall may have occurred is called change point identification.

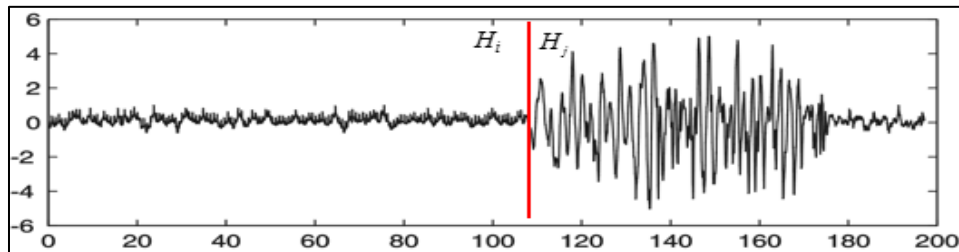


Figure 3.29 - Signal change detection.

III.2.4.4.1 Results of signal changing detection

Many scenarios containing different ADLs (walking, sitting, standing, lying down, and falling down) took place. Activities were made with different ways like soft and hard falls, fast and slow walking, falling from sitting and falling from walking. The aim is to detect the signal changing when fall occurs on time in order to discriminate between falling and non-falling states. The “Figure 3.30” shows the signal changing when a falling down occurs. Signals are normalized before being drawn.

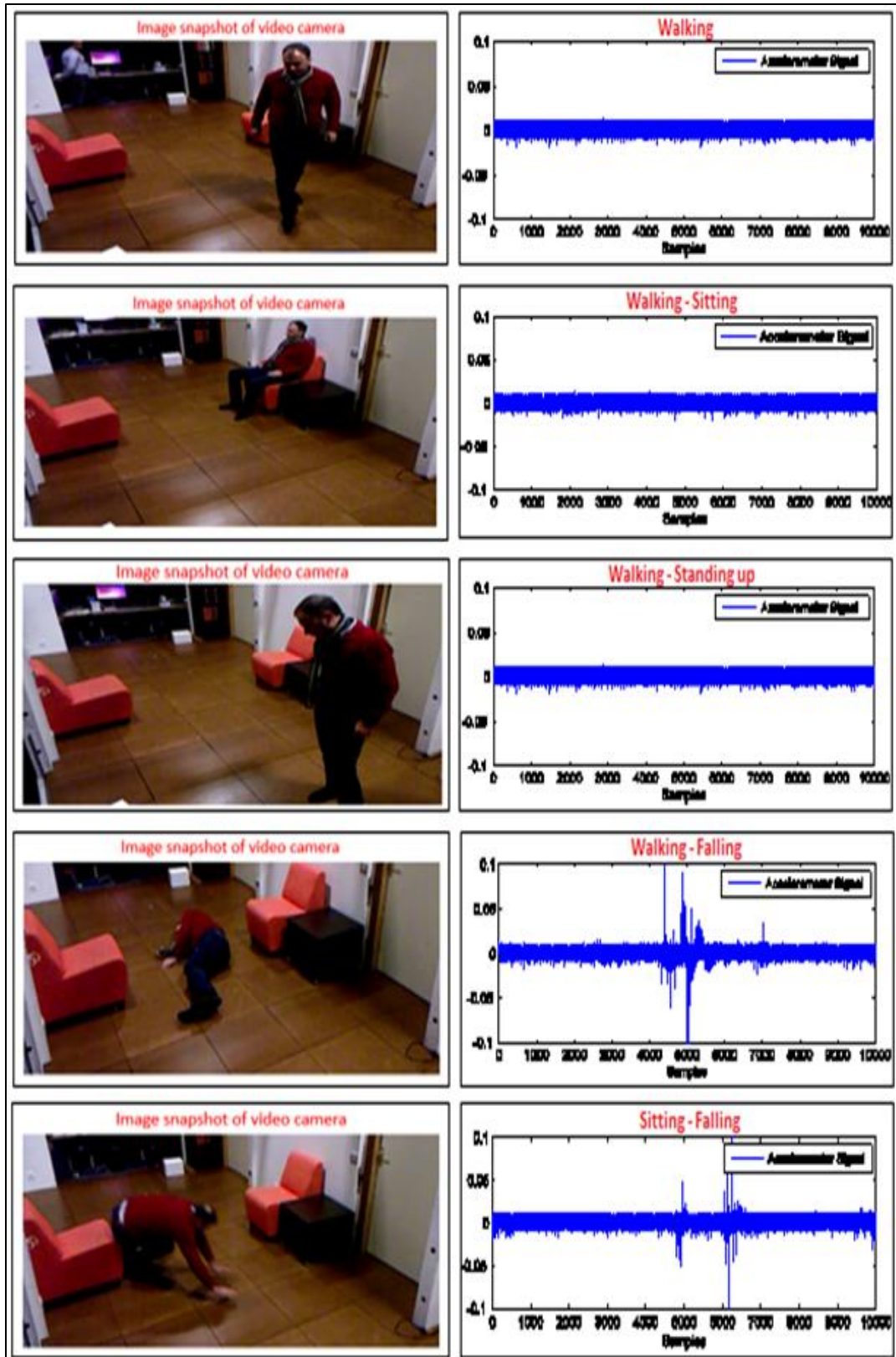


Figure 3.30 – An image snapshot taken from a RGB-D Kinect camera (left). The correspondent accelerometer signal (right). One can see the signal changing when a falling down case occurs.

Based on the hypothesis that most of extracted parameters have a high peak in case of human falls, we developed a threshold-based algorithm to detect the signal change when a fall down occurs. The “Figure 3.31” shows the extracted parameter “D5” from the accelerometer signal in (a), and the fall detection with a good accuracy in (b). The changing point identification has been also specified.

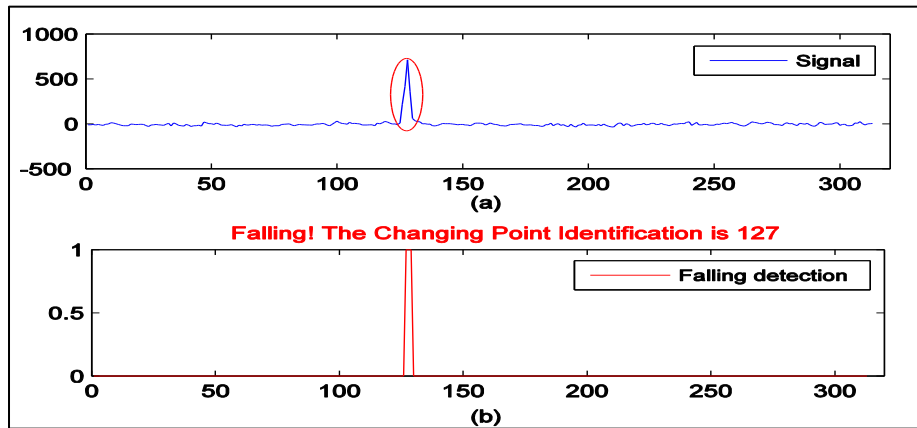


Figure 3.31 – Parameter changing detection when a fall occurs.

Thirty four falling down cases are tested using the proposed system. The results were very promising with a sensitivity of 94.1%.

III.2.5 Evaluation

Evaluation is an essential phase in this work to systematically assess the obtained results. Indeed, the ROC (Receiver Operating Characteristic) curves are frequently used as a tool for diagnostic test evaluation. A ROC curve is a graphical plot that illustrates the performance of a binary classifier system as its discrimination threshold is varied. It has been used for decades in many domains such as data mining and machine learning [150].

Consider a two-class prediction problem (binary classification), in which the outcomes are labeled either as positive (p) or negative (n). There are four possible outcomes from a binary classifier represented in a confusion matrix. If the outcome from a prediction is p and the actual value is also p, then it is called a true positive (TP); however if the actual value is n then it is said to be a false positive (FP). Conversely, a true negative (TN) has occurred when both the prediction outcome and the actual value are n, and false negative (FN) is when the prediction outcome is n while the actual value is p (see Figure 3.32).

		prediction outcome		total
		<i>p</i>	<i>n</i>	
actual value	<i>p'</i>	True Positive	False Negative	<i>P'</i>
	<i>n'</i>	False Positive	True Negative	<i>N'</i>
total		<i>P</i>	<i>N</i>	

Figure 3.32 – Confusion matrix

A ROC space is defined by FPR and TPR as *x* and *y* axes respectively, which depicts relative trade-offs between true positive (benefits) and false positive (costs). Since TPR is equivalent to sensitivity and FPR is equal to (1 - specificity), the ROC graph is sometimes called the sensitivity vs (1 - specificity) plot (see Figure 3.33). Each prediction result or instance of a confusion matrix represents one point in the ROC space.

- TPR is also known as sensitivity, recall or probability of detection = $\frac{\sum TP}{\sum \text{Positive Condition}}$

$$i.e. TPR = \frac{TP}{TP + FN} \tag{3.9}$$

- FPR is also known as fall-out or probability of false alarm = $\frac{\sum FP}{\sum \text{Negative Condition}}$

$$i.e. FPR = \frac{FP}{FP + TN} = 1 - \textit{Specificity} \tag{3.10}$$

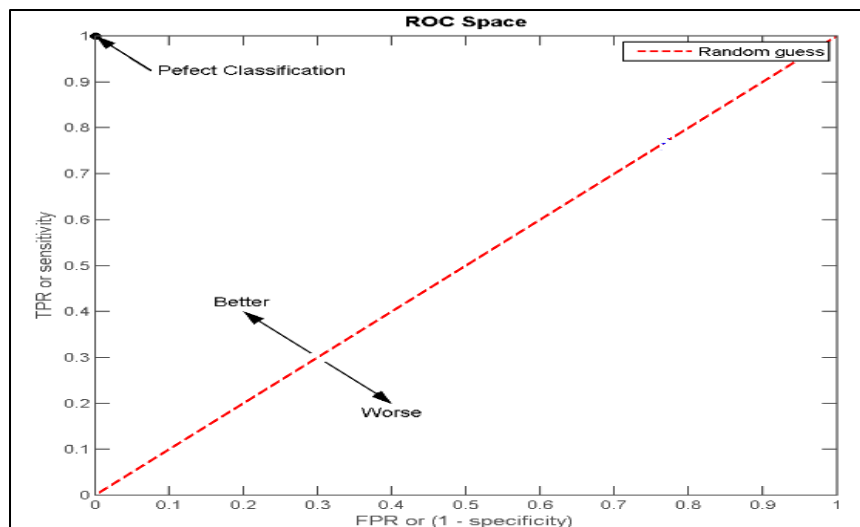


Figure 3.33 - ROC space.

The best prediction method would return a point coordinate (0,1) of the ROC space in the upper left corner, representing 100% sensitivity (no false negatives) and 100% specificity (no false positives). The (0,1) point is also called a perfect classification. A chance guess would give a point along a diagonal. The points above the diagonal represent good classification results, while the opposite points represent poor results.

In this work, the ROC curve is applied and the area under the curve (AUC) is calculated to compute the ability of each parameter to discriminate between falling and non-falling postures. AUC is chosen because it is the most used as an evaluation metric [151]. The more the AUC value is high, the more the parameter is discriminative (see Figure 3.34).

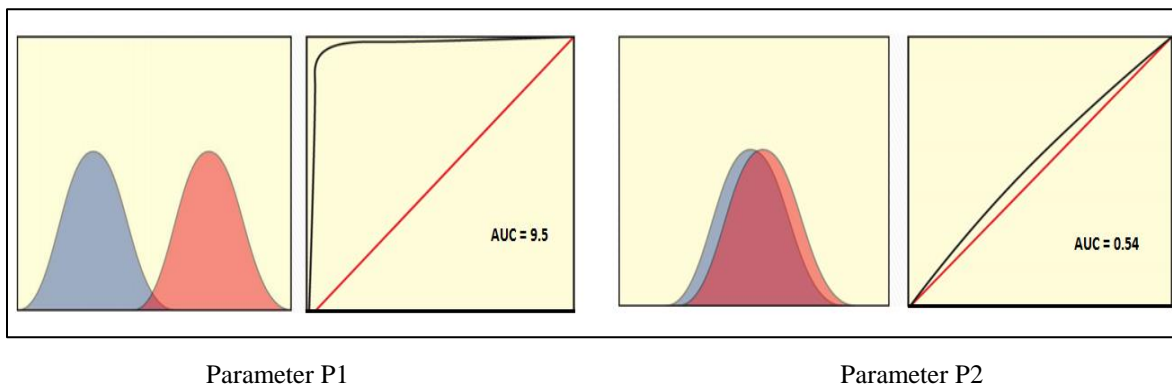


Figure 3.34 – For two parameters P1 and P2, the distribution probability (left) and the corresponding AUC (right).

Therefore, we compute the distribution probability of each parameter for all the falling cases and the non-falling cases then we calculate the AUC for each one in order to estimate each capability to discriminate between falling and non-falling cases. The results are presented in the “Table 3.5”.

Parameters	AUC	Accuracy	Sensitivity	Specificity	Test result
D5	0.875	0.875	1	0.75	Good
D6	0.875	0.875	1	0.75	Good
W3	0.85	0.85	0.75	0.75	Good
D4	0.75	0.75	0.75	0.75	Fair
W4	0.75	0.75	1	0.5	Fair
W5	0.725	0.75	1	0.5	Fair

W1	0.675	0.75	1	0.5	Poor
W2	0.675	0.75	1	0.5	Poor
MPF	0.65	0.75	0.5	1	Poor
D2	0.65	0.75	1	0.5	Poor
D3	0.65	0.75	0.75	0.5	Poor
D7	0.625	0.75	0.75	0.5	Poor
D8	0.625	0.75	0.5	0.5	Poor
LE	0.625	0.75	0.5	0.5	Poor
D9	0.575	0.625	0.75	0.75	Fail
DFA	0.575	0.625	0.75	0.75	Fail
TR	0.55	0.625	0.5	0.75	Fail
D1	0.525	0.625	0.75	0.5	Fail
D0	0.525	0.625	0.75	0.75	Fail
SE	0.5	0.625	0.5	0.5	Fail

Table 3.5 – The results of each parameter’s discrimination ability.

The first column contains the parameters extracted from the accelerometer signals. The second, third, fourth, and fifth columns contain the calculated values of the AUC, Accuracy, sensitivity, and specificity respectively. The sixth column describes the test result of each parameter based on the AUC interpretation values below [152].

AUC Interpretation:

- *0.91-1.0: Excellent*
- *0.81-0.9: Good*
- *0.71-0.8: Fair*
- *0.61-0.7: Poor*
- *0.51-0.6: Fail*
- *Remember that <0.5 is worse than guessing*

III.2.6 Conclusion

The objective of using the accelerometer under the tiles is to discriminate between falling and non-falling postures (see Figure 3.35). Upon this aim, a database was built from the collected accelerometer sensing floor signals.

Thereafter, many parameters were extracted from accelerometer signals. These parameters are stored in a smaller output dataset that are used in this work in order to increase the efficiency of the proposed system. The efficiency appears by improving the computational speed and the prediction accuracy of the proposed system.

Later, a novel and efficient algorithm called “HCM” was developed that aims to select the most relevant features. Results show a good efficiency in both accuracy and computation time compared to well-known methods in literature. Then, we apply a signal detection algorithm on the most pertinent feature to detect the signal’s changing in case of fall.

Results show that the proposed approach can easily distinguish between falling down and non-falling situations with a high accuracy.

The next contribution of this work is the merging between the load pressure sensors and the accelerometers decisions to get profit in both human fall detection and ADLs recognition.

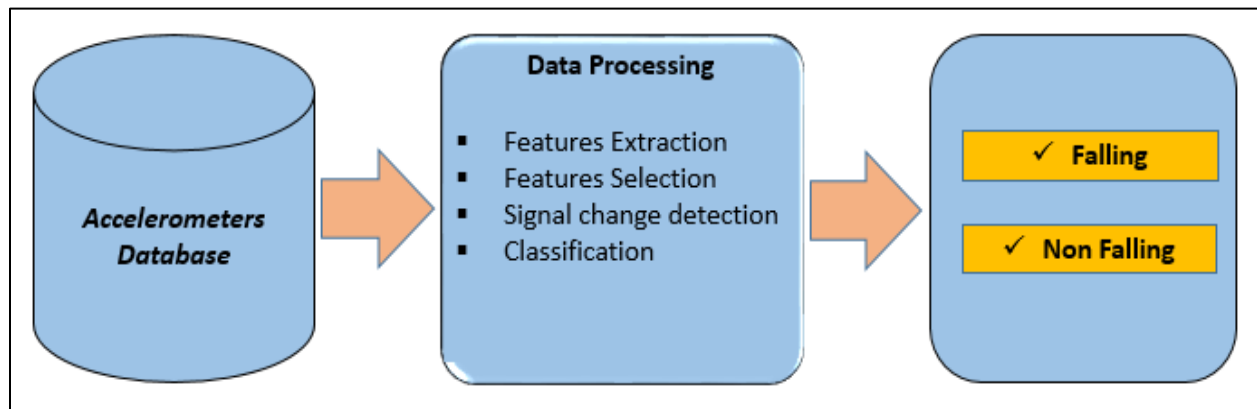


Figure 3.35 - Falling detection using accelerometer.

Section 3: Merging between the load pressure sensors results and the accelerometers decisions

III.3.1 Introduction

The previous two sections explored the capabilities the Inria Smart apartment and its sensing floor prototype as a tool for AmI.

First we started by exploiting the load pressure sensing floor. We gave an extensive account of the data collection and processing to localize, track and recognize elderly ADLs, using the weight information provided by the load sensing floor. We showed that the pressure sensors signals can be used to differentiate among walking, standing, and sitting states, but they confuse between falling down and lying down postures (see Figure 3.36).

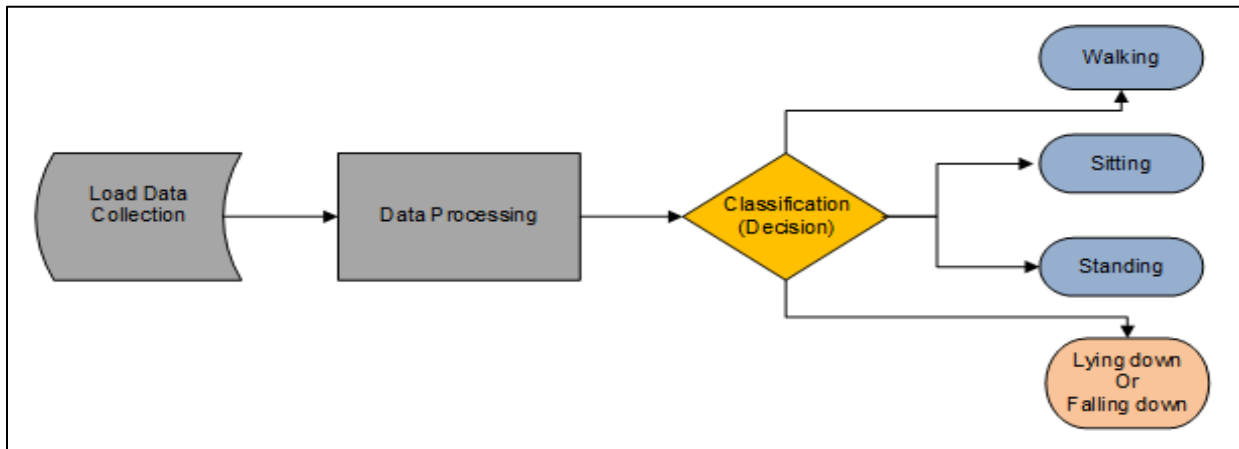


Figure 3.36 – ADLs recognition using load data.

Second, we have used the LSM tri-axial accelerometers embedded in the floor tiles to detect people falls. We finally succeed to differentiate between falling down cases and normal ADLs performed by humans (see Figure 3.37).

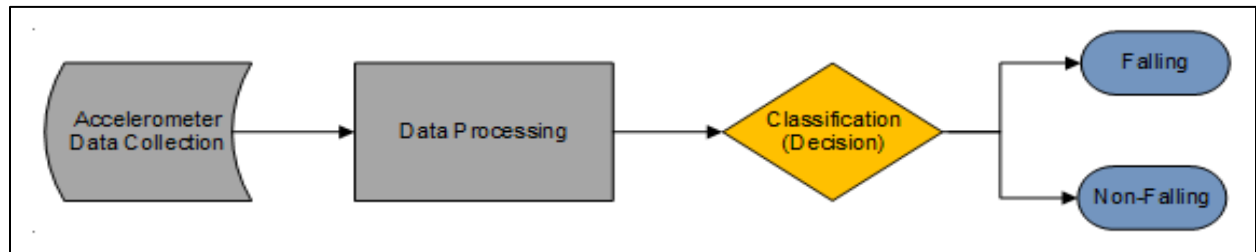


Figure 3.37 – Fall detection using accelerometer data.

Therefore, we propose to fuse the load sensor results with the accelerometer decisions to get profit in both elderly fall detection and ADLs recognition.

III.3.2 Merging between the load sensors results and the accelerometer decisions

We showed that the load pressure sensors can be used to differentiate between walking, standing, and sitting states, but they confuse between falling and lying down postures. We also showed that accelerometers could easily differentiate between the falling and non-falling states. Hence, by fusing the load sensors results and the accelerometers decisions, we can have a system that recognizes elderly ADLs and detect falling cases. The complete process flow chart of the system is shown in the “Figure 3.38”.

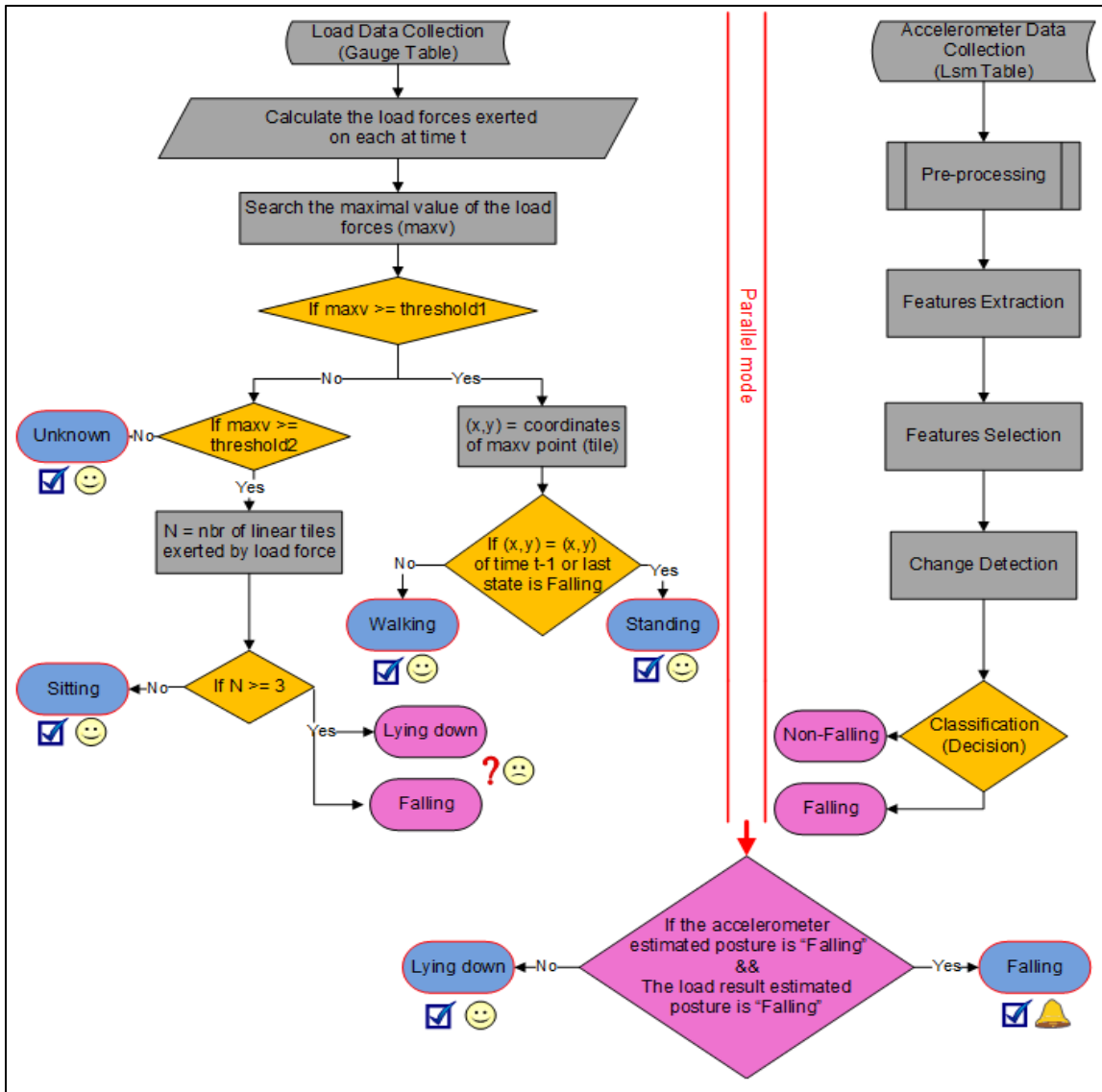


Figure 3.38 – Flow chart diagram of fusing the load sensors results and the accelerometer decisions.

III.3.3 Results

To test and validate the proposed system, ten different sequences with six different subjects were tested to show the accuracy and the efficiency of the proposed system. The “Table 3.6” shows the sensitivity results of both falling down detection and ADLs’ postures estimations.

Real postures	Estimated postures	Sensitivity
60 Unknown	60 Unknown	100%
150 Walking	148 Walking + 2 Standing Up	98.7%
65 Standing Up	60 Standing Up + 3 sitting + 2 Unknown	92.3%
42 Sitting	40 Sitting + 2 Unknown	95.2%
20 Lying down	18 Lying down + 1 Falling down	95%
34 Falling down	32 Falling down + 2 Lying down	94.1%

Table 3.6 – Sensitivity of falling down detection and ADLs’ postures estimations.

Thus, one can see that the proposed methods are accurate (the system sensitivity is greater than 94% for the fall detection of persons and more than 92% for the discrimination between the different ADLs).

III.3.4 Conclusion

This section shows how can the merging between the load pressure sensors results and the accelerometers decisions serve to enhance the system accuracy. By combining the load sensors results with the accelerometers decisions, the Inria Nancy - Grand Est sensing floor permits non-intrusively to locate and track elder, recognize their activities, and detect falling down cases (see Figure 3.39”). This would meet the practical objective of this thesis in AmI domain by offering assistive technology for elders living in their senior home.

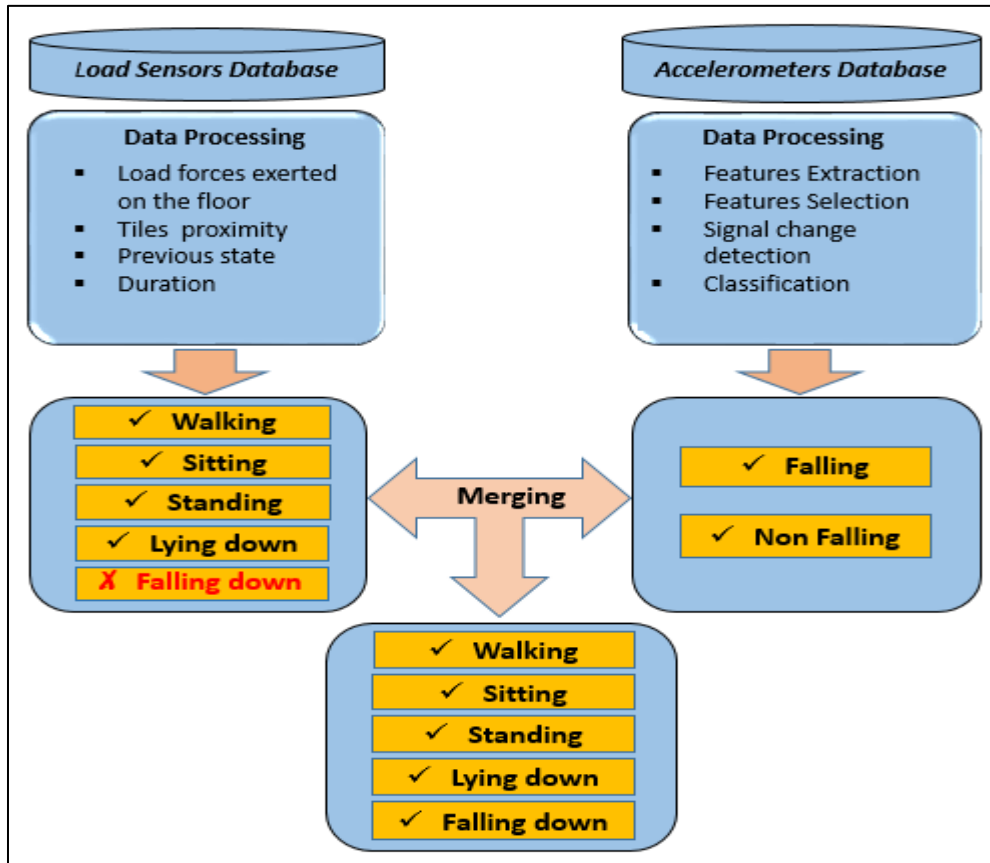


Figure 3.39 – ADLs recognition and fall detection.

General Conclusion

This chapter proposes a fine elder tracking, activities recognition, and fall detection system using a set of non-intrusive sensors. The proposed system is based on the merging between the results of the load pressure sensors and the accelerometers that are concealed under the smart tiles.

Actually, most of existing fall detection systems use wearable sensors mounted on the person or a camera-based systems that are uncomfortable to the elderly. Moreover, most of prevailing sensing floors are used to track, locate and detect human fall cases. Whereas, the idea behind this work is to provide a system that not only tracks, locates and detects elders' falls, but also recognizes their activities (walking, standing, sitting, lying down, and the transitions between them), using a set of non-intrusive sensors that grants privacy and comfort to the elders.

Indeed, the large-scale deployments of the proposed system require a large number of sensors and are expensive. However, due to the recent rapid advancement in information and communication technologies, sensors will be cheaper in the near future to reduce the cost of the system installation.

The main problem that emerged during this work is the faulty measurements that can be derived from sensors defects, which leads to significant false alarms. Another limitation of the previous algorithm is that it cannot track different people if they are close and exist on the same tile.

Consequently, the work is geared towards tracking people and adding a fault tolerance fusion method in the area of faulty sensors, which consist the core of the next chapter.

To end up, our challenge is to offer a user-friendly system with higher privacy and integrity within a reliable, efficient and affordable framework.

Chapter IV - Multisensory data fusion with detection and exclusion of faults based on Kullback-Leibler divergence

- Personal Localization System -

Overview

In the previous chapter, we have study how a network of load sensors combined with accelerometers concealed under smart tiles can be exploited to perform object localization and tracking, ADLs recognition and fall detection. One can observe that by merging load sensors and accelerometers decisions, we can locate and track people, recognize their main ADLs, and detect any falling case. This would meet the practical objective of this work in AmI domain by offering assistive technology for elders desiring live in their senior home. However, sensors are vulnerable to a plethora of different fault types and erroneous measurements that can compromise system accuracy and performance after their deployment.

Consequently, the work is geared towards tracking person(s) and adding a fault-tolerant fusion method in the area of faulty sensors. Therefore, there is a necessity of more than one data provider to permit the detection and exclusion of faulty measurements. Upon this aim, we propose integrating the distributed load pressure sensors with a simulated inertial measurement unit (IMU) assumed to be held by a person. IMU is chosen since it has a large usage in navigation and tracking applications, thus it can be used to track people while the load pressure sensors can provide redundant data to correct erroneous estimated tracks.

The main contributions of the work presented in this chapter are:

- Developing a method able simultaneously to localize people in addition to detecting and excluding the faulty sensors and erroneous measurements,
- Developing of a distributed architecture for multi-sensors data fusion with a measurements diagnosis,

- Developing of a residual for detection and isolation of erroneous measurements using an informational metrics based on the use of the Kullback-Leibler divergence.

The chapter is composed of two sections and a general conclusion:

- Section 1 presents the work positioning with a brief state of art,
- Section 2 is dedicated for the description of the proposed approach,
- General conclusion evaluates the performance of the developed approach and presents the perspectives.

Section 1: State of the art and work positioning

IV.1.1 Multisensory data fusion: definition and objectives

In general, data fusion refers to all tasks that demand any type of parameter estimation from multiple sources. Information fusion is typically employed as synonyms of data fusion; but in some scenarios, the term information fusion is employed to define already processed data, while the term data fusion is used for the data obtained directly from the sensors (raw data). In this sense, the term information fusion implies a higher semantic level than data fusion. Other terms associated with data fusion that typically appear in the literature include decision fusion, data combination, data aggregation, multi-sensors data fusion and sensors fusion [153].

Researchers in this field agree that the most accepted definition of data fusion was provided by the Joint Directors of Laboratories (JDL) workshop [154]: “A multi-level process dealing with the association, correlation, combination of data and information from single and multiple sources to achieve refined position, identify estimates and complete and timely assessments of situations, threats and their significance.”

In other words, data fusion can be defined as the combination of multiple data sources to provide a robust and complete description of an environment or process of interest. The goal is to obtain a lower detection error probability and a higher integrity and reliability by using data from multiple distributed sources. Data fusion is commonly used in detection and classification tasks in different application domains, such as military applications, positioning systems and robotics [155].

IV.1.2 Data fusion methods

The data fusion can be implemented using one of three theoretical frameworks: probability theory, belief theory, and possibilities theory. But, usually all of them share the following four steps [156]:

- Modeling: it consists in representing the information to be merged;
- Estimation: it depends on the modeling. It is not systematic but often necessary. For example, it consists in estimating the distributions of probabilities;
- Combination: this is the main step of the merge in which the data is grouped in order to obtain better information;

- **Decision:** this is the last step of the merger system. In this step, a decision criterion is used to judge the result of the fusion.

However, the most widely used data fusion methods employed in robotics, recognition, and navigation originate in the fields of statistics, estimation and control. Most of them are based on control system theory and employ the laws of probability to compute a vector state from a measurements vector or a stream of vector measurements. Indeed, probabilistic methods are now considered the standard approach to data fusion in all tracking and navigation applications [157]. Probabilistic data fusion methods are generally based on Bayes' rule for combining prior and observation information. Practically, this may be implemented in a number of ways: through the use of the Kalman and extended Kalman filters, through sequential Monte Carlo methods, or through the use of functional density estimates. Furthermore, there are a number of alternatives to probabilistic methods that include the theory of evidence and interval methods. These alternative techniques are not as widely used, but they still have special characteristics that may be useful in specific problems.

IV.1.2.1 Bayes' rule

Bayes' rule lies at the heart of most data fusion methods and it is based on probability theory and graph theory. To construct a Bayesian network, we must define an acyclic oriented graph representing knowledge. Each node of the graph is a random variable and the relations between the nodes are modeled in a probabilistic way [158]. In general, Bayes' rule provides a means to make inferences about an object or environment of interest described by a state \mathbf{x} , given an observation \mathbf{z} . These are methods Bayes' rule provides a means to make inferences about an object or environment of interest described by a state \mathbf{x} , given an observation \mathbf{z} using probability distribution $P(\mathbf{x}, \mathbf{z})$ [159].

$$P(\mathbf{x}|\mathbf{z}) = \frac{P(\mathbf{z}|\mathbf{x})P(\mathbf{x})}{P(\mathbf{z})} \quad (4.1)$$

IV.1.2.2 Kalman filter

In 1960, Rudolph Emil Kalman has introduced the Kalman filter (KF). It is an iterative mathematical process that uses a set of equations and consecutive data inputs to quickly estimate the true value (position, velocity, etc.) of the object being measured, when the measured values

contain unpredicted or random error, uncertainty, or variation. KF is a very popular fusion method that has been subject to extensive research and becoming a widely used tool when dealing with noisy systems [160]. The algorithm works in a two-step process: the prediction and the update. In the prediction step, the KF produces estimates of the current state variables, along with their uncertainties. Once the outcome of the next measurement (necessarily corrupted with some amount of error, including random noise) is observed, these estimates are updated using a weighted average, with more weight being given to estimates with higher certainty. The algorithm can run in real time recursively, using only the present input measurements and the previously calculated state and its uncertainty matrix; no additional past information is required.

KF yields the exact conditional probability estimate in the case that all errors are Gaussian-distributed. Extended Kalman filter (EKF) method that works on nonlinear systems has also been developed. The “Figure 4.1” shows the schema of how KF works.

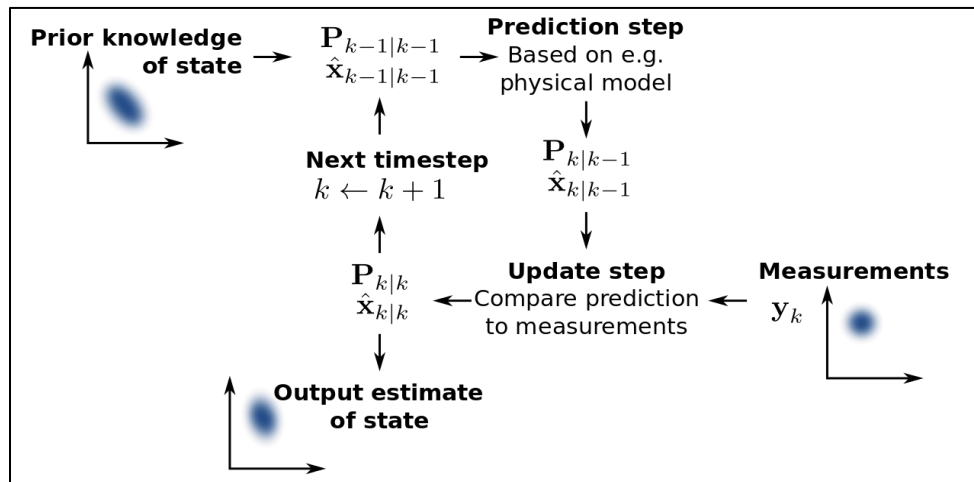


Figure 4.1 - Kalman filter schema: prediction and correction phase.

IV.1.2.3 The information filter for data fusion

The informational filter (IF) uses the informational form of the state vector and the covariance matrix respectively named information vector (y) and informational matrix (Y). Like the KF, the IF is broken down into two steps: a prediction step from the system evolution model and a correction step resulting from the use of the observations in the estimation procedure. Some advantages of the IF over KF are listed below [161,162]:

1. Computationally simple correction step that permits to easily manage a relatively high number of observations,
2. Although the prediction equations are more complex, prediction depends on a propagation coefficient, which is independent of the observations. Thus, it is easy to decouple and decentralize where the number of observations varies over time,
3. There are no gain or innovation covariance matrices and the maximum dimension of a matrix to be inverted is the state dimension, which is usually smaller than the observation dimensions in a multi-sensors system.

These characteristics provide the scalability and the fault tolerance to the system. Furthermore, in order to develop the information estimation method for nonlinear systems, the extended information filter (EIF) is used. The idea consists in applying the analytical approximations used in the case of the EKF [163,164].

IV.1.2.4 Sequential Monte Carlo Methods

Monte Carlo (MC) filter methods describe probability distributions as a set of weighted samples of an underlying state space. MC filtering then uses these samples to simulate probabilistic inference usually through Bayes' rule. Many samples or simulations are performed. By studying the statistics of these samples as they progress through the inference process, a probabilistic picture of the process being simulated can be built up. Probability distributions in this method are described in terms of a set of support points (state space values) x^i , $i = 1, \dots, N$, together with a corresponding set of normalized weights w^i , $i = 1, \dots, N$, where $\sum_i w^i = 1$. The support points and weights can be used to define a probability density function in the form: $P(x) \approx \sum_{i=1}^N w^i \delta(x - x^i)$. This particulate filter has two steps, a prediction step where the particles evolve according to the state model and a correction step where the weights are adjusted according to the observations [165,166].

IV.1.2.5 Alternatives to probability

The representation of uncertainty is essential to the problem of information fusion where a number of alternative modeling techniques have been proposed to deal with perceived limitations in probabilistic methods: the complexity, the inconsistency, and the precision of models. Three

main techniques put forward to address these issues; interval calculus [167], fuzzy logic [168], and the theory of evidence (Dempster-Shafer methods) [169].

IV.1.3 Data fusion consequences

Several issues may occur during multisource information fusion, such as the data inadequacy, correlation, inconsistency and disparateness [170]. One of the major problems in the sensors fusion is that the provided measurements may be false leading to an erroneous estimation. Hence the necessity of a diagnostic layer that can detect and locate sensor defects in order to exclude them from the fusion procedure to avoid loss of integrity of the method and provide a fault-tolerant system.

IV.1.4 Fault-tolerant multi-sensors data fusion

Fault tolerance means the ability of a system to perform a task despite the occurrence of defects, whether drift, bias, blockage, software fault of a noisy environment influencing the performance of the sensor. One of the ways to make a multi-sensors data fusion fault-tolerant method is to add a diagnostic layer of sensor measurements before using a recursive Bayesian filter. The diagnostic methods of faults are divided into three functions:

- Fault detection: detects the presence of a fault in the system,
- Fault isolation: locates or classifies the fault,
- Fault identification: determines the type and amplitude of the fault.

The objective of the proposed approach is to add a diagnostic layer that can detect and locate sensor defects in order to exclude them from the fusion procedure to avoid loss of integrity of the method. Thus, we focus on the isolation and elimination of these erroneous measurements from the fusion procedure (Fault Detection and Exclusion (FDE)) [171,172,173]. In this work, erroneous measurements can be derived from different circumstances (Such circumstances include IMU error measurements, load pressure sensor defect, tile vibration, offset error, and electromagnetic noise, etc.).

IV.1.4.1 Related works

Several fault-tolerant data fusion related works are presented in the two past decades [174]. A set of them is described below.

Dixon et al.

In 2001, Dixon et al. developed a method for wheeled mobile robot (WMR) fault detection based on kinematic and dynamic models of the WMR in the presence of faults [175]. They employ a torque filtering technique to develop a prediction error based fault detection residual. The structure of the prediction error allows for fault detection despite parametric uncertainty in the WMR model.

Escher et al.

In 2002, Escher et al. proposed a method of detection and exclusion of satellite defects based on a bank of Kalman filters [176]. This method was widely used in the area of GNSS to ensure the location integrity.

Kobayashi and Simon

In 2003, Kobayashi and Simon proposed an approach that uses a bank of Kalman filters for aircraft gas turbine engine sensor and actuator fault detection and isolation [177]. Each filter is designed to detect a specific sensor or actuator fault.

Xue et al.

In 2007, Xue et al. presented faulty detection and exclusion system for sensor defects of an aircraft engine using a bank of KF [178]. Each KF is designed on the base of a specific hypothesis, sensitive to a single sensor defect. If a fault occurs, all filters except the one using the correct assumption produce an error significant.

Ricquebourg et al.

Ricquebourg et al. proposed in 2007 a method based on the sensors redundancy and on the analysis of conflicts between data sources [179]. A source is considered to be failing if its conflict with the others is high. After detecting the failing source, its effect on the final decision is enfeebled without discarding it from the fusion procedure.

IV.1.4.2 Information tools for fault-tolerant data fusion

One of the first researchers who emphasized the importance of the IF in the field of data fusion was Durrant-Whyte [180]. The information form is often known by the canonic representation of the Gaussian distribution [181]. Nowadays, for the reason that IF has several advantages, and despite the fact that it is still less known than the KF, different applications use this filter especially in the localization and mapping domain [162]. The main advantage of the IF over the KF remains in the relative simplicity of the correction phase. This aspect seems very beneficial for the diagnostic methods based on this type of filter. For a system with n sensors, the fused information of the correction phase is simply the linear sum of information contributions from all sensors because the products of likelihoods are turned into sums [182].

The benefits of using information tools for fault-tolerant data fusion is explicitly shown in [183] where authors propose a new approach based on information filter and information theory to detect and to exclude the faulty sensors using Kullback-Leibler divergence. This approach is tested in two applications with very promising results. The first application is the fault-tolerant collaborative localization of a multi-robots system, while the second is the localization in outdoor environments using GNSS/odometer with a fault-tolerant aspect. The results show an interesting performance.

IV.1.5 Multi-sensors data fusion for positioning systems

Positioning system is a mechanism for determining the location of an object in space. Several technologies for this task exist ranging from worldwide coverage with meter accuracy to workspace coverage with centimeter accuracy [184]. It can be divided into two main categories based on application usage: outdoor and indoor positioning systems.

In outdoor scenarios, several well-known and widely used navigation systems such as the Global Positioning System (GPS), the Global Navigation Satellite System (GLONASS), BeiDou Navigation Satellite System (BDS) and Galileo Positioning System (GALILEO) [185]. All of these are satellite-based systems, which are not suitable to indoor location service, since satellite signal losses due to obstructions from buildings that decline sharply the system accuracy.

However, knowing the exact position of a person in real time is essential to many applications like personal localization system (PLS) for elderly and disabled people during emergency situations. They actually use radio waves, magnetic fields, or other sensory information collected

by mobile devices with diverse technologies (GPS, Wi-Fi, Bluetooth, ZigBee, Ultra-Wide Band, Ultrasounds, Infrared, etc). These technologies vary significantly in terms of accuracy, coverage, efficiency, security cost and power consumption which remain important challenges in indoor location systems [186,187].

Recently, due to the big demands of elderly care systems, several techniques have been developed by fusing two or more types of the existing technologies using a proper algorithm to get the needed performance.

IV.1.5.1 PLS related works

Over the two past decades, a large number of commercial and research in PLS domain have been developed. They generally aim to provide a high accuracy system (<30cm) in a small area.

WiFi Kid Tracker

In 2004, the cooperation between Bluesoft and KidSpotter companies has successfully deployed a child tracking application within LEGOLAND Denmark, one of the Europe's largest amusement parks [188]. The approach based on Bluesoft's AeroScout System that combines the RFID technology with the wireless sensor network technology for a tracking application. Parents rent the AeroScout WiFi tags with a wristband that their children wear inside the park. If the child gets separated from them, they simply send a text message (i.e., SMS) from their smart phones and receive an automated response indicating them the accurate location of the child.

Jin et al.

In 2007, Jin et al. presented an indoor positioning system called the Best Beacon Match (BBM) positioning method that uses the Zigbee technology [189]. The proposed system is suitable for a smart home system prototype. It has low infrastructure cost, needs low power consumption, and provides a high level security for persons. Unfortunately the accuracy was 1-10 meters.

Renaudin et al.

Renaudin et al. proposed in 2007 a hybrid system that combines Radio-frequency identification (RFID) beacons and dead reckoning [190]. The idea is that the first person must deploy an RFID beacon at a defined location and the system estimates the position of the following persons based

on the known location of the beacon. However, the position of the RFID beacons must be known and preinstalled, also the number of required beacons would be high.

Woodman and Harle

Woodman and Harle proposed in 2008 a pedestrian localization system for indoor environments that uses foot-mounted inertial unit, a detailed building model, and a particle filter [191]. Results show that the system can track a person to within 0.73 m 95% of the time.

Girard et al.

In 2011, Girard et al. described a real time indoor navigation that uses a combination of foot-mounted IMU, ultrasonic ranging, particle filtering and model-based navigation [192]. It uses a constant step length that is not suitable for real situations and some of the assumptions could be modified to further improve the overall performance of the system.

Chen and Lin

In 2012, Chen and Lin presented an indoor positioning system based on neural network. They trained the neural network with ZigBee link quality indicator to perform indoor location tracking. Results showed that the proposed system is useful [193].

Lee and Yim

In 2012, Lee and Yim described a few Wi-Fi based indoor positioning systems [194]. Two systems built by the fingerprinting technique that used the K-nearest neighbor (KNN) and the decision tree methods. They also described the extended Kalman filter (EKF) method for Wi-Fi based indoor positioning.

Rida et al.

In 2015, Rida et al. have designed an indoor location system based on Receive Signal Strength indicator (RSSI) of the Bluetooth low energy 4.0 (BLE) [195]. The system deploys equidistant access points (APs) on the ceiling that transmit a periodic beacon (every 0.4 second). Once a smart device pass in the broadcasting area, it locates the three APs having the highest signal strength. This information can be calculated using a localization algorithm (Dilatation). The method needs a large numbers of APs and has about [0.5-1] meter of error.

a) Current status of PLS

Despite the large number of commercial systems on the market, there still is no standard for PLS, and there is a lot of faintness [184]. In 2015, Poosamani and Rhee pointed out the weaknesses of existing methods as follows [196]:

- Most practical PLS use radio frequency signals or beacons that need particular devices.
- Fingerprinting methods using WiFi signal need deployment overhead and extensive calibration.
- PLS using smartphone sensors suffers from the high consuming battery energy.
- PLS using averaged received signal strength (RSS) of 2G cellular signals is difficult because RSS is related to many aspects.

This work presents a novel approach for PLS to locate elderly in their senior apartment by using wearable sensor(s) and sensory equipped infrastructure. The approach uses an informational framework for a fault-tolerant and multi-sensors data fusion with fault detection and exclusion.

Section 2: Proposed approach

IV.2.1 Problem statement

The main purpose of PLS is to track and locate people within a certain area. It is quite challenging due to the people random movements and considering that a person walking can have either one or two feet in contact with the floor depending on the phase of the step. Furthermore, multiple people can be moving on the same tile simultaneously, increasing the complexity and leading to an association problem as well, that is, the classified position corresponds to one or more persons being tracked. Moreover, signals from the IMU and the load pressure sensors are noisy and may be erroneous due to a sensor faulty, leading to incorrect localization and classification. To overcome these issues, we employ the popular EKF approach, where we assign one estimator to each person being tracked. We are interested in probabilistic methods in order to take advantage of the mathematical framework as well as statistical tools in order to develop a localization method tolerant to sensor defects. This is a method that can work in real time.

The main idea of this localization procedure is the fusion between the simulated IMU sensor measurements (used in the frame of an pedometer prediction model) that tracks the motion and the position of the elder person (this prediction model is named in the next by IMU prediction model) and the load pressure sensors concealed under the tiles that give a representation of the load distribution exerted by the person on the tiles (observation model for correction). These techniques aim to improve the localization integrity of the overall system considering the fact that a person's movement is more erratic when compared, for instance, with a robot being tracked.

In this work, the sensors redundancy makes the FDE algorithms more feasible in order to exclude the faulty sensors from the fusion procedure. Moreover, we present a distributed FDE method based on a bank of Extended Information Filter (EIF) [177] with residual tests based on the Kullback-Leibler divergence (KLD) [162,197,198]. The efficiency of the KLD is proven for the fault detection and exclusion for the case of a single person moving in the smart apartment.

IV.2.2 Inertial measurement unit (IMU)

An inertial measurement unit (IMU) is an electronic device that measures and reports a body's specific force, angular rate, and sometimes the magnetic field surrounding the body, using a combination of accelerometers, gyroscopes and magnetometers [199]. IMUs are very small in

size and can be installed on the person in such a way that they do not disturb his normal movements.

IV.2.2.1 IMU components, measurements and uses

An IMU is typically composed of the following components:

- Three accelerometers,
- Three gyroscopes,
- Digital signal processing hardware/software,
- Power conditioning,
- Communication hardware/software,
- An enclosure.

Three accelerometers and three gyroscopes are mounted at right angles to each other. Thus the acceleration can be measured independently in three axes: X, Y and Z (see Figure 4.2). The angular rate can be also measured around each of the acceleration axes [200].



Figure 4.2 – IMU axes.

IMU works by detecting linear acceleration using one or more accelerometers and rotational rate using one or more gyroscopes. Some also include a magnetometer, which is commonly used as a heading reference. Signals from the accelerometers and gyroscopes are processed through signal processing at a very high rate. Generally, IMUs are integrated into Inertial Navigation Systems (INS) that uses their raw measurements to calculate attitude, angular rates, linear velocity and position relative to a global reference frame. The IMU equipped INS forms the backbone for the navigation and control of many commercial and military vehicles such as manned aircraft, missiles, ships, submarines, and satellites.

Moreover, the low cost of IMUs has encouraged their propagation in many fields. They serve as orientation sensors in many consumer products such as smartphones and tablets. Some gaming

systems, fitness trackers and animation applications may also include IMUs to measure motion [201].

IV.2.2.2 IMU performance and erroneous measurements

Different variety of IMUs exists with the following performance range depending on applications types. Performance is based on levels of precision of both accelerometers and gyroscopes [202].

- From $0.1^\circ/\text{s}$ to $0.001^\circ/\text{h}$ for gyroscope.
- From 0.1 m/s^2 to 0.00001 m/s^2 for accelerometer.

Several types of errors can occur and limit the sensor accuracy [199]:

- Bias or offset error: this error derives from the difference between the nominal and actual offset points;
- Scale factor error: is the slope of the sensor signal (the relation between input and output);
- Misalignment error: due to imperfect mechanical mounting;
- Cross axis sensitivity: parasitical interference made by solicitation between orthogonal sensor axes;
- Noise: is a stochastic process and can be minimized using statistical techniques;
- Environment sensitivity: mainly sensitivity to thermal gradients and accelerations;
- Timing error (Latency): is the difference between the time when the IMU measures a motion and the time that an external source like the Global Navigation Satellite System (GNSS) measure the same motion.

An important factor for having a high performance is to understand the types of errors in the system and developing ways to reduce or remove them. The “Figure 4.3” shows some of these erroneous measurements.

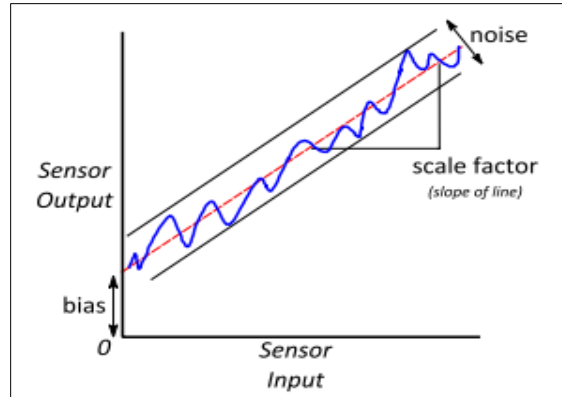


Figure 4.3 - Some of IMUs erroneous measurements.

The IMU chosen to build the IMU prediction model is the SparkFun 9DoF Razor IMU M0⁶ that combines a SAMD21 microprocessor with an MPU-9250 9DoF (9 Degrees of Freedom) sensor to create a tiny, reprogrammable and multi-purpose sensor (monitor and log motion, transmit Euler angles over a serial port or even act as a step-counting pedometer). It has three 3-axis sensors; an accelerometer, gyroscope and magnetometer; that offer the ability to sense linear acceleration, angular rotation velocity and magnetic field vectors.

IV.2.3 The load pressure sensors of the Inria Nancy – Grand Est platform

A load pressure sensor is a device that measures electrical resistance changes in response to, and proportional of strain, pressure or force applied to the device. Each tile of the Inria Nancy - Grand Est sensing floor is equipped with four load sensors concealed under the corners that measure the load forces exerted on the floor (see Chapter III, Section 1).

IV.2.4 IMU and load pressure sensors data fusion – Problem formulation

This work aims to offer a reliable and fault-tolerant system to track and monitor elderly. Upon this aim, we propose integrating the load pressure sensors and the simulated IMU measurements.

The data reported by the IMU is fed into a processor which calculates altitude, velocity and position of the person being tracked relative to a global reference frame. The angular rate collected from the gyroscope is used to calculate angular position. This is fused with the gravity vector measured by the accelerometers in a KF to estimated attitude. This attitude is used to transform acceleration measurements into an inertial reference frame where they are integrated once to get

⁶ <https://www.sparkfun.com/products/14001>

linear velocity, and twice to get global position. Thus, we can build an IMU prediction model to estimate the change in position over time. Such system has a good accuracy in the short term, but it drifts as soon as the distance traveled becomes great. Therefore, the position of the person needs to be corrected periodically.

Hence, the data reported by the load pressure sensors is used to correct this position based on the total weight of the person pressing on a tile and its distribution on the four sensors.

In this way, EIF is used and it consists of the following two phases:

- The evolution phase (or prediction step) where an IMU prediction model resulting from the IMU sensor measurements are used to locate and track the trajectory followed by a subject in order to derive the evolution model,
- The correction phase (or update step) where the relative observations of the load pressure sensors values are used to correct the predicted position. A certain translation is made to convert from the local position (derived from the load pressure distributions on the tiles) to the global position (derived from the IMU prediction model).

Note that the tracking of one person is presented here, where this approach can be generalized to more than one person by assigning one estimator to each of them.

IV.2.4.1 Prediction step using an evolution model

The propagation equations of the EIF are described using the IMU prediction model. At instant k , the state vector of a person is considered to be the position (x, y) and the orientation (θ) , namely the pose of the elder:

$$X_k = [x_k \ y_k \ \theta_k]^T \quad (4.2)$$

The propagation model is as shown below:

$$X_{k+1/k} = X_{k/k} + A_k u_k + w_k = f(X_{k/k}, u_k) + w_k \quad (4.3)$$

Where:

- $X_{k+1/k}$ is the estimate of X at time $k + 1$ given observations up to time k ,
- A_k is the input matrix,

$$A_k = \begin{bmatrix} \cos \theta_k & 0 \\ \sin \theta_k & 0 \\ 0 & 1 \end{bmatrix} \quad (4.4)$$

- u_k is the input vector, it consists of the elementary displacement and rotation of the person; which is usually calculated from the IMU measurements: $u = [\Delta, \omega]^T$. Δ is calculated using the distance formula derived from the Pythagorean theorem; for two points (x_1, y_1) and (x_2, y_2) , $\Delta = \sqrt{(x_2 - x_1)^2 + (y_2 - y_1)^2}$, and ω is given by gyroscope. In this work, Δ and ω are calculated using a camera-based sensing approach. By means of the mass center coordinates extracted from a simple RGB-D camera [203], we calculate Δ using the Pythagoras's theorem and ω using the arctangent function, i.e. $\omega = \arctan\left(\frac{y_2 - y_1}{x_2 - x_1}\right)$.
- w_k is the process state noise modeled as Gaussian white noise with zero mean and covariance matrix Q_k ,

$$X_{k+1/k} = \begin{bmatrix} x_{k+1} \\ y_{k+1} \\ \theta_{k+1} \end{bmatrix} = \begin{bmatrix} x_k \\ y_k \\ \theta_k \end{bmatrix} + \begin{bmatrix} \Delta_k \cos \theta_k \\ \Delta_k \sin \theta_k \\ w_k \end{bmatrix} + w_k = f(X_k, u_k) + w_k \quad (4.5)$$

Since the model is nonlinear, the EIF is applied. Therefore, the Jacobian matrices $F_k = \left. \frac{\partial f}{\partial X} \right|_{X_{k/k}}$ and $B_k = \left. \frac{\partial f}{\partial u} \right|_{u_k}$ are computed:

$$F_k = \begin{bmatrix} 1 & 0 & -\Delta_k \sin \theta_{k/k} \\ 0 & 1 & \Delta_k \cos \theta_{k/k} \\ 0 & 0 & 1 \end{bmatrix} \quad (4.6)$$

$$B_k = \begin{bmatrix} \cos \theta_{k/k} & -\Delta_k \sin \theta_{k/k} \\ \sin \theta_{k/k} & \Delta_k \cos \theta_{k/k} \\ 0 & 1 \end{bmatrix} \quad (4.7)$$

The covariance matrix corresponding to this evolution model is the following:

$$P_{k+1/k} = F_k P_{k/k} F_k^T + B_k (Q_u)_k B_k^T + Q_k \quad (4.8)$$

Where:

- $(Q_u)_k$ is covariance matrix associated with the noise of measurements associated to the input vector u_k .

Therefore, the informational matrix denoted $(Y_{k+1/k})$ and the information vector denoted $(y_{k+1/k})$ can be calculated as the following:

$$Y_{k+1/k} = P_{k+1/k}^{-1} \quad (4.9)$$

$$y_{k+1/k} = Y_{k+1/k} X_{k+1/k} \quad (4.10)$$

IV.2.4.2 Correction step using an observation model

The IMU prediction model used for tracking people suffers from accumulated error driven from measurement errors, however small, are gathered over time. This leads to 'drift': an ever-increasing difference between where the system estimates it is located and the actual real location. Thus, when a person presses on tiles, the weight is distributed over the pressure sensors under the tiles being exerted. These load pressures will be used to update the EIF that correct the person position on a tile.

The fusion of the load pressure sensors observations with the data coming from the IMU prediction model is carried out using the IF:

$$Y_{k/k} = Y_{k/k-1} + \sum_{i=1}^N I_i(k) \quad (4.11)$$

$$y_{k/k} = y_{k/k-1} + \sum_{i=1}^N i_i(k) \quad (4.12)$$

$$I_i(k) = H_{i,k}^T R_i^{-1}(k) H_{i,k} \quad (4.13)$$

$$i_i(k) = H_{i,k}^T R_i^{-1}(k) [(W_{i,k} - \widehat{W}_{i,k}) + H_{i,k} X_{k/k-1}] \quad (4.14)$$

A development of the IF and the EIF from the Bayes rules can be found in the reference [204].

Where

- $I_i(k)$ and $i_i(k)$ are the informational contributions associated with the measurement of the i^{th} load pressure sensor.
- $\widehat{W}_{i,k}$ is the estimated load pressure amount of the i^{th} load pressure sensor.
- $W_{i,k}$ is the measure received from the i^{th} load pressure sensor.

- $H_{i,k}$ is the i^{th} line of the matrix H_k that relates the parameters to be estimated to the observation measurements.
- N is the number of load pressure sensors under a tile.
- The noise associated with the load pressure sensors measurements is assumed to be uncorrelated. Similarly, each noise is assumed to be a Gaussian white noise of zero mean value and a covariance matrix R_i .

a) Load pressure estimation (\widehat{W}_i calculation)

As it is described in the “Chapter III, Section 1”, each tile of the Inria SmartTiles prototype is maintained by four load pressure sensors. For a person having a weight (W) and a position coordinates (x_L, y_L) in a tile plan of dimension L (see Figure 4.4), the estimated load pressures amount of the i^{th} load pressure sensor (\widehat{W}_i) can be calculated using the Newton's laws assuming the following criteria:

- The tiles and the sensors are rigid and flat (no vertical and horizontal displacement),
- The only points of contact between the tiles surface and the ground are the sensors,
- The ground is considered infinitely rigid,
- The surface is not supposed to be deformed,
- The weight ($W=mg$) is normal; where m is mass, and g is the gravitational field strength (about 9.81 m/s^2 on Earth); and the vertical forces “ \widehat{W}_i ” applied are perpendicular to its plane,
- The system is considered stable vertically and horizontally (using of pinned or fixed supports), than the system becomes statically determinate (or isostatic) [205].

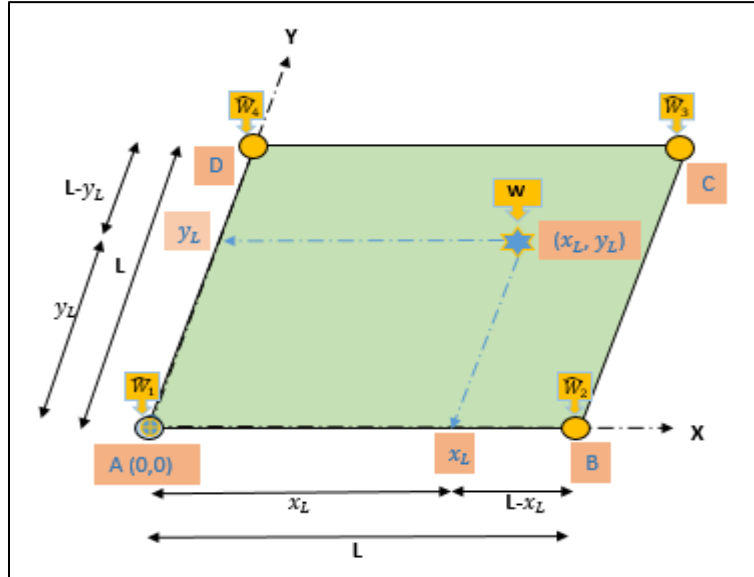


Figure 4.4 – A person having a weight of (W) and a position coordinates (x_L, y_L) in a tile plan of dimension L .

For a two-dimensional body and based on Newton's laws of motion, the available equilibrium equations are [206]:

- (i) $\sum \vec{F} = 0$: The vectorial sum of the forces acting on the body equals zero;
- (ii) $\sum \vec{M}_A = 0$: The sum of the moments (about an arbitrary point) of all forces equals zero.

$$(i): \sum \vec{F} = 0 \rightarrow W = \widehat{W}_1 + \widehat{W}_2 + \widehat{W}_3 + \widehat{W}_4$$

As the tile is square shaped and the only points of contact between the tiles surface and the ground are A, B, C and D, thus the weight (W) can be divided into two parts such that the ($\widehat{W}_1 + \widehat{W}_4$) on [AD] and ($\widehat{W}_2 + \widehat{W}_3$) on [BC] (see Figure 4.5).

Where:

$$\begin{cases} \widehat{W}_1 + \widehat{W}_4 = \frac{W \times (L - x_L)}{L} \\ \widehat{W}_2 + \widehat{W}_3 = \frac{W \times x_L}{L} \end{cases}$$

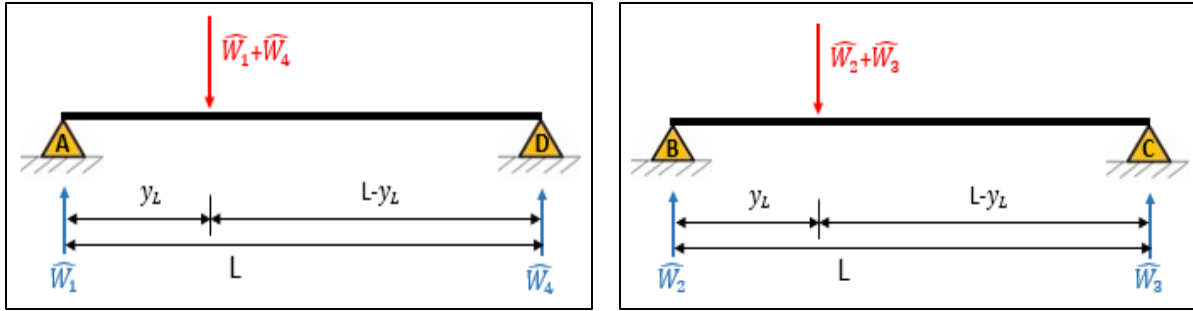


Figure 4.5 - The weight (W) is divided into two parts: $(\widehat{W}_1 + \widehat{W}_4)$ on [AD] (left) and $(\widehat{W}_2 + \widehat{W}_3)$ on [BC] (right).

$$(ii): \sum \overrightarrow{M}_A = 0 \Rightarrow -\widehat{W}_1 \times 0 + (\widehat{W}_1 + \widehat{W}_4) \times y_L - \widehat{W}_4 \times L = 0 \Rightarrow \widehat{W}_4 = \frac{W \times (L - x_L)y_L}{L^2}$$

$$\widehat{W}_1 = \frac{W \times (L - x_L)}{L} - \widehat{W}_4 \Rightarrow \widehat{W}_1 = \frac{W \times (L - x_L)(L - y_L)}{L^2}$$

$$\sum \overrightarrow{M}_B = 0 \Rightarrow -\widehat{W}_2 \times 0 + (\widehat{W}_2 + \widehat{W}_3) \times y_L - \widehat{W}_3 \times L = 0 \Rightarrow \widehat{W}_3 = \frac{W \times x_L y_L}{L^2}$$

$$\widehat{W}_2 = \frac{W \times x_L}{L} - \widehat{W}_3 \Rightarrow \widehat{W}_2 = \frac{W \times x_L(L - y_L)}{L^2}$$

$$\text{Thus, } \widehat{W} = \begin{bmatrix} \widehat{W}_1 \\ \widehat{W}_2 \\ \widehat{W}_3 \\ \widehat{W}_4 \end{bmatrix} = \begin{bmatrix} \frac{W \times (L - x_L)(L - y_L)}{L^2} \\ \frac{W \times x_L(L - y_L)}{L^2} \\ \frac{W \times x_L y_L}{L^2} \\ \frac{W \times (L - x_L)y_L}{L^2} \end{bmatrix}$$

Since the platform has a rectangular form with $(n \times m)$ tiles (see Figure 4.9), we can calculate the position (x, y) using the following equations:

$$x_L = x - [(i - 1) \% n] = x - k_1$$

$$y_L = y - (i \text{ div } n) = y - k_2$$

Where:

- $\%$ operation (modulo) is the remainder of the Euclidean division,
- div operation is the Euclidean division,

- i is the identifier for the tile,
- x_L and y_L are the local position coordinates (the origin is at the Bottom-Left of current tile having the identifier equal to i),
- x and y are the global position coordinates of a person where the origin (0,0) is at the bottom left corner of the platform (see Figure 4.6).

Therefore,

$$\hat{W} = \begin{bmatrix} \hat{W}_1 \\ \hat{W}_2 \\ \hat{W}_3 \\ \hat{W}_4 \end{bmatrix} = \begin{bmatrix} \frac{W \times (L - x + k_1)(L - y + k_2)}{L^2} \\ \frac{W \times (x - k_1)(L - y + k_2)}{L^2} \\ \frac{W \times (x - k_1)(y - k_2)}{L^2} \\ \frac{W \times (L - x + k_1)(y - k_2)}{L^2} \end{bmatrix} = h(X_k) \quad (4.15)$$



Figure 4.6 - The position coordinates of a person in the platform plan.

b) H_k calculation

As the observation model is non-linear, its linearization around the predicted pose yields the Jacobian:

$$H_k = \left. \frac{\partial h}{\partial X} \right|_{X=X_{k/k-1}} \Rightarrow H_k = \left[\frac{\partial W_i}{\partial X_k} \right] = \begin{bmatrix} \frac{\partial W_1}{\partial X_k} \\ \frac{\partial W_2}{\partial X_k} \\ \frac{\partial W_3}{\partial X_k} \\ \frac{\partial W_4}{\partial X_k} \\ \frac{\partial W_4}{\partial X_k} \end{bmatrix}$$

Where $\frac{\partial W_i}{\partial X_k} = \begin{bmatrix} \frac{\partial W_i}{\partial x} & \frac{\partial W_i}{\partial y} & \frac{\partial W_i}{\partial \theta} \end{bmatrix}$

$$\Rightarrow H_k = \begin{bmatrix} \frac{\partial W_1}{\partial x} & \frac{\partial W_1}{\partial y} & \frac{\partial W_1}{\partial \theta} \\ \frac{\partial W_2}{\partial x} & \frac{\partial W_2}{\partial y} & \frac{\partial W_2}{\partial \theta} \\ \frac{\partial W_3}{\partial x} & \frac{\partial W_3}{\partial y} & \frac{\partial W_3}{\partial \theta} \\ \frac{\partial W_4}{\partial x} & \frac{\partial W_4}{\partial y} & \frac{\partial W_4}{\partial \theta} \\ \frac{\partial W_4}{\partial x} & \frac{\partial W_4}{\partial y} & \frac{\partial W_4}{\partial \theta} \end{bmatrix}_{k/k-1}$$

$$\begin{cases} \frac{\partial W_1}{\partial x} = \frac{-W}{L^2}(L - y + k_2) \\ \frac{\partial W_1}{\partial y} = \frac{-W}{L^2}(L - x + k_1) \\ \frac{\partial W_1}{\partial \theta} = 0 \end{cases}$$

$$\begin{cases} \frac{\partial W_2}{\partial x} = \frac{W}{L^2}(L - y + k_2) \\ \frac{\partial W_2}{\partial y} = \frac{-W}{L^2}(x - k_1) \\ \frac{\partial W_2}{\partial \theta} = 0 \end{cases}$$

$$\begin{cases} \frac{\partial W_3}{\partial x} = \frac{W}{L^2}(y - k_2) \\ \frac{\partial W_3}{\partial y} = \frac{W}{L^2}(x - k_1) \\ \frac{\partial W_3}{\partial \theta} = 0 \end{cases}$$

$$\begin{cases} \frac{\partial W_4}{\partial x} = \frac{-W}{L^2}(y - k_2) \\ \frac{\partial W_4}{\partial y} = \frac{W}{L^2}(L - x + k_1) \\ \frac{\partial W_4}{\partial \theta} = 0 \end{cases}$$

$$\text{Then, } H_k = \begin{bmatrix} \frac{-W(L-y+k_2)}{L^2} & \frac{-W(L-x+k_1)}{L^2} & 0 \\ \frac{W(L-y+k_2)}{L^2} & \frac{-W(x-k_1)}{L^2} & 0 \\ \frac{W(y-k_2)}{L^2} & \frac{W(x-k_1)}{L^2} & 0 \\ \frac{-W(y-k_2)}{L^2} & \frac{W(L-x+k_1)}{L^2} & 0 \end{bmatrix}_{k/k-1} \quad (4.16)$$

IV.2.5 Fault detection and exclusion using informational framework

The FDE aims to enable systems to continue to operate in the presence of some erroneous measurements.

IV.2.5.1 Fault detection

In this section, we propose a method for detection and exclusion of defects based on the use of *KLD* for residual synthesizing. The *KLD* permit to compute the divergence between two probability density functions (pdf) [10]. Recall that the *KLD* from pdf q to pdf p is defined as:

$$KL(p||q) = \int p(X) \log\left(\frac{p(X)}{q(X)}\right) dX \quad (4.17)$$

The *KLD* can be written in the form:

$$\begin{aligned} KLD(f(x)||g(x)) \\ = \frac{1}{2} \left[\text{trace}(P_2^{-1}P_1) + \log\left(\det\left(\frac{P_2}{P_1}\right)\right) - d \right. \\ \left. + (\mu_1 - \mu_2)^T P_2^{-1}(\mu_1 - \mu_2) \right] \end{aligned} \quad (4.18)$$

Where \log represents the natural logarithm, and (P_1, μ_1) , (P_2, μ_2) are the covariance matrices and the means of two Gaussian distributions $f(x)$ and $g(x)$.

This informational metric can be considered as the expected Log Likelihood Ratio (LLR) [207]. It takes in consideration the Mahalanobis distance and the orientation and the compactness of the data distributions represented by the trace and the determinant of the covariance matrices.

The *KLD* between the data distribution obtained in the predicted step of the EIF ($g(k/k-1)$) and the equation obtained in the corrected step ($g(k/k)$) is called the Global Kullback-Leibler Divergence (*GKLD*) [30] and has the form:

$$\begin{aligned} GKLD &= KLD(g(k/k-1) \| g(k/k)) \\ &= \frac{1}{2} \left[\text{trace}(Y_{k/k} Y_{k/k-1}^{-1}) + \log \frac{|Y_{k/k-1}|}{|Y_{k/k}|} - M \right. \\ &\quad \left. + (X_{k/k} - X_{k/k-1})^T Y_{k/k} (X_{k/k} - X_{k/k-1}) \right] \end{aligned} \quad (4.19)$$

Where M is the dimension of the state vector.

The efficiency of this divergence has been proven for sensors fault detection and exclusion for a system of one or more robots moving in indoor or outdoor environments [162,183].

This equation takes the form of a residual test to detect the presence of the defect in the load pressure sensors as well as in the simulated IMU.

The *GKLD* measures the divergence between the posterior and the prior distributions obtained from the informational filter. If the *GKLD* exceeds a predetermined threshold, this implies a divergence of the estimate obtained after incorporating observations from the load pressure sensors with respect to the estimate obtained from the IMU prediction model. Once the convergence of the informational filter is obtained, this divergence is the sign of a defect.

Note that the threshold is preset based on the determination of a false alarm probability.

IV.2.5.2 Fault isolation

After a faulty measurement detection, the erroneous measurement must be identified in order to be excluded from the fusion procedure. For that reason, N (EIF _{j}) filters are designed in such way that each filter uses the measurements of the load pressure sensor j . The statistical test associated with each filter is obtained from the calculation of the KL divergence between the corrected state using the j^{th} load sensor measurements and the predicted state using the IMU prediction model. This residual is named the Partial Kullback-Leibler Divergence (*PKLD*) and can be represented by the equation below:

$$\begin{aligned}
 PKLD_{j,k} = & \frac{1}{2} \text{trace}(Y_{j,k/k} Y_{k/k-1}^{-1}) + \frac{1}{2} \log \frac{|Y_{k/k-1}|}{|Y_{j,k/k}|} - \frac{1}{2} M \\
 & + \frac{1}{2} (X_{j,k/k} - X_{k/k-1})^T Y_{j,k/k} (X_{j,k/k} - X_{k/k-1}) \quad (4.20)
 \end{aligned}$$

Where:

$$Y_{j,k/k} = Y_{k/k-1} + I_j(k) \quad (4.21)$$

$$y_{j,k/k} = y_{k/k-1} + i_j(k) \quad (4.22)$$

$$X_{j,k/k} = (Y_{j,k/k})^{-1} y_{j,k/k} \quad (4.23)$$

In the case where a $PKLD_j$ surpasses a predefined threshold, yet the j^{th} load pressure sensor may be then defected, and consequently it will be taken out from the fusion process. A significant increasing in all $PKLD_j$ implies that the erroneous measurements come probably from the simulated IMU, so the faulty IMU prediction model measurements will be excluded from the fusion procedure. While a significant increasing in at most three of the four $PKLD_j$ implies that the corresponding sensors are defected, and then the four load pressure sensors of the same tile are excluded from the fusion procedure. The “Fig. 5” shows the procedure for fault detection and exclusion using the filter bank with the corresponding residues.

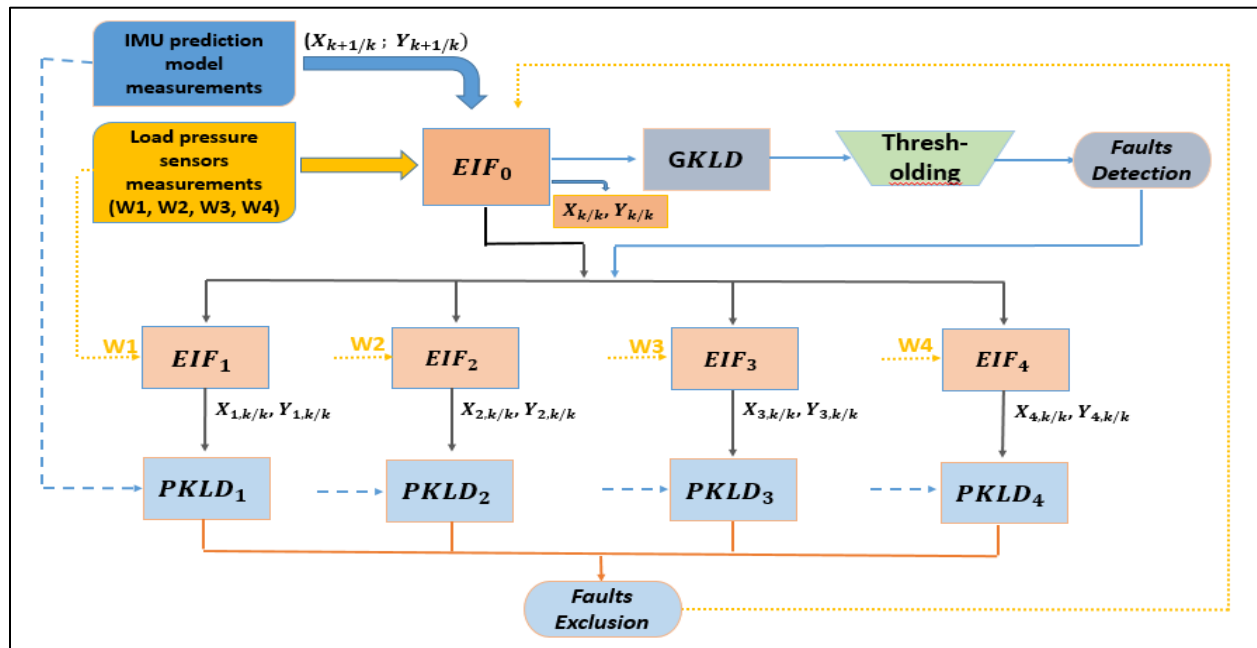


Figure 4.7 – The detection and exclusion procedure of defect.

IV.2.6 Experimentation and validation of results

In order to test the performance of the proposed approach, experiments with real data are prepared. A person considered as holding an IMU starts moving on the Inria sensing floor and performing some ADLs such as walking, standing, sitting, lying down, and also falling down.

For the following scenario where a person starts walking from the tile 7, then is sitting on a chair at tile 5 and finally exits from tile 18. This scenario is shown in the “Figure 4.8” where the real trajectory of the person (named in the next by reference trajectory) has been drawn manually in yellow color.

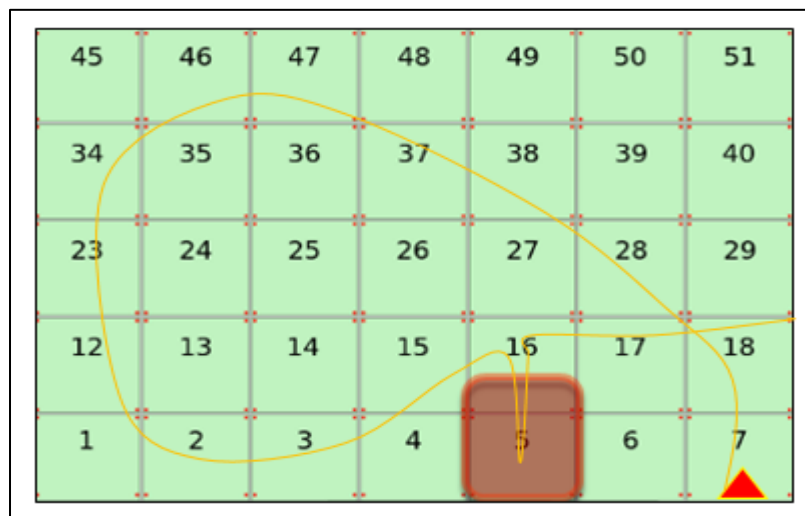


Figure 4.8 – The reference trajectory drawn manually.

For this scenario, the “Figure 4.9” shows the predicted trajectory derived from the IMU prediction model (in blue color) compared to the reference trajectory. One can see that the IMU prediction model trajectory is not very accurate especially on the following tiles 7, 18, 35, 24, 23, 16, 17 and 18.

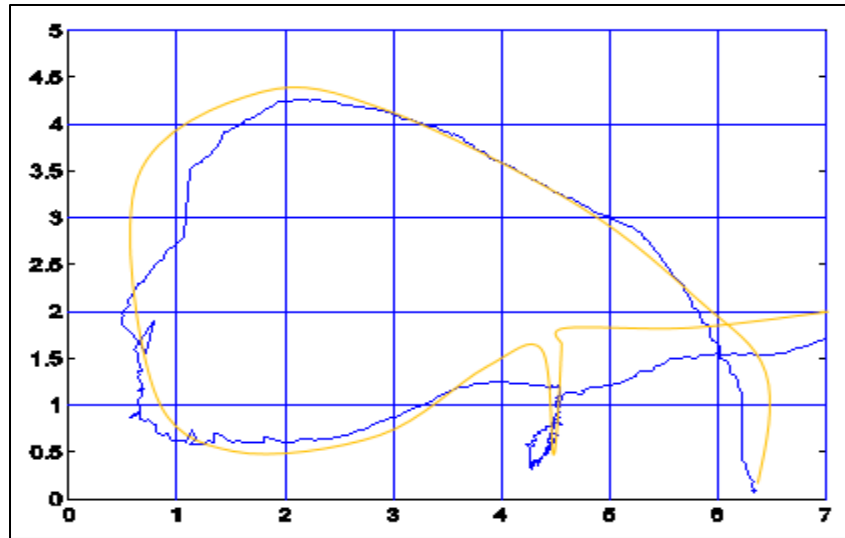


Figure 4.9 – The estimated trajectory derived from the IMU prediction model compared to the reference trajectory.

After the fusion between the IMU prediction model and the load pressure sensors’ measurements, one can see clearly that the estimated trajectory becomes closer to the reference trajectory and particularly after FDE. The “Figure 4.10 (a)” shows the trajectory before FDE (in red color) compared to the reference trajectory (in yellow color). On the other hand, the “Figure 4.10 (b)” shows the same trajectory after FDE.

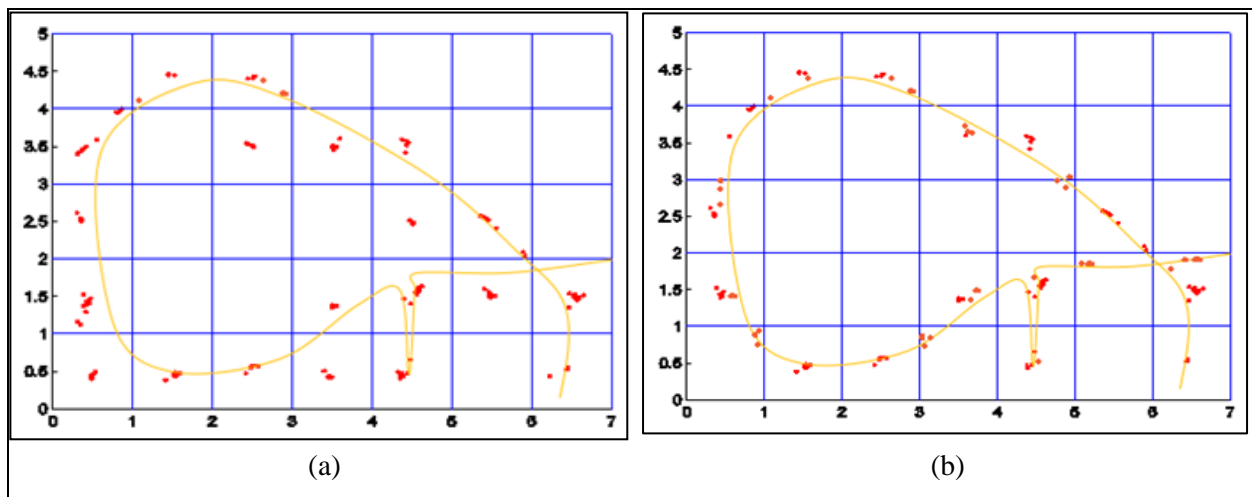


Figure 4.10 – (a) The estimated trajectory before FDE of a person after data fusion between IMU prediction model and tiles measurements (in red color) compared to the reference trajectory (in yellow color), (b) the same trajectory after FDE.

As it is mentioned in the “Paragraph IV.2.5.1” above, faults are detected using the *GKLD*. This quantity measures the divergence between the IMU prediction model and corrected load pressure

sensors estimates. The results, which are illustrated in the “Figure 4.11”, show several jumps above a predefined threshold indicating the presence of erroneous measurements.

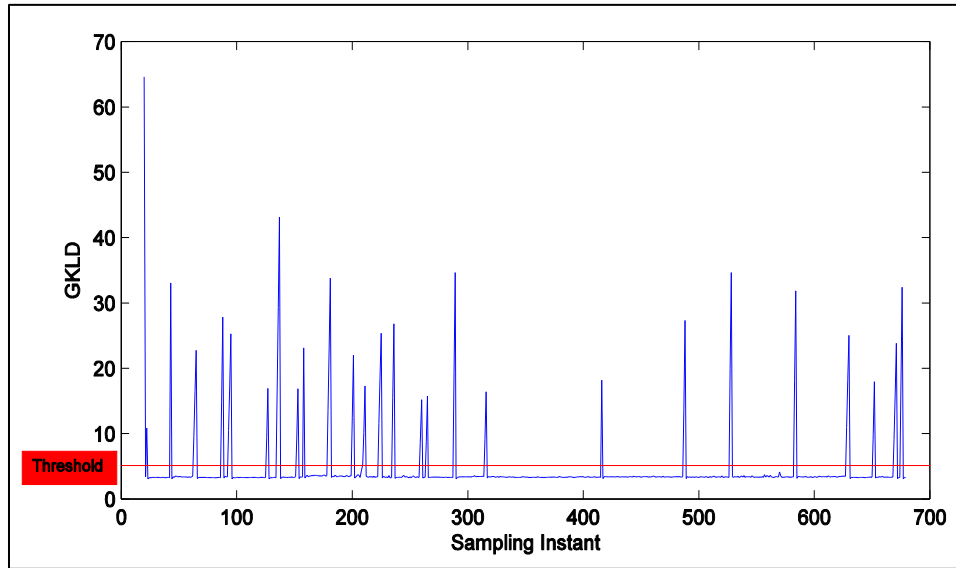


Figure 4.11 - The *GKLD* used for fault detection.

As an example of FD, the “Figure 4.12” shows a zoom in on a certain part of the *GKLD* for the observed jumps of $k = 626$ to $k = 632$.

One can see that from $k = 627$ to 631 the *GKLD* is above the threshold declaring fault measurements detection.

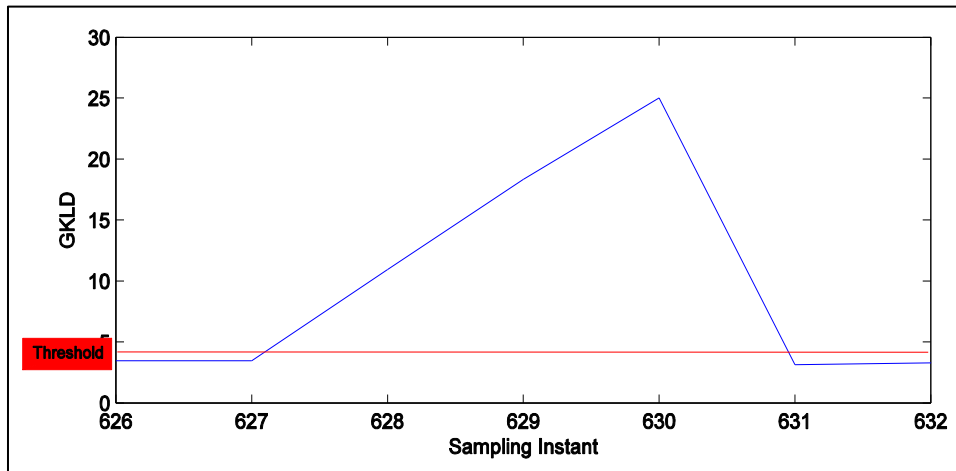


Figure 4.12 - The jump in the *GKLD* representing fault detection.

Once defects are detected using the *GKLD*, the erroneous measurement must be excluded from the fusion procedure. A significant increasing in *GKLD* and in all $PKLD_j$ implies the necessity of

excluding the faulty IMU prediction model measurements from the fusion procedure, while a significant increasing in $GKLD$ and in maximum three of the four $PKLD_j$ implies the necessity of excluding the faulty tile measurements from the fusion procedure. The “Figure 4.13” shows the residues $PKLD_j$ used for the exclusion of defects.

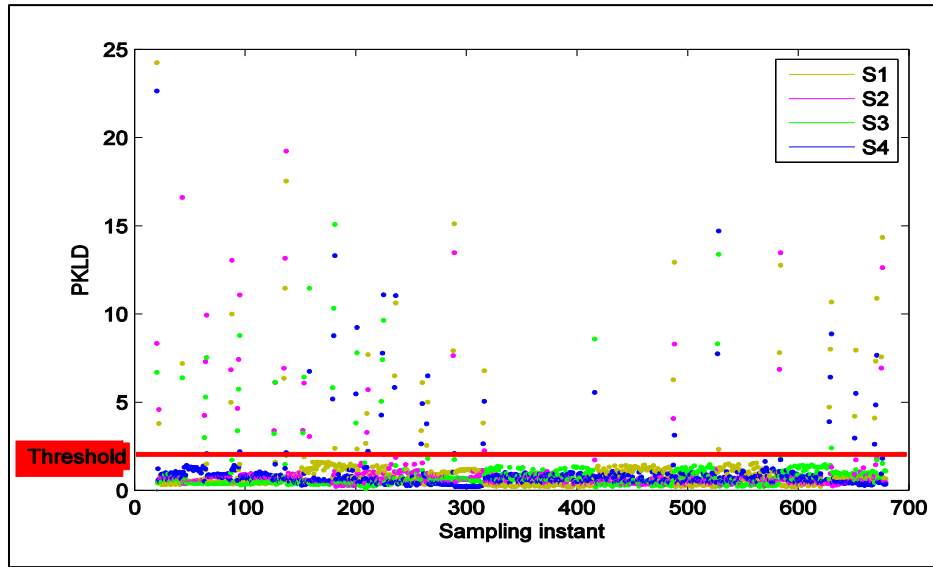


Figure 4.13 - The residues $PKLD$ used for the exclusion of defects.

For instance, the $PKLD_i$ analysis for a sampling instant $k = 627$ to 631 provided in the “Figure 4.14” shows that the $PKLD_3$ has a jump at instant $k = 627$, while $PKLD_1$, $PKLD_2$ and $PKLD_4$ remain below the threshold. This result indicates that 1 of the 4 load pressures sensors (noticed the third sensor) is defected, involving the necessity of excluding the corresponding tile from the fusion procedure during this interval.

Similarly, jumps at $PKLD_1$ and $PKLD_4$ indicate that 2 load pressure sensors are defected, then the corresponding tile should be excluded from the fusion at $k = 628$.

At $k = 629$, the $PKLD_1$, $PKLD_3$ and $PKLD_4$ have jumps indicating the defect of 3 load pressure sensors measurements then the corresponding tile must be excluded from the fusion.

The $PKLD_1$, $PKLD_2$, $PKLD_3$ and $PKLD_4$ have jumps at $k = 630$ indicating that the corresponding simulated IMU measurements must be excluded from the fusion procedure. Indeed, in this case, all pressure sensors give estimations that diverge from the predicted one obtained from the IMU. Therefore, the estimated IMU measurement is more likely to be erroneous.

Consequently, the proposed method is capable of handling the FDE in a relevant manner.

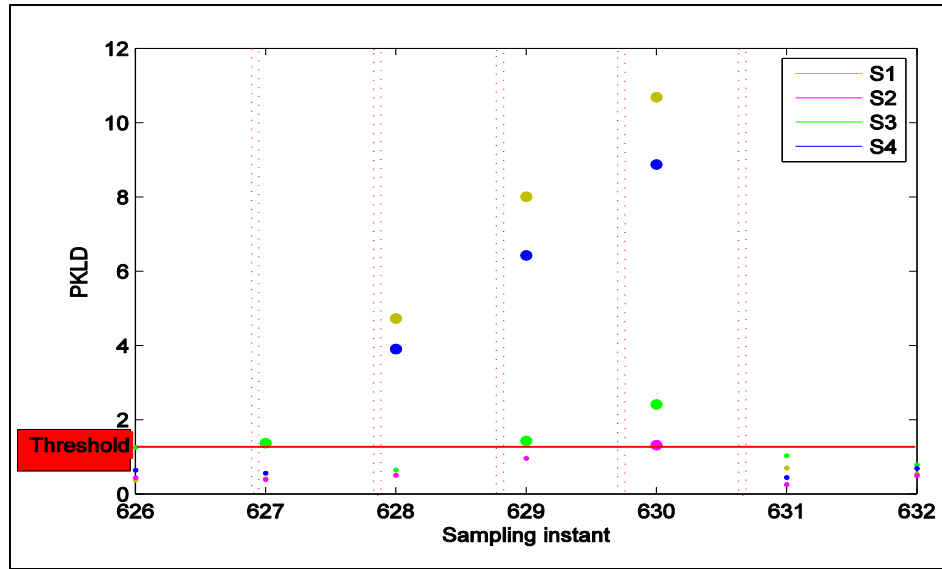


Figure 4.14 – Example of different faults exclusion using *PKLD*.

Conclusion

This chapter aims to show the performance of the developed approach on PLS application in an indoor environment using a multi-sensor fusion between a simulated IMU and load pressure sensors measurements with FDE. The FDE step is formulated using the *KLD* between the predicted and the corrected distributions of the IF. The residual tests based on the *KLD* has many advantages as they take into account the Bregman matrix divergence between covariance matrices as well as the Mahalanobis distance. The *GKLD* test detects the presence of faulty sensors in the load pressure sensors measurements and in the simulated IMU.

First, we presented the different methods and techniques used in the data fusion using a distributed FDE method based on a bank of EIF with residual tests taking the form of the *KLD*.

Second, related works on PLS are also presented and a description of the IMU sensor is provided as well as an IMU prediction model is built to estimate the personal trajectory.

Third, the fusion of the load pressure sensors measurements and the simulated IMU sensor measurements using EKF and IF is detailed, in addition to a load pressure estimation distribution method. IF is used in the correction step for its advantages over KF besides it allows a distributed or decentralized data fusion architecture.

Fourth, we present the proposed PLS with a phase of detection and exclusion of erroneous measurements using the *KLD*.

Finally, an experiment study of the proposed framework is done on real data is carried out in order to test the proposed approach. The estimation of the trajectories after FDE proves the efficiency of the proposed approach.

As a perspective of this work, we will work on tracking multiple persons simultaneously and developing an adaptive threshold optimization using the information theory metrics.

Chapter V - Conclusion and future works

V.1 Conclusion

Aging population is a major defy that modern societies will face in the next few years. It's one of the greatest social and economic challenges of the 21st century. By 2050, the proportion of people over the age of 60 will reach 30% in the developed countries and in particular France. In this age group, falling down is one of the most serious life-threatening events that can occur. It is the principal cause of injury in elderly people and the leading reason of accidental death. Moreover, it has dramatic psychological, medical and social consequences.

However, advances in ambient intelligence (AmI) can deliver key skills remotely and enable home-based care and reduce the cost of premature institutionalization.

This thesis explores the abilities of the Inria Nancy platform as an AmI smart home to offer a high integrity PLS for elderly in their independent living senior apartments, (ADLs) recognition, and automatic fall detection system, using a non-intrusive sensors network system that performs integrity, reliability, efficiency, and easy to use.

As a first step, we present the state of the art of FD systems and sensing floors domain, including performance and accuracy evaluations for several studies. Then, we explore the Inria Nancy sensing floor as a PAL system. The main ADLs (unknown, walking, standing, sitting, and lying down) are defined and an approach is introduced to distinguish between them. The results show that by using the load sensors concealed under tiles, the proposed system can track humans and recognize the ADLs postures defined above, but it fails to detect the falling down cases and they are estimated as "Lying down" postures. Thus, we proceeded to the accelerometer signals to detect falling down cases. We had started by extracting some useful parameters and then selecting the pertinent one that discriminates between the falling and lying down postures. By extracting and selecting some meaningful features from the collected data, the size of the dataset is reduced and becomes more efficient. The efficiency appears by improving the computational speed and the prediction accuracy of the proposed system. After that, we merge between the load pressure sensor

measurements and the accelerometer sensor decisions to recognize the ADLs and automatically detect each falling case.

Second, we take in consideration the erroneous or noisy sensors measurements that can affect the PLS accuracy. In this way, we present a generic and accurate method that localizes tracks people as well as detects and excludes faulty measurements from used sensors. The main idea of this localization procedure is the fusion between the simulated IMU (used in the frame of an pedometer prediction model) that tracks the motion and the position of the elder person and the load pressure sensors concealed under the tiles that give a representation of the load distribution exerted by the person on the tiles (observation model for correction). In this part, we have shown the benefit of using the informational form (IF) of a KF, which makes it possible to simplify the fusion of the multi-sensors data. We have concluded that the IF is adapted to the design of a fusion method for which we have integrated a diagnostic layer with a distributed architecture. Moreover, we have adapted a residue based on the Kullback-Leibler divergence between the a priori and a posteriori distributions which include the Mahalanobis distance performing a test on the averages and the Bregman divergence matrix allowing a test on the covariance matrices. The importance of this residue is shown in the detection of faulty measurements having a direct impact on the position and the tracking of the elder. These techniques aim to improve the localization integrity of the overall system.

The obtained results are very promising; a fault-tolerant system that localizes and tracks people in their home with a high accuracy, recognizes their ADLs with a sensitivity greater than 92% for all estimated postures, and automatically detects falling down cases with more than 94% sensitivity.

However, certain limitations can be pointed out and can be used as a basis for future works.

V.2 Perspectives and future works

As a perspective of this work, we will work on:

- Tracking different people simultaneously,
- Developing an adaptive threshold optimization using the information theory metrics. Choosing the threshold is a critical step in making the right decision about the presence of erroneous measurements in the system. An optimized thresholding method can be developed

based on the information gain gained during the transition from the a priori distribution to the a posteriori distribution,

- Detecting and correcting sensors faulty measurements: when a faulty measurement from a load pressure sensor is detected, the whole tile (4 load pressure sensors) is excluded from the merging process, while it is important to develop a method to detect and isolate only the defected sensor. On the other hand, this work provides diagnostic methods that can detect and exclude sensors defects. However, because the number of observations is limited, it is interesting to identify the amplitude of the default and correct it without being excluded from the fusion procedure. In such way, we can provide a layer of error detection and correction.
- Preventing falling down cases of elderly by processing the database through different diagnostics and studies of many properties such as movement, activity, and gait analysis.

References

- [1] J. C. Augusto. "Ambient intelligence: Basic concepts and applications." In *International Conference on Software and Data Technologies*, pp. 16-26. Springer Berlin Heidelberg, 2006.
- [2] J. C. Nugent, C. D. Augusto "A new architecture for smart homes based on ADB and temporal reasoning." In *Toward A Human-Friendly Assistive Environment: ICOST'2004, 2nd International Conference on Smart Home and Health Telematics*, p. 106. IOS Press, 2004.
- [3] Z. Zhou, W. Dai, J. Eggert, J. T. Giger, J. Keller, M. Rantz, and Z. He. "A real-time system for in-home activity monitoring of elders." In *2009 Annual International Conference of the IEEE Engineering in Medicine and Biology Society*, pp. 6115-6118. IEEE, 2009.
- [4] http://www.un.org/en/development/desa/population/publications/pdf/ageing/WPA2015_Report.pdf. April, 2016
- [5] Y. Zhang, and F.W. Goza. "Who will care for the elderly in China?: A review of the problems caused by China's one-child policy and their potential solutions." *Journal of Aging Studies* 20, no. 2 (2006): 151-164.
- [6] M. E. Tinetti, and M. Speechley. "Prevention of falls among the elderly." *New England journal of medicine* 320, no. 16 (1989): 1055-1059.
- [7] J. A. Stevens. "Falls among older adults—risk factors and prevention strategies." *Journal of safety research* 36, no. 4 (2005): 409-411.
- [8] A. Bueno-Cavanillas, F. Padilla-Ruiz, J. J. Jimenez-Moleon, C. A. Peinado-Alonso, and R. Galvez-Vargas. "Risk factors in falls among the elderly according to extrinsic and intrinsic precipitating causes." *European journal of epidemiology* 16, no. 9 (2000): 849-859.
- [9] G. F. Fuller. "Falls in the elderly." *American family physician* 61, no. 7 (2000): 2159-68.
- [10] N. El-Bendary, Q. Tan, F. C. Pivot, and A. Lam. "Fall detection and prevention for the elderly: A review of trends and challenges." *Int. J. Smart Sens. Intell. Syst* 6, no. 3 (2013): 1230-1266.
- [11] K. James, D. Eldemire-Shearer, J. Gouldbourne, and C. Morris, —Falls and Fall Prevention in the Elderly: The Jamaican Perspective, *West Indian Medical Journal*, vol. 56, no. 6, 2007, pp. 534-539.
- [12] Long-term care services in the United States: 2013 overview. Tech. rep. U.S. Department of Health and Human Services, Centers for Disease Control and Prevention, National Center for Health Statistics, 2013. url: http://www.cdc.gov/nchs/data/nsltcp/long_term_care_services_2013.pdf.
- [13] Etude sur le marché de l'offre de soins, d'hébergement et de services destinés aux personnes âgées dépendantes. Tech. rep. Ernst & Young, 2008. url: <http://www.senat.fr/commission/missions/Dependance/etude.pdf>.
- [14] J. A. Stevens. "Falls among older adults—risk factors and prevention strategies." *Journal of safety research* 36, no. 4 (2005): 409-411.
- [15] V. Spasova, and I. Iliev. "Computer Vision and Wireless Sensor Networks in Ambient Assisted Living: State of the Art and Challenges." *Journal of Emerging Trends in Computing and Information Sciences* 3, no. 4 (2012): 585-595.
- [16] A. Bamis, D. Lymberopoulos, T. Teixeira, and A. Savvides. "Towards precision monitoring of elders for providing assistive services." In *Proceedings of the 1st international conference on Pervasive Technologies Related to Assistive Environments*, p. 49. ACM, 2008.
- [17] N. Pepin, O. Simonin, and F. Charpillet. "Intelligent Tiles-Putting Situated Multi-Agents Models in Real World." In *ICAART*, pp. 513-519. 2009.
- [18] M. Andries, O. Simonin, and F. Charpillet, "Localisation of humans and objects interacting on load-sensing floors," *IEEE Sensors Journal* 16, no. 4 (2016): 1026-1037.
- [19] M. Daher, M. El Badaoui El Najjar, A. Diab, M. Khalil, and F. Charpillet. "Elder Tracking and Fall Detection System using Smart Tiles". In *IEEE Sensors Journal* 11/2016 PP(99):1-1. DOI:10.1109/JSEN.2016.2625099, November 2016.
- [20] M. Daher, M. El Badaoui El Najjar, A. Diab, M. Khalil, and F. Charpillet. "Automatic Fall Detection System using Sensing Floors". In *International Journal of Computing & Information Sciences* Vol. 12, No. 1, pp. 75-82, September 2016.
- [21] M. Daher, M. El Badaoui El Najjar, A. Diab, M. Khalil, and F. Charpillet. "Towards a usable and an efficient elder fall detection system." *2015 International Conference on Advances in Biomedical Engineering (ICABME). IEEE*, 2015.

- [22] Prima team, Inria. Casper project. url: <https://raweb.inria.fr/rapportsactivite/RA2010/prima/uid91.html>.
- [23] P Couturier, S Moine, F Favre-Reguillon, Y Caritu, F Giraud-By, R Guillemaud, P Barralon, N Noury, M Berenguer, H Provost et al. "Actidom: Monitoring of activity in frail elderly in their daily life." In *Proceeding of the international meeting on Micro and NAnoTECHnology, MINATEC2003, Grenoble, France*. 2003.
- [24] Pulsarteam, Inria. GerhomeProject. url:<http://www-sop.inria.fr/members/Francois.Bremond/topicsText/gerhomeProject.html>.
- [25] D. P. Chau, F. Bremond, and M. Thonnat. "Online evaluation of tracking algorithm performance." In *Crime Detection and Prevention (ICDP 2009), 3rd International Conference on*, pp. 1-6. IET, 2009.
- [26] P. Jallon, B. Dupre, and M. Antonakios. "A graph based method for timed up & go test qualification using inertial sensors." In *2011 IEEE International Conference on Acoustics, Speech and Signal Processing (ICASSP)*, pp. 689-692. IEEE, 2011.
- [27] P. Robert, E. Castelli, P. C. Chung, T. Chiroux, C. F. Crispim-Junior, P. Mallea, and F. Bremond. "SWEET-HOME ICT technologies for the assessment of elderly subjects." *IRBM* 34, no. 2 (2013): 186-190.
- [28] D. Hewson, J., Jacques Duchêne, F. Charpillat, J. Saboune, V. Michel-Pellegrino, H. Amoud, M. Doussot, J. Paysant, A. Boyer, and J. Y. Hogrel. "The PARACHUTE project: remote monitoring of posture and gait for fall prevention." *EURASIP Journal on Applied Signal Processing* 2007, no. 1 (2007): 109-109. Michael C Mozer. "The neural network house: An environment hat adapts to its inhabitants". In: Proc. AAAI Spring Symp. Intelligent Environments. 1998, pp. 110–114.
- [29] M. C. Mozer. "The neural network house: An environment hat adapts to its inhabitants." In *Proc. AAAI Spring Symp. Intelligent Environments*, vol. 58. 1998.
- [30] C. D. Kidd, R. Orr, G. D. Abowd, C. G. Atkeson, I. A. Essa, B. MacIntyre, E. Mynatt, T. E. Starner, and W. Newstetter. "The aware home: A living laboratory for ubiquitous computing research." In *International Workshop on Cooperative Buildings*, pp. 191-198. Springer Berlin Heidelberg, 1999.
- [31] S. K. Das, D. J. Cook, A. Battacharya, E. O. Heierman, and T. Y. Lin. "The role of prediction algorithms in the MavHome smart home architecture." *IEEE Wireless Communications* 9, no. 6 (2002): 77-84.
- [32] S. Helal, W. Mann, H. El-Zabadani, J. King, Y. Kaddoura, and E. Jansen. "The gator tech smart house: A programmable pervasive space." *Computer* 38, no. 3 (2005): 50-60.
- [33] Y. Nishida, T. Hori, T. Suehiro, and S. Hirai. "Sensorized environment for self-communication based on observation of daily human behavior." In *Intelligent Robots and Systems, 2000.(IROS 2000). Proceedings. 2000 IEEE/RSJ International Conference on*, vol. 2, pp. 1364-1372. IEEE, 2000.
- [34] H. Noguchi, T. Mori, and T. Sato. "Construction of network system and the first step of summarization for human daily action data in the sensing room." In *Knowledge Media Networking, 2002. Proceedings. IEEE Workshop on*, pp. 17-22. IEEE, 2002.
- [35] K. Matsuoka. "Aware home understanding life activities." In *Proceedings of 2nd International Conference On Smart Homes and Health Telematic, ICOST*, vol. 4, pp. 186-193. 2004.
- [36] G. Williams, K. Doughty, and D. A. Bradley. "A systems approach to achieving CarerNet-an integrated and intelligent telecare system." *IEEE transactions on Information Technology in Biomedicine* 2, no. 1 (1998): 1-9.
- [37] S. Guillen, M. T. Arredondo, V. Traver, J. M. García, and C. Fernandez. "Multimedia telehomecare system using standard TV set." *IEEE Transactions on Biomedical Engineering* 49, no. 12 (2002): 1431-1437.
- [38] B. Brumitt, B. Meyers, J. Krumm, A. Kern, and S. Shafer. "Easyliving: Technologies for intelligent environments." In *International Symposium on Handheld and Ubiquitous Computing*, pp. 12-29. Springer Berlin Heidelberg, 2000.
- [39] X. Yu, "Approaches and Principles of Fall Detection for Elderly and Patient", 10th IEEE Intl. Conf. on e-Health Networking, Applications and Service (HEALTHCOM 2008), July 2008.
- [40] G. Z. Yang, and M. Yacoub. "Body sensor networks." (2006): 500.
- [41] Y. S. Delahoz, and M. A. Labrador. "Survey on fall detection and fall prevention using wearable and external sensors." *Sensors* 14, no. 10 (2014): 19806-19842.
- [42] F. Wu, H. Zhao, Y. Zhao, and H. Zhong. "Development of a wearable-sensor-based fall detection system." *International journal of telemedicine and applications* 2015 (2015): 2.
- [43] Y.T. Chen, Y. C. Lin, and W. H. Fang. "A hybrid human fall detection scheme." In *2010 IEEE International Conference on Image Processing*, pp. 3485-3488. IEEE, 2010.

- [44] A. Williams, G. Deepak, and A. Hanson. "Aging in place: fall detection and localization in a distributed smart camera network." In *Proceedings of the 15th ACM international conference on Multimedia*, pp. 892-901. ACM, 2007.
- [45] Vaidehi, V.; Ganapathy, K.; Mohan, K.; Aldrin, A.; Nirmal, K. Video based automatic fall detection in indoor environment. In *Proceedings of the International Conference on Recent Trends in Information Technology (ICRTIT)*, Chennai, Tamil Nadu, India, 3–5 June 2011; pp. 1016–1020.
- [46] W. K. Wong, H. L. Lim, C. K. Loo, and W. S. Lim. "Home alone faint detection surveillance system using thermal camera." In *Computer Research and Development, 2010 Second International Conference on*, pp. 747-751. IEEE, 2010.
- [47] C. Rougier, J. Meunier, A. St-Arnaud, and J. Rousseau. "Fall detection from human shape and motion history using video surveillance." In *Advanced Information Networking and Applications Workshops, 2007, AINAW'07. 21st International Conference on*, vol. 2, pp. 875-880. IEEE, 2007.
- [48] R. Hegde, B. Sudarshan, S. Kumar, S. Hariprasad, and B. Satyanarayana. "Technical advances in fall detection system—a review." *Int. J. Comput. Sci. Mob. Comput* 2 (2013): 152-160.
- [49] N. M. Peel, R. J. McClure, and J. K. Hendrikz. "Psychosocial factors associated with fall-related hip fractures." *Age and ageing* 36, no. 2 (2007): 145-151.
- [50] K. Ozcan, A. K. Mahabalagiri, M. Casares, and S. Velipasalar. "Automatic fall detection and activity classification by a wearable embedded smart camera." *IEEE journal on emerging and selected topics in circuits and systems* 3, no. 2 (2013): 125-136.
- [51] W. S. Baek, D. M. Kim, F. Bashir, and J. Y. Pyun. "Real life applicable fall detection system based on wireless body area network." In *2013 IEEE 10th Consumer Communications and Networking Conference (CCNC)*, pp. 62-67. IEEE, 2013.
- [52] M. Lan, A. Nahapetian, A. Vahdatpour, L. Au, W. Kaiser, and M. Sarrafzadeh. "SmartFall: an automatic fall detection system based on subsequence matching for the SmartCane." In *Proceedings of the Fourth International Conference on Body Area Networks*, p. 8. ICST (Institute for Computer Sciences, Social-Informatics and Telecommunications Engineering), 2009.
- [53] O. Almeida, M. Zhang, and J.C. Liu. "Dynamic fall detection and pace measurement in walking sticks." In *High Confidence Medical Devices, Software, and Systems and Medical Device Plug-and-Play Interoperability, 2007. HCMDS-MDPNP. Joint Workshop on*, pp. 204-206. IEEE, 2007.
- [54] F. Werner, J. Diermaier, S. Schmid, and P. Panek. "Fall detection with distributed floor-mounted accelerometers: An overview of the development and evaluation of a fall detection system within the project eHome." In *2011 5th International Conference on Pervasive Computing Technologies for Healthcare (PervasiveHealth) and Workshops*, pp. 354-361. IEEE, 2011.
- [55] A. Sengto, and T. Leauhatong. "Human falling detection algorithm using back propagation neural network." In *Biomedical Engineering International Conference (BMEiCON), 2012*, pp. 1-5. IEEE, 2012.
- [56] Y. T. Chen, Y. C. Lin, and W. H. Fang. "A hybrid human fall detection scheme." In *2010 IEEE International Conference on Image Processing*, pp. 3485-3488. IEEE, 2010.
- [57] A. Sorvala, E. Alasaarela, H. Sorvoja, and R. Myllylä. "A two-threshold fall detection algorithm for reducing false alarms." In *2012 6th International Symposium on Medical Information and Communication Technology (ISMICT)*, pp. 1-4. IEEE, 2012.
- [58] M. Humenberger, S. Schraml, C. Sulzbachner, A. N. Belbachir, A. Srp, and F. Vajda. "Embedded fall detection with a neural network and bio-inspired stereo vision." In *2012 IEEE Computer Society Conference on Computer Vision and Pattern Recognition Workshops*, pp. 60-67. IEEE, 2012.
- [59] A. N. Belbachir, M. Litzenberger, S. Schraml, M. Hofstätter, D. Bauer, P. Schön, M. Humenberger, C. Sulzbachner, T. Lunden, and M. Merne. "CARE: a dynamic stereo vision sensor system for fall detection." In *2012 IEEE International Symposium on Circuits and Systems*, pp. 731-734. IEEE, 2012.
- [60] D. Chen, W. Feng, Y. Zhang, X. Li, and T. Wang. "A wearable wireless fall detection system with accelerators." In *Robotics and Biomimetics (ROBIO), 2011 IEEE International Conference on*, pp. 2259-2263. IEEE, 2011.
- [61] M. Yuwono, S. W. Su, and B. Moulton. "Fall detection using a Gaussian distribution of clustered knowledge, augmented radial basis neural-network, and multilayer perceptron." In *Broadband and Biomedical Communications (IB2Com), 2011 6th International Conference on*, pp. 145-150. IEEE, 2011.

- [62] O. Ojetola, E. I. Gaura, and J. Brusey. "Fall detection with wearable sensors--safe (Smart Fall Detection)." In *Intelligent Environments (IE), 2011 7th International Conference on*, pp. 318-321. IEEE, 2011.
- [63] B. Kuris, and T. Dishongh. "SHIMMER-Sensing Health with Intelligence, Modularity, Mobility, and Experimental Reusability." *Intel Corp* 23 (2006): 104-107.
- [64] M. Shoaib, R. Dragon, and J. Ostermann. "View-invariant fall detection for elderly in real home environment." In *Image and Video Technology (PSIVT), 2010 Fourth Pacific-Rim Symposium on*, pp. 52-57. IEEE, 2010.
- [65] A. Dubois. "Mesure de la fragilité et détection de chutes pour le maintien à domicile des personnes âgées." PhD diss., Université de Lorraine, 2014.
- [66] J. Dai, X. Bai, Z. Yang, Z. Shen, and D. Xuan. "PerFallD: A pervasive fall detection system using mobile phones." In *Pervasive Computing and Communications Workshops (PERCOM Workshops), 2010 8th IEEE International Conference on*, pp. 292-297. IEEE, 2010.
- [67] F. Sposaro, and G. Tyson. "iFall: an Android application for fall monitoring and response." In *2009 Annual International Conference of the IEEE Engineering in Medicine and Biology Society*, pp. 6119-6122. IEEE, 2009.
- [68] Y. Shi, Y. Shi, and X. Wang. "Fall detection on mobile phones using features from a five-phase model." In *Ubiquitous Intelligence & Computing and 9th International Conference on Autonomic & Trusted Computing (UIC/ATC), 2012 9th International Conference on*, pp. 951-956. IEEE, 2012.
- [69] Y. G. Wu, and Sheng-Lun Tsai. "Fall detection system design by smart phone." *International Journal of Digital Information and Wireless Communications (IJDIWC)* 4, no. 4 (2014): 474-485.
- [70] B. Aguiar, T. Rocha, J. Silva, and I. Sousa. "Accelerometer-based fall detection for smartphones." In *Medical Measurements and Applications (MeMeA), 2014 IEEE International Symposium on*, pp. 1-6. IEEE, 2014.
- [71] Sensorband II. Available online: <http://www.vigilio.fr>. Accessed on December 10, 2016.
- [72] Sensorband II. Available online: <http://fate.upc.edu/index.php>. Accessed on December 10, 2016.
- [73] Sensorband II. Available online: <http://www.caretech.com.au/products-/fall-sensor.html>. Accessed on December 10, 2016.
- [74] Vitalbase. Available online: <http://www.vitalbase.fr/teleassistance/>. Accessed on December 10, 2016.
- [75] V. Spasova, and I. Iliev. "Computer Vision and Wireless Sensor Networks in Ambient Assisted Living: State of the Art and Challenges." *Journal of Emerging Trends in Computing and Information Sciences* 3, no. 4 (2012): 585-595.
- [76] A. Bamis, D. Lymberopoulos, T. Teixeira, and A. Savvides. "Towards precision monitoring of elders for providing assistive services." In *Proceedings of the 1st international conference on Pervasive Technologies Related to Assistive Environments*, p. 49. ACM, 2008.
- [77] M.D. Addlesee, A. Jones, F. Livesey, and F. Samaria. "The ORL active floor." *IEEE Personal Communications* 4 (1997): 35-41.
- [78] J. Paradiso, C. Ablner, K.Y. Hsiao, and M. Reynolds. "The magic carpet: physical sensing for immersive environments." In *CHI'97 Extended Abstracts on Human Factors in Computing Systems*, pp. 277-278. ACM, 1997.
- [79] N. Griffith, and M. Fernström. "LiteFoot-A Floor Space for Recording Dance and Controlling Media." In *ICMC*. 1998.
- [80] R. J. Orr, and G. D. Abowd. "The smart floor: A mechanism for natural user identification and tracking." In *CHI'00 extended abstracts on Human factors in computing systems*, pp. 275-276. ACM, 2000.
- [81] S. Helal, W. Mann, H. El-Zabadani, J. King, Y. Kaddoura, and E. Jansen. "The gator tech smart house: A programmable pervasive space." *Computer* 38, no. 3 (2005): 50-60.
- [82] C. D. Kidd, R. Orr, G. D. Abowd, C. G. Atkeson, I. A. Essa, B. MacIntyre, E. Mynatt, T.E. Starner, and W. Newstetter. "The aware home: A living laboratory for ubiquitous computing research." In *International Workshop on Cooperative Buildings*, pp. 191-198. Springer Berlin Heidelberg, 1999.
- [83] T. Mori, and T. Sato. "Robotic room: Its concept and realization." *Robotics and Autonomous Systems* 28, no. 2-3 (1999): 141-148.
- [84] T. Sato, T. Harada, and T. Mori. "Environment-type robot system" RoboticRoom" featured by behavior media, behavior contents, and behavior adaptation." *IEEE/ASME Transactions on Mechatronics* 9, no. 3 (2004): 529-534.

- [85] Debraj De, Shaojie Tang, Wen-Zhan Song, Diane Cook and Sajal K. Das. "ActiSen: Activity-aware Sensor Network in Smart Environments". In: *Journal of Pervasive and Mobile Computing (PMC)* (2012).
- [86] K. Nakajima, Y. Mizukami, K. Tanaka and T. Tamura. "Footprint-based personal recognition." *IEEE Transactions on Biomedical Engineering* 47, no. 11 (2000): 1534-1537.
- [87] M. Razeghi, and M. E. Batt. "Foot type classification: a critical review of current methods." *Gait & posture* 15, no. 3 (2002): 282-291.
- [88] A. Schmidt, M. Strohbach, K. V. Laerhoven, A. Friday, and H-W. Gellersen. "Context acquisition based on load sensing." In *International Conference on Ubiquitous Computing*, pp. 333-350. Springer Berlin Heidelberg, 2002.
- [89] M. Alwan, Rajendran, P. J., Kell, S., Mack, D., Dalal, S., Wolfe, M., & Felder, R. (2006, April). A smart and passive floor-vibration based fall detector for elderly. In *2006 2nd International Conference on Information & Communication Technologies* (Vol. 1, pp. 1003-1007). IEEE.
- [90] R. Glaser, C. Lauterbach, D. Savio, M. Schnell, S. Karadal, W. Weber, S. Kornely, and A. Stohr. "Smart Carpet: A textile-based large-area sensor network." (2007).
- [91] D. Savio, and Thomas Ludwig. "Smart carpet: A footstep tracking interface." In *Advanced Information Networking and Applications Workshops, 2007, AINAW'07. 21st International Conference on*, vol. 2, pp. 754-760. IEEE, 2007.
- [92] Y. L. Shen, and C. S. Shin. "Distributed sensing floor for an intelligent environment." *IEEE Sensors Journal* 9, no. 12 (2009): 1673-1678.
- [93] R. E. Reilly, M. R. Amirinia, and R. W. Soames. "A two-dimensional imaging walkway for gait analysis." In *Computer-Based Medical Systems, 1991. Proceedings of the Fourth Annual IEEE Symposium*, pp. 145-152. IEEE, 1991.
- [94] H. Morishita, R. Fukui, and T. Sato. "High resolution pressure sensor distributed floor for future human-robot symbiosis environments." In *Intelligent Robots and Systems, 2002. IEEE/RSJ International Conference on*, vol. 2, pp. 1246-1251. IEEE, 2002.
- [95] J. S. Yun, S. H. Lee, W. T. Woo, and J. H. Ryu. "The user identification system using walking pattern over the ubifloor." In *Proceedings of International Conference on Control, Automation, and Systems*, vol. 1046, p. 1050. 2003.
- [96] J. Yun, G. D. Abowd, J. Ryu, and W. Woo. "User identification with user's stepping pattern over the UbiFloorII." *International Journal of Pattern Recognition and Artificial Intelligence* 22, no. 03 (2008): 497-514.
- [97] S. Pirttikangas, J. Suutala, J. Riekk, and J. Rönig. "Footstep identification from pressure signals using Hidden Markov Models." In *Proc. Finnish Signal Processing Symposium (FINSIG'03)*, pp. 124-128. 2003.
- [98] D. Gouwanda, and S. M. N. A. Senanayake. "Real time multi-sensory force sensing mat for sports biomechanics and human gait analysis." *International Journal of Intelligent Systems and Technologies* 3, no. 3 (2008): 149-154.
- [99] B. Richardson, K. Leydon, M. Fernstrom, and J. A. Paradiso. "Z-Tiles: building blocks for modular, pressure-sensing floorspaces." In *CHI'04 extended abstracts on Human factors in computing systems*, pp. 1529-1532. ACM, 2004.
- [100] S. Rangarajan, A. Kidane, G. Qian, S. Rajko, and D. Birchfield. "The design of a pressure sensing floor for movement-based human computer interaction." In *European Conference on Smart Sensing and Context*, pp. 46-61. Springer Berlin Heidelberg, 2007.
- [101] G. Qian, J. Zhang, and A. Kidané. "People identification using gait via floor pressure sensing and analysis." *Smart sensing and context* (2008): 83-98.
- [102] G. Qian, J. Zhang, and A. Kidane. "People identification using floor pressure sensing and analysis." *IEEE Sensors Journal* 10, no. 9 (2010): 1447-1460.
- [103] W. H. Liao, C. L. Wu, and L. C. Fu. "Inhabitants tracking system in a cluttered home environment via floor load sensors." *IEEE Transactions on Automation Science and Engineering* 5, no. 1 (2008): 10-20.
- [104] R. Bose, and A. Helal. "Observing walking behavior of humans using distributed phenomenon detection and tracking mechanisms." In *Applications and the Internet, 2008. SAINT 2008. International Symposium on*, pp. 405-408. IEEE, 2008.
- [105] R. Rajalingham, Y. Visell, and J. R. Cooperstock. "Probabilistic tracking of pedestrian movements via in-floor force sensing." In *Computer and Robot Vision (CRV), 2010 Canadian Conference on*, pp. 143-150. IEEE, 2010.

- [106] H. Rimminen, J. Lindström, M. Linnavuo, and R. Sepponen. "Detection of falls among the elderly by a floor sensor using the electric near field." *IEEE Transactions on Information Technology in Biomedicine* 14, no. 6 (2010): 1475-1476.
- [107] Tzeng, H. W., Chen, M. Y., & Chen, J. Y. (2010, July). Design of fall detection system with floor pressure and infrared image. In *2010 International Conference on System Science and Engineering* (pp. 131-135). IEEE.
- [108] M. Lombardi, A. Pieracci, P. Santinelli, R. Vezzani, and R. Cucchiara. "Sensing floors for privacy-compliant surveillance of wide areas." In *Advanced Video and Signal Based Surveillance (AVSS), 2013 10th IEEE International Conference on*, pp. 105-110. IEEE, 2013.
- [109] A. Heller, T. Senior, and J. Wheat. "The smartfloor: A large area force-measuring floor for investigating dynamic balance and motivating exercise." *Procedia engineering* 72 (2014): 226-231.
- [110] C. Lauterbach, A. Steinhage, and A. Techmer. "Large-area wireless sensor system based on smart textiles." In *International Multi-Conference on Systems, Signals & Devices*. 2012.
- [111] <http://www.future-shape.com/en/>. Accessed in January 2017.
- [112] Tarkett. FloorInMotion. url: <http://professionnels.tarkett.fr/content/floor-motion-care-tarkett>. Accessed in January 2017.
- [113] M. Andries. "Object and human tracking, and robot control through a load sensing floor." PhD diss., Université de Lorraine, 2015.
- [114] A. Dib. "Vers un système de capture du mouvement humain en 3D pour un robot mobile évoluant dans un environnement encombré." PhD diss., Université de Lorraine, 2016.
- [115] A. Bautin, O. Simonin, and F. Charpillet. "Minpos: A novel frontier allocation algorithm for multi-robot exploration." *Intelligent Robotics and Applications* (2012): 496-508.
- [116] R. Sapsford, and V. Jupp, eds. *Data collection and analysis*. Sage, 2006.
- [117] M. Rio, F. Colas, M. Andries, and F. Charpillet.. "Probabilistic sensor data processing for robot localization on load-sensing floors." 2016 IEEE International Conference on Robotics and Automation (ICRA). IEEE, 2016.
- [118] G. Sannino, I. De Falco, and G. De Pietro, "Automatic Extraction of an Effective Rule Set for Fall Detection for a Real-Time Mobile Monitoring System." *Developments in eSystems Engineering (DeSE), 2013 Sixth International Conference on*. IEEE, 2013.
- [119] M. Daher, A. Dib, M. El Badaoui El Naijar, A. Diab, M. Khalil, and F. Charpillet. "Ambient Assistive Living System Using RGB-D Camera." Accepted to be published in *Advances in Biomedical Engineering (ICABME), 2017 International Conference*. IEEE, 2017.
- [120] D. M. Karantonis, M. R. Narayanan, M. Mathie, N. H. Lovell, and B. G. Celler. "Implementation of a real-time human movement classifier using a triaxial accelerometer for ambulatory monitoring." *IEEE transactions on information technology in biomedicine* 10, no. 1 (2006): 156-167
- [121] M. J. Mathie, B. G. Celler, N. H. Lovell, and A. C. F. Coster. "Classification of basic daily movements using a triaxial accelerometer." *Medical and Biological Engineering and Computing* 42, no. 5 (2004): 679-687.
- [122] I. H. Witten, E. Frank, M. A. Hall, and C. J. Pal. *Data Mining: Practical machine learning tools and techniques*. Morgan Kaufmann, 2016.
- [123] D. Cabric, S. M. Mishra, and R. W. Brodersen. "Implementation issues in spectrum sensing for cognitive radios." In *Signals, systems and computers, 2004. Conference record of the thirty-eighth Asilomar conference on*, vol. 1, pp. 772-776. Ieee, 2004.
- [124] J. Terrien, T. Steingrimsdottir, C. Marque, and B. Karlsson, "Synchronization between EMG at different uterine locations investigated using time–frequency ridge reconstruction: comparison of pregnancy and labor contractions," *EURASIP J. Adv. Signal Process.* 2010, 1–10 (2010).
- [125] W.L. Maner, R.E. Garfield, H. Maul, G. Olson, and G. Saade, "Predicting term and preterm delivery with transabdominal uterine electromyography." *Obstet. Gynecol.* 101(6), 1254–1260 (2003).
- [126] J. Sikora, A. Matonia, R. Czabanski, K. Horoba, J. Jezewski, and T. Kupka, "Recognition of premature threatening labour symptoms from bioelectrical uterine activity signals," *Arch. Perinat. Med.* 17(2), 97–103 (2011).
- [127] C. Marque, H. Leman, M.L. Voisine, J. Gondry, and P. Naepels, "Traitement de l'électromyogramme utérin pour la caractérisation des contractions pendant la grossesse," *RBM-News* 21(9), 200–211 (1999).

- [128] G. Fele-Žorž, G. Kavšek, Ž. Novak-Antolič, and F. Jager, "A comparison of various linear and non-linear signal processing techniques to separate uterine EMG records of term and pre-term delivery groups." *Med. Biol. Eng. Comput.* 46(9), 911–922 (2008).
- [129] M. Y. Gokhale, & D. K. Khanduja, (2010). Time domain signal analysis using wavelet packet decomposition approach. *Int'l J. of Communications, Network and System Sciences*, 3(03), 321.
- [130] D. Alamedine, M. Khalil, and C. Marque, Comparison of different EHG feature selection methods for the detection of preterm labor. *Computational and mathematical methods in medicine 2013* (2013).
- [131] M. O. Diab, C. Marque, and M. A. Khalil, "Classification for uterine EMG signals: Comparison between AR model and statistical classification method", *International Journal of computational cognition*, vol. 5, no. 1, pp.8-14, 2007.
- [132] G. Weiss. "Time-reversibility of linear stochastic processes." *Journal of Applied Probability* 12, no. 04 (1975): 831-836.
- [133] C.K. Peng, S. Havlin, H.E. Stanley, and A.L. Goldberger. "Quantification of scaling exponents and crossover phenomena in nonstationary heartbeat time series." *Chaos: An Interdisciplinary Journal of Nonlinear Science* 5, no. 1 (1995): 82-87.
- [134] A. Diab, M. Hassan, C. Marque, and B. Karlsson, "Quantitative performance analysis of four methods of evaluating signal nonlinearity: application to uterine EMG signals." Presented at the 34th Annual International IEEE EMBS Conference. San Diego, USA (2012).
- [135] T. Ivancevic, L. Jain, J. Pattison, A. Hariz, et al, "Preterm birth analysis using nonlinear methods." *Recent Patents Biomed. Eng.* 1(3), 160–170 (2008).
- [136] H.H. Hsu, C.W Hsieh, and M.D Lu, "Hybrid feature selection by combining filters and wrappers," *Expert Systems with Applications* 38.7 (2011): 8144-8150.
- [137] P. Langley and others, "Selection of relevant features in machine learning". *Defense Technical Information Center*, 1994.
- [138] H. Liu and L. Yu, "Toward integrating feature selection algorithms for classification and clustering," *Knowl. Data Eng. IEEE Trans. On*, vol. 17, no. 4, pp. 491–502, 2005.
- [139] H. Liu and H. Motoda, Feature extraction, construction and selection: A data mining perspective. Springer Science & Business Media, 1998..
- [140] M. A. Hall, "Correlation-based Feature Subset Selection for Machine Learning". *PhD Thesis*, University of Waikato, 1999.
- [141] A. L. Blum and P. Langley, "Selection of relevant features and examples in machine learning," *Artif. Intell.*, vol. 97, no. 1, pp. 245–271, 1997.
- [142] M. Dash and H. Liu, "Feature selection for classification," *Intell. Data Anal.*, vol. 1, no. 3, pp. 131–156, 1997.
- [143] T. M. Phuong, Z. Lin et R. B. Altman. Choosing SNPs using feature selection. *Proceedings / IEEE Computational Systems Bioinformatics Conference, CSB. IEEE Computational Systems Bioinformatics Conference*, pages 301-309, 2005. PMID 16447987.
- [144] Phuong, T. M., Lin, Z., & Altman, R. B. (2006). Choosing SNPs using feature selection. *Journal of bioinformatics and computational biology*, 4(02), 241-257.
- [145] B. Duval, J.-K. Hao et J. C. Hernandez Hernandez. "A memetic algorithm for gene selection and molecular classification of cancer." In *Proceedings of the 11th Annual conference on Genetic and evolutionary computation*, pp. 201-208. ACM, 2009.
- [146] G.H. John, R. Kohavi and K. Pfleger, "Irrelevant Features and the Subset Selection Problem," *Proceedings of the Eleventh International Conference on Machine Learning*, 1994, 121–129.
- [147] I. Kononenko, "Estimating Attributes: Analysis and Extensions of RELIEF," *European Conference on Machine Learning*, 1994, 171–182.
- [148] Y. W. Chang, and C. J. Lin. "Feature ranking using linear SVM." *WCCI Causation and Prediction Challenge*. 2008.
- [149] M. Basseville, and I. V. Nikiforov. *Detection of abrupt changes: theory and application*. Vol. 104. Englewood Cliffs: Prentice Hall, 1993.
- [150] J.A. Swets. *Signal detection theory and ROC analysis in psychology and diagnostics: Collected papers*. Psychology Press, 2014.

- [151] D. J. Hand, and R. J. Till. "A simple generalisation of the area under the ROC curve for multiple class classification problems." *Machine learning* 45, no. 2 (2001): 171-186.
- [152] <https://www.aub.edu.lb/sharp/Documents/ROC.pdf>. Accessed on June 10, 2017.
- [153] F. Castanedo. "A review of data fusion techniques." *The Scientific World Journal* 2013 (2013).
- [154] JDL, Data Fusion Lexicon. "Technical Panel for C3." FE White, San Diego, Calif, USA, Code 420 (1991).
- [155] R. R. Brooks, and S. S. Iyengar. Multi-sensor fusion: fundamentals and applications with software. Prentice-Hall, Inc., 1998.
- [156] A. Martin. "La fusion d'informations." *Polycopié de cours ENSIETA-Réf1484* (2005): 117.
- [157] S. Thrun, W. Burgard, and D. Fox. Probabilistic robotics. MIT press, 2005.
- [158] L.D. Stone, T.L. Corwin, and C.A. Barlow. "Bayesian Multiple Target Tracking, Artech House." Inc., Norwood, MA (1999).
- [159] C. Aynaoud. "Localisation précise et fiable de véhicules par approche multisensorielle." PhD diss., Université Blaise Pascal-Clermont-Ferrand II, 2015.
- [160] R.E. Kalman. "A new approach to linear filtering and prediction problems." *Journal of basic Engineering* 82, no. 1 (1960): 35-45.
- [161] B.DO. Anderson, and J.B. Moore."Optimal filtering." *Englewood Cliffs*21 (1979): 22-95.
- [162] J. Al Hage. "Fusion de données tolérante aux défaillances: application à la surveillance de l'intégrité d'un système de localisation." PhD diss., Lille 1, 2016.
- [163] S. Thrun, D. Koller, Z. Ghahramani, H. Durrant-Whyte, and A. Y. Ng. "Simultaneous mapping and localization with sparse extended information filters: Theory and initial results." In *Algorithmic Foundations of Robotics V*, pp. 363-380. Springer Berlin Heidelberg, 2004.
- [164] A. Gasparri and F. Pascucci. "An interlaced extended information filter for self-localization in sensor networks." *IEEE Transactions on Mobile Computing* 9, no. 10 (2010): 1491-1504
- [165] J. Laneurit. "Perception multisensorielle pour la localisation d'un robot mobile en environnement extérieur, application aux véhicules routiers." PhD diss., Université Blaise Pascal-Clermont-Ferrand II, 2006.
- [166] A. Doucet. "On sequential simulation-based methods for Bayesian filtering." (1998).
- [167] R.E. Moore: Interval Analysis (Prentice Hall, Upper Saddle River 1966)
- [168] D.J. Dubois. Fuzzy sets and systems: theory and applications. Vol. 144. Academic press, 1980.
- [169] D. Pagac, E.M. Nebot, H. Durrant-Whyte. "An evidential approach to map-building for autonomous vehicles." *IEEE Transactions on Robotics and Automation* 14, no. 4 (1998): 623-629.
- [170] B. Khaleghi, A. Khamis, F.O. Karray, and S.N. Razavi. "Multisensor data fusion: A review of the state-of-the-art." *Information Fusion* 14, no. 1 (2013): 28-44.
- [171] A. Frikha, H. Moalla. Analytic hierarchy process for multi-sensor data fusion based on belief function theory, *Eur. J. Oper. Res.* 241 (2015) 133-147.
- [172] H. Durrant-Whyte. Introduction to decentralised data fusion. The University of Sydney, Sydney, Australia, 2004.
- [173] S.J. Wellington, J.K. Atkinson, R.P. Sion. Sensor validation and fusion using the Nadaraya-Watson statistical estimator, in: Proc. Fifth Int. Conf. Inf. Fusion, vol.1, 2002, pp. 321-326.
- [174] K. Bader. "Tolérance aux fautes pour la perception multi-capteurs: application à la localisation d'un véhicule intelligent." PhD diss., Compiègne, 2014.
- [175] W. E. Dixon, I. D. Walker, and D. M. Dawson. "Fault detection for wheeled mobile robots with parametric uncertainty." In *Advanced Intelligent Mechatronics, 2001. Proceedings. 2001 IEEE/ASME International Conference on*, vol. 2, pp. 1245-1250. IEEE, 2001.
- [176] A.C. Escher, C. Macabiau, N. Martin, B. Roturier, and V. Vogel. "GNSS/IRS hybridization: fault detection and isolation of more than one range failure." In *ION GPS 2002, 15th International Technical Meeting of the Satellite Division of the Institute of Navigation*, pp. pp-2619. 2002.
- [177] T. Kobayashi, and D.L. Simon. "Application of a bank of Kalman filters for aircraft engine fault diagnostics." *ASME Paper No. GT2003-38550*(2003).
- [178] W. Xue, Y.Q. Guo, and X.D. Zhang. "A bank of Kalman filters and a robust Kalman filter applied in fault diagnosis of aircraft engine sensor/actuator." In *Innovative Computing, Information and Control, 2007. ICICIC'07. Second International Conference on*, pp. 10-10. IEEE, 2007.

- [179] V. Ricquebourg, M. Delafosse, L. Delahoche, B. Marhic, A. Jolly-Desodt, and D. Menga. "Fault detection by combining redundant sensors: a conflict approach within the tbm framework." *Cognitive Systems with Interactive Sensors, COGIS* (2007).
- [180] M. Kumar, D.P. Garg, R.A. Zachery. A method for judicious fusion of inconsistent multiple sensor data, *IEEE Sens. J.* 7 (2007) 723–733.
- [181] R. M. Eustice, H. Singh, and J. J. Leonard. "Exactly sparse delayed-state filters for view-based SLAM." *IEEE Transactions on Robotics* 22, no. 6 (2006): 1100-1114.
- [182] H. Durrant-Whyte and T. C. Henderson. "Multisensor data fusion." In *Springer Handbook of Robotics*, pp. 585-610. Springer Berlin Heidelberg, 2008.
- [183] J. Al Hage, M.E. El Najjar, and D. Pomorski. "Multi-Sensor Fusion Approach with Fault Detection and Exclusion based on the Kullback-Leibler Divergence: Application on Collaborative Multi-Robot System." *Information Fusion* (2017).
- [184] https://en.wikipedia.org/wiki/Positioning_system. Accessed on April 20, 2017.
- [185] D. Dardari, P. Closas, and P.M. Djurić. "Indoor tracking: Theory, methods, and technologies." *IEEE Transactions on Vehicular Technology* 64, no. 4 (2015): 1263-1278.
- [186] H. Huang, and G. Gartner. "A survey of mobile indoor navigation systems." *Cartography in Central and Eastern Europe* (2010): 305-319.
- [187] Y. Gu, A. Lo, and I. Niemegeers. "A survey of indoor positioning systems for wireless personal networks." *IEEE Communications surveys & tutorials* 11, no. 1 (2009): 13-32.
- [188] <http://www.mobiletechnews.com/info/2004/04/27/011106.html>. Accessed on May 15, 2017.
- [189] M.H. Jin, C.H. Yu, H.R. Lai, and M.W. Feng. "Zigbee positioning system for smart home application." In *Frontiers of High Performance Computing and Networking ISPA 2007 Workshops*, pp. 183-192. Springer Berlin/Heidelberg, 2007.
- [190] V. Renaudin, O. Yalak, P. Tomé, and B. Merminod. "Indoor navigation of emergency agents." *European Journal of Navigation* 5, no. 3 (2007): 36-45.
- [191] O. Woodman, and R. Harle. "Pedestrian localisation for indoor environments." In *Proceedings of the 10th international conference on Ubiquitous computing*, pp. 114-123. ACM, 2008.
- [192] G. Girard, S. Côté, S. Zlatanova, Y. Barette, J. St-Pierre, and P. Van Oosterom. "Indoor pedestrian navigation using foot-mounted IMU and portable ultrasound range sensors." *Sensors* 11, no. 8 (2011): 7606-7624.
- [193] R.C. Chen, and Y.H. Lin. "Using ZeeBee Sensor Network with artificial neural network for indoor location." In *Natural Computation (ICNC), 2012 Eighth International Conference on*, pp. 290-294. IEEE, 2012.
- [194] G. Lee, and J. Yim. "A review of the techniques for indoor location based service." *International Journal of Grid and Distributed Computing* 5, no. 1 (2012): 1-22.
- [195] M.E. Rida, F. Liu, Y. Jadi, A.A.A. Algawhari, and A. Askourih. "Indoor location position based on bluetooth signal strength." In *Information Science and Control Engineering (ICISCE), 2015 2nd International Conference on*, pp. 769-773. IEEE, 2015.
- [196] N. Poosamani, and I. Rhee. "Towards a practical indoor location matching system using 4G LTE PHY layer information." In *Pervasive Computing and Communication Workshops (PerCom Workshops), 2015 IEEE International Conference on*, pp. 284-287. IEEE, 2015.
- [197] A.M. Martins, A.D. Neto, J.D. Melo. "Comparison between mahalanobis distance and kullback-leibler divergence in clustering analysis." *Wseas Transactions on Systems* 3 (2004): 501-505.
- [198] F. Pérez-Cruz. Kullback–Leibler divergence estimation of continuous distributions, in: *Inf. Theory 20 08 ISIT 20 08 IEEE Int. Symp. On*, IEEE, 2008, pp. 1666–1670.
- [199] https://en.wikipedia.org/wiki/Inertial_measurement_unit. Accessed on May 17, 2017.
- [200] <https://www.novatel.com/assets/Documents/Bulletins/APN064.pdf>. Accessed on May 19, 2017.
- [201] B. Tessenorf, F. Gravenhorst, B. Arnrich, and G. Tröster. "An imu-based sensor network to continuously monitor rowing technique on the water." In *Intelligent Sensors, Sensor Networks and Information Processing (ISSNIP), 2011 Seventh International Conference on*, pp. 253-258. IEEE, 2011.
- [202] <https://www.thalesgroup.com/en/worldwide/aerospace/topaxyz-inertial-measurement-unit-imu/infographic>. Accessed on May 19, 2017.

- [203] A. Dubois, and F. Charpillet. "Detecting and preventing falls with depth camera, tracking the body center." The 12th European Association for the Advancement of Assistive Technology in Europe (2013): 77-82.
- [204] S. Thrun, Y. Liu, D. Koller, A. Y. Ng, Z. Ghahramani, and H. Durrant-Whyte. "Simultaneous localization and mapping with sparse extended information filters." *The International Journal of Robotics Research* 23, no. 7-8 (2004): 693-716.
- [205] <http://www.mechanicalbooster.com/2016/11/types-of-support.html>. Accessed on Feb 05, 2017.
- [206] https://en.wikipedia.org/wiki/Statically_indeterminate. Accessed on Feb 05, 2017.
- [207] S. Eguchi, J. Copas. Interpreting Kullback–Leibler divergence with the Neyman—Pearson lemma, *J. Multivar. Anal.* 97 (2006) 2034–2040.